ROLES OF MoFe PROTEIN α-274-HISTIDINE, α-276-TYROSINE AND α-277-ARGININE RESIDUES IN *Azotobacter vinelandii* NITROGENASE CATALYSIS

by

JOAN SHEN

Dissertation submitted to the faculty of the
Virginia Polytechnic Institute and State University
in partial fulfillment of the requirements for the degree of

DOCTOR OF PHILOSOPHY

in

Biochemistry and Anaerobic Microbiology

APPROVED:

William E. Newton, Chairman

Jiann-Shin Chen

Dennis R. Dean

Eugene M. Gregory

Thomas O. Sitz

November, 1994
Blacksburg, Virginia

ROLES OF MoFe PROTEIN α-274-HISTIDINE, α-276-TYROSINE AND α-277-ARGININE RESIDUES IN *Azotobacter vinelandii* NITROGENASE CATALYSIS

by

JOAN SHEN

Committee Chairman: William E. Newton
Biochemistry and Anaerobic Microbiology

(ABSTRACT)

Previous studies revealed that α-275-Cys provides an essential ligand to one of the Fe atoms on the FeMo-cofactor, and its substitutions resulted in inactive nitrogenase. In order to study the structural-functional relationship of the protein environment in this region with respect to the FeMo-cofactor, subtle changes were introduced through substitutions using a site-directed mutagenesis and gene-replacement method at α-274-His, α-276-Tyr and α-277-Arg in *Azotobacter vinelandii* nitrogenase. Characterization of mutants strains resulting from amino acid substitutions at residues, α-274-His, α-276-Tyr or α-277-Arg, using activity assays, resulted in mixed Nif phenotypes. Therefore, none of these residues is absolutely required for nitrogenase activity. However, the changed EPR spectra of the altered MoFe proteins from some strains with substitutions at either α-276-Tyr or α-277-Arg indicated that the FeMo-cofactor environment had been perturbed by these substitutions.

Together with its changed EPR spectrum, substituting α-277-Arg with His showed some extraordinary catalytic features, such as its inability to reduce N_2, while retaining respectable C_2H_2- and H^+-reduction activities. It was also found that this altered protein used a higher percentage of total electron flux for H_2 evolution under an C_2H_2/Ar atmosphere than did wild type. Further characterization of the purified α-277^{his} MoFe protein in parallel with its wild type

counterpart revealed that the alteration in the α-277^{his} MoFe protein caused a lower affinity for C_2H_2 binding, whereas it did not affect the CO binding. Interestingly, CO-induced cooperativity during C_2H_2 reduction was observed in this altered MoFe protein clearly indicating two sites for C_2H_4 evolution, one of which might be in the vicinity of this residue. Furthermore, the α-277^{his} MoFe protein does not bind or reduce N_2 leading to the proposal of a nonexistent E_4 redox state in the MoFe protein catalytic cycle which was supported by stopped-flow spectrophotometric evidence. This altered α-277^{his} MoFe protein showed comparable physical stabilities to that of the wild-type protein, and its ATP hydrolysis rates remained constant under a number of substrates assayed. Therefore, the substitution has not affected the overall protein structure, rather, it has changed the local FeMo-cofactor environment.

When we studied the purified α-276^{his} and α-274^{gln}/α-276^{his} MoFe proteins and compared the results with the data from the α-277^{his} and wild-type MoFe protein, we found that there is no direct correlation between the additional set of EPR signals observed in these altered MoFe proteins and their catalytic activities. The current understanding concerning the functionality of these residues is that they are involved in maintaining a proper environment for FeMoco to bind and in stabilizing the different redox states of the enzyme during catalysis.

Acknowledgement

First of all, I would like to thank my advisor, Dr. Bill Newton, for his support, patience and fatherly care for me. I would not have accomplished this much without his scientific guidance. I would like to thank Dr. Dennis Dean for his support and encouragement that played important roles in my dissertation research. From Dr. J.-S. Chen, I benefited very much from his precise methodology and appreciated his valuable advice both as a professor and a friend. I would also thank my committee members, Dr. Gregory and Dr. Sitz, for their support, encouragement and understanding. This excellent combination of professional expertise in my committee provided me with such valuable experience that I would always cherish.

I would like to thank all the faculty members in this department, Dr. Bender, Dr. Niehause, Dr. Bunce, Dr. Kennelly, and Dr. Anderson, to name a few. I appreciate their effort in helping me and encouragements.

I am grateful to Peggy, Mary Jo, Karen and Sheila for their effort in helping me whenever I need. Thanks also go to Mrs. Anderson for her kindness and warm heart. I enjoyed talking to Barbara as a friend everyday.

Fortunately, I have known a good number of both present and former fellow graduate students and coworkers. I will never be able to replace the friendship, knowledge and help gained from my colleagues, C-H. Kim, John Cantwell, John Peters, Richard Jack, Tamaki Kurusu, Krissie Thrasher, Val Cash, Christie Dapper, Mark Sadler. Special thanks also go to Drs. Limin Zheng and Karl Fisher for their help and encouragements, both as coworkers and friends.

As a student far from home, I would not have enjoyed these years as much without my friends, Lily Lin, Yan Wang, Alex Wang, Lance Wang, Jia Li, Christina Wong, Keith Oxenrider, and Michael Zhang. Numerous former and

present graduate students in this department have been very encouraging and helpful. I treasure the friendship with Mr. Walter Maloney whose kindness and support have been important during my thesis preparation.

Finally, I would like to thank my parents for their endless love, for always inspiring my interest in science and for their constant encouragement, my gratitude toward them is beyond words. My family, my parents, my brother and sister, have been behind me throughout these years. Most important of all, I thank my husband, Kin Shum, whose love, understanding and support have always accompanied me.

This work was supported by a grant from the National Institute of Health (DK-37255).

Table of Contents

List of Figures

List of Tables

Chapter 1 Literature Review

1.1 Biological Nitrogen Fixation

The growth and survival of all living organisms on the Earth is ultimately dependent on the availability in the soil of fixed forms of nitrogen, which can be utilized by the plant, if sunlight and water supply are not limiting factors for crop growth. However, atmospheric dinitrogen (N_2) is chemically unreactive because of its strong triple bond, and thus cannot be utilized directly by plants or animals. Crucial steps in the nitrogen cycle involve the natural conversion of N_2 into more reactive forms, either non-biologically to the highly oxidized states (nitrate or nitrite) or biologically to the reduced state (ammonia). There is no evidence for the occurrence of biological oxidative nitrogen fixation. The ability to reduce N_2 to ammonia and thus make it available as a nitrogen source for plant and bacterial growth is restricted to certain prokaryotic organisms, which are called diazotrophs.

Diazotrophy is a characteristic shared by many different genera of prokaryotes with representatives among Gram-positive and Gram-negative eubacteria and also in the archaebacteria (Eady, 1992). This ability is distributed through a broad spectrum of microorganisms and plant-microorganism symbionts with little in common other than their ability to reduce N_2.

The process of nitrogen fixation has been effectively industrialized at high temperatures and pressures (350°C and 400 atmospheres, Leigh, 1981) in the Haber-Bosch process. In the presence of a catalyst of finely divided iron containing Mo, K and Al oxides, N_2 is reduced by H_2 to ammonia as the basis for the manufacture of ammonia-based fertilizers. However, the use of commercial fertilizers in agriculture has a number of disadvantages, such as the need for expensive and sophisticated industrial installations, the high cost in energy and transportation to the field and the potential hazard to the natural ecosystem.

Globally, nitrogen fixation contributes a total of 2.5×10^8 tones of nitrogen per year fixed by both chemical and biological routes (Eady, 1992). Diazotrophs add annually about 60% of the earth's newly fixed nitrogen, while industrially fixed nitrogen contributes only about 25% of the bulk, with the remaining 15% produced by lightning, UV radiation, etc (Eady, 1992). Although biological nitrogen fixation is essential for maintaining the nitrogen cycle in the Earth's biosphere, it still has an energy requirement of 355 kJ (mol $NH_4^+)^{-1}$. This energy input is required to overcome the activation energy for the reduction of dinitrogen. The organisms that possess this capacity to fix nitrogen operate at ambient temperatures and pressures with the sun as the ultimate energy source. The agronomic significance of symbiotic microorganisms that fix and deliver nitrogen to their hosts is well established. Nitrogen fixation has become a major topic of research in hope for a better understanding of the molecular mechanism of nitrogen fixation. Such knowledge should prove valuable to efforts aimed at duplicating the activity of nitrogenase in chemical systems, as well as improving the economy of nitrogen fixation through genetic manipulation of N_2-fixing species. Therefore, progress in nitrogen fixation research could represent real contributions to the long-term solution of the World food supply problem and in upgrading the nutritional status of the World's population.

1.2 Nitrogenase

There are three genetically distinct, although related, nitrogenase systems capable of catalyzing the reduction of dinitrogen to ammonia. One is based on molybdenum (Mo-nitrogenase) (Bulen *et al.*, 1965; Lowe *et al.*, 1985; Eady, 1986), another on vanadium (Hales *et al.*, 1986a, b; Robson, *et al.*, 1986), and a third that functions without molybdenum or vanadium (Chisnell *et al.*, 1988). The latter two, also called alternative nitrogenases, have only recently been discovered

and isolated, because the addition of Mo to the bacterial growth medium prevents their expressions (Pau *et al.*, 1989). The alternative nitrogenases will not be discussed in any detail because they were not part of the author's research.

All Mo-nitrogenases are comprised of two oxygen-labile metalloproteins, the iron protein (Fe-protein) and molybdenum-iron protein (MoFe-protein). Both components of the enzyme complex contain non-heme iron and acid labile sulphur. It catalyzes the following nitrogen-reduction reaction.

$$N_2 + 8H^+ + 8e^- + 16MgATP \rightarrow 2NH_3 + H_2 + 16MgADP + 16Pi$$

Besides N_2, nitrogenase also catalyzes the reduction of a number of nonphysiological substrates, such as, C_2H_2, H^+ and N_3^- and so on (for details, see section 1.7.3).

1.2.1 The Fe Protein

The Fe protein is a homodimer, encoded by the *nifH* gene, with M_r *ca.* 63,000 Dalton. Its two identical subunits are bridged by a single 4Fe:4S cluster. Among all diazotrophic eubacteria whose Fe protein sequences are known, there are five conserved cysteinyl residues: Cys-39, Cys-86, Cys-98, Cys-133 and Cys-185 (numbers refer to the amino-acid sequence of the *A. vinelandii* Fe protein) (reviewed by Dean & Jacobson, 1992). The three-dimensional crystal structure of the Fe protein (Georgiadis *et al.*, 1992) confirmed the hypothesis (Hausinger & Howard, 1983; Howard *et al.*, 1989) that the 4Fe:4S cluster is symmetrically coordinated by Cys-98 and Cys-133 from each subunit. The two subunits are related by a molecular two-fold rotation axis that passes through the 4Fe:4S cluster, which is located at one end of the dimer and at the subunit-subunit interface. Figure 1 shows a ribbon diagram of the nitrogenase Fe protein from *Azotobacter vinelandii*.

It was shown in the earlier studies that, upon removal of the cluster, the

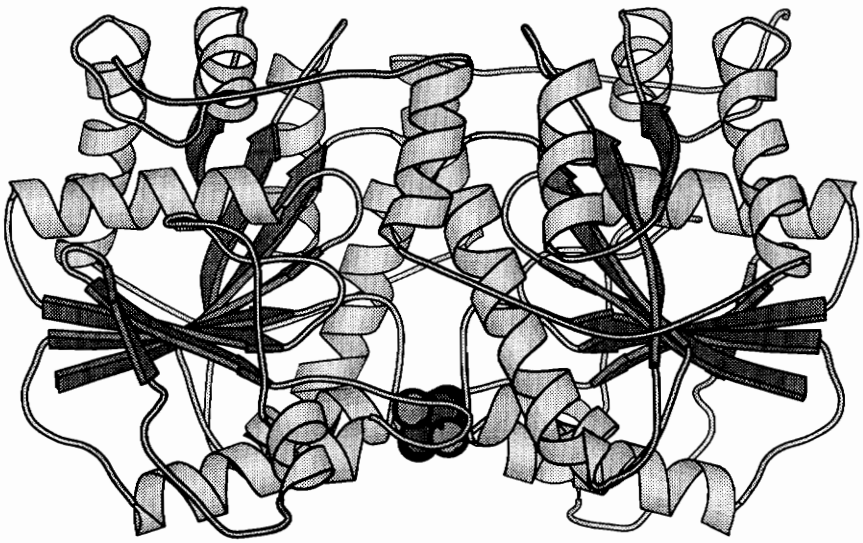

Figure 1. Ribbon structure of Fe protein from *A. vinelandii* nitrogenase, the figure was generated using program MOLSCRIPT (Kraulis, 1991) from data kindly provided by Dr. Jeff Bolin at Purdue University.

dimer structure of the Fe protein was still well maintained (Howard *et al.*, 1989). The crystal structure subsequently offered an excellent explanation for this observation, that there are numerous hydrophobic and salt interactions in the interface beneath the cluster that help to stabilize the dimer structure (Georgiadis *et al.*, 1992). The single 4Fe:4S cluster undergoes a one-electron redox cycle between the $2Fe^{2+}2Fe^{3+}$ state and the $3Fe^{2+}Fe^{3+}$ state. In contrast to the protected environment of the 4Fe:4S clusters observed in ferredoxin-type proteins, a striking feature of the Fe protein is the exposure of the cluster to solvent, a property anticipated by the spectroscopic studies (Morgan *et al.*, 1990). There is little contact between the 4Fe:4S cluster and the amino-acid side chains other than the cysteinyl ligands.

In order for electron transfer to occur, the nitrogenase component proteins, MoFe protein (see section 1.2.2) and Fe protein, are proposed to be brought together and dock in a specific manner such that the Fe-protein 4Fe:4S cluster is located near the MoFe-protein P cluster (for more detailed descriptions, see section 1.5). Insight into this docking orientation has come from studies of the regulatory mechanism of photosynthetic microorganisms (Eady, 1986). ADP ribosylation of the Arg-100 residue was shown to block the binding of the Fe protein to the MoFe protein (Pope *et al.*, 1985; Murrell *et al.*, 1988). Later, Glu-112 of the Fe protein was proved to be involved in the interaction with the MoFe-protein by chemical cross-linking studies (Willing, *et al.*, 1989; Willing & Howard, 1990). The x-ray crystallographic structure of Fe protein from *A. vinelandii* shows that both Arg-100 and Glu-112 are located on the protein surface close to the 4Fe:4S cluster (Georgiadis *et al.*, 1992).

The other principal functional feature of the Fe protein is its ability to bind the nucleotides, MgATP and MgADP. Two nucleotide-binding sites per Fe protein, one on each subunit, have been reported (Hageman *et al.*, 1980). The

crystal structure shows that the presumed binding site for the terminal nucleotide phosphates (where hydrolysis occurs) is located ~20 Å from the 4Fe:4S cluster, which indicates that the nucleotide does not interact directly with the cluster. Rather, the location of the cluster and nucleotide-binding sites at the interface between the subunits suggests that there is an allosteric coupling mechanism that connects these two functional sites.

In summary, the 4Fe:4S cluster is believed to be responsible for accepting and delivering single electrons to the MoFe protein. Binding of MgATP to the Fe protein and its subsequent hydrolysis appears to be essential for the electron transfer process. However, the relationship of MgATP hydrolysis, electron transfer and component protein association and dissociation is not well understood (for a recent review, see Howard & Rees, 1994; Dean & Jacobson, 1994; and the references cited therein).

1.2.2 The MoFe Protein

The MoFe protein from all nitrogenase sources has a native M_r of about 230,000 and is composed of two non-identical subunits as an $\alpha_2\beta_2$ tetramer: the α-subunit is coded by the *nifD* gene with M_r *ca.* 55,000 and the β-subunit by the *nifK* gene with M_r *ca.* 60,000. The holoprotein contains 30 Fe, 32-34 sulfides, and two Mo atoms per native molecule distributed among its two types of prosthetic groups, the P cluster and FeMo-cofactor (FeMoco) (two copies of each per MoFe protein).

Sequence comparison studies revealed strong interspecies sequence conservation of the MoFe-protein α- and β-subunits among different species reflecting their critical relevance to the MoFe-protein function. A striking interspecies conservation in the folding of the individual subunits is suggested by a remarkable conservation of residues that are frequently located within reverse turns (e.g.,

glycine and proline). Further, there are five Cys residues conserved among all known α-subunit sequences: Cys-62, Cys-88, Cys-154, Cys-183, and Cys-275, and three Cys residues conserved among all known β-subunit sequences: Cys-70, Cys-95, and Cys-153 (numbers refer to the amino-acid sequence of *A. vinelandii* MoFe protein). Among these conserved cysteine residues, it was proposed that the first three from the α-subunit together with those in the β-subunit provided the polypeptide environment for the P clusters (Dean *et al.*, 1990b) while the remaining two cysteine residues from the α-subunit were involved in accommodating the FeMoco (Brigle *et al.*, 1985). These predictions were subsequently proved by site-directed mutagenesis studies and the crystal structure (for details refer to section 1.2.3 and 1.4). In addition, according to the crystallographic studies, the strictly conserved His residue at position α-442 is directly ligated to the Mo atom of the FeMoco thus it is also involved in providing the FeMoco environment (Kim & Rees, 1992a). Figure 2 is a schematic representation of the primary sequences of the α- and β-subunits of the MoFe proteins and the residues that are involved in P-cluster and FeMoco binding.

Recently, the x-ray crystallographic structure of the MoFe protein from both the *A. vinelandii* and *C. pasteurianum* nitrogenases has been solved which provides us with much needed detailed structural information. Figure 3 is a ribbon diagram of *A. vinelandii* MoFe protein as an $\alpha\beta$ dimer and the relative positions of the P cluster and FeMoco in the protein.

1.2.3 MoFe Protein Metal Clusters: P Cluster and FeMoco

It was found that about 16 Fe atoms can be extruded from each MoFe protein molecule as approximately four 4Fe:4S clusters by treatment of the native protein with thiols in a denaturing organic solvent (Kurtz *et al.*, 1979). These

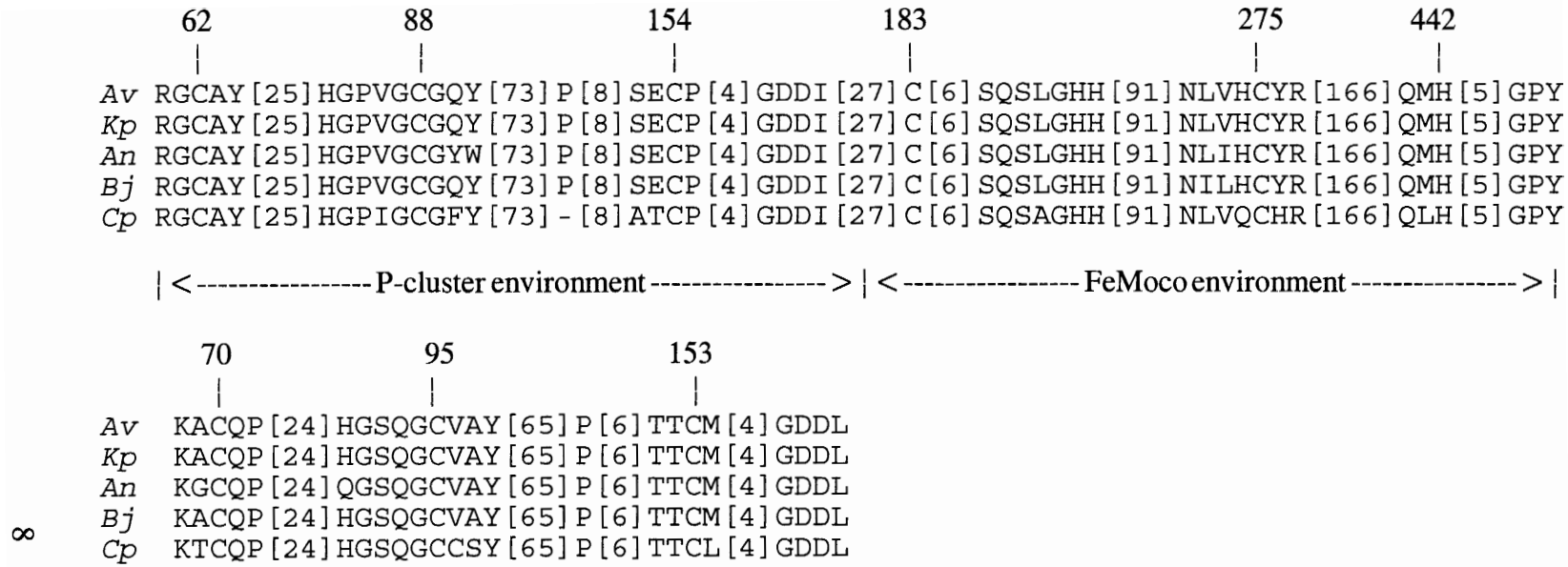

Figure 2. Sequence alignment of relevant regions containing conserved Cys residues (and His residues) from the MoFe protein α- and β-subunits from *A.vinelandii*, *K. pneumoniae, Anabaena* 7120, *B. japonicum*, *C. pasteurianum*. Numbers refer to the *A.vinelandii* sequence. P-cluster and FeMoco environments in the α- and β-subunits are indicated. Adapted from Dean and Jacobson, 1992.

Figure 3. Ribbons diagram of *Azotobacter vinelandii* MoFe protein $\alpha\beta$ subunit dimer with space-filling models for the FeMoco in the α-subunit and the P cluster bridging the α- and β-subunit. The graph was generated using MOLSCRIPT (Kraulis, 1991) from data kindly provided by Dr. Jeff Bolin at Purdue University.

protein-bound Fe-S clusters have been described by their redox properties and their Mössbauer, circular dichroism (CD) and magnetic circular dichroism (MCD) spectroscopic features (Stephens *et al.*, 1979; Kurtz *et al.*, 1979; McLean *et al.*, 1987; Lindahl *et al.*, 1988). They are called P clusters because of their covalently protein-bound nature revealed by the earlier studies (Zimmerman *et al.*, 1978).

Although originally their redox and spectroscopic properties were thought to be compatible with their formulation as four 4Fe:4Fe clusters, the spectroscopic properties of the P clusters are very unusual. Hagen *et al.* (1985) first proposed the possibility of the P clusters existing as two 8Fe:8S clusters and early X-ray anomalous diffraction data supported this notion by indicating that the P-cluster Fe atoms were associated with just two regions of high electron density in the tetramer (Bolin, *et al.*, 1990). Indeed, the x-ray crystallographic studies model each P cluster as an 8Fe:8S center containing two 4Fe:4S clusters, with two Fe atoms of each cluster involved in bridging through the cysteine (Cys) thiols (from α88 and β95), with the four remaining Fe atoms terminally ligated by singly coordinating cysteine thiols (from residues α62, α154, β70 and β153). Thus the P clusters reside *ca.* 10 Å below the surface and at the interface of the α- and β-subunits with both nonbridging cysteines coordinated to one specific 4Fe:4S cluster from the same subunit. In addition to the cysteine ligands, β-188-Ser is close to Fe6 and may coordinate this site along with β-153-Cys (Figure 4, Kim & Rees, 1992a). It is proposed that, in the *Azotobacter vinelandii* MoFe protein structure, the two 4Fe:4S sub-clusters in the P cluster are bridged additionally by a disulfide bond between two inorganic sulfurs (see Figure 4). The presence of the disulfide bridge in the P cluster pair implies that this center may be able to serve as a two-electron redox group. There is no definite evidence concerning the biosynthesis of the P clusters. Isolation of FeMoco-less apo-MoFe protein (*nifB*$^-$) that can be

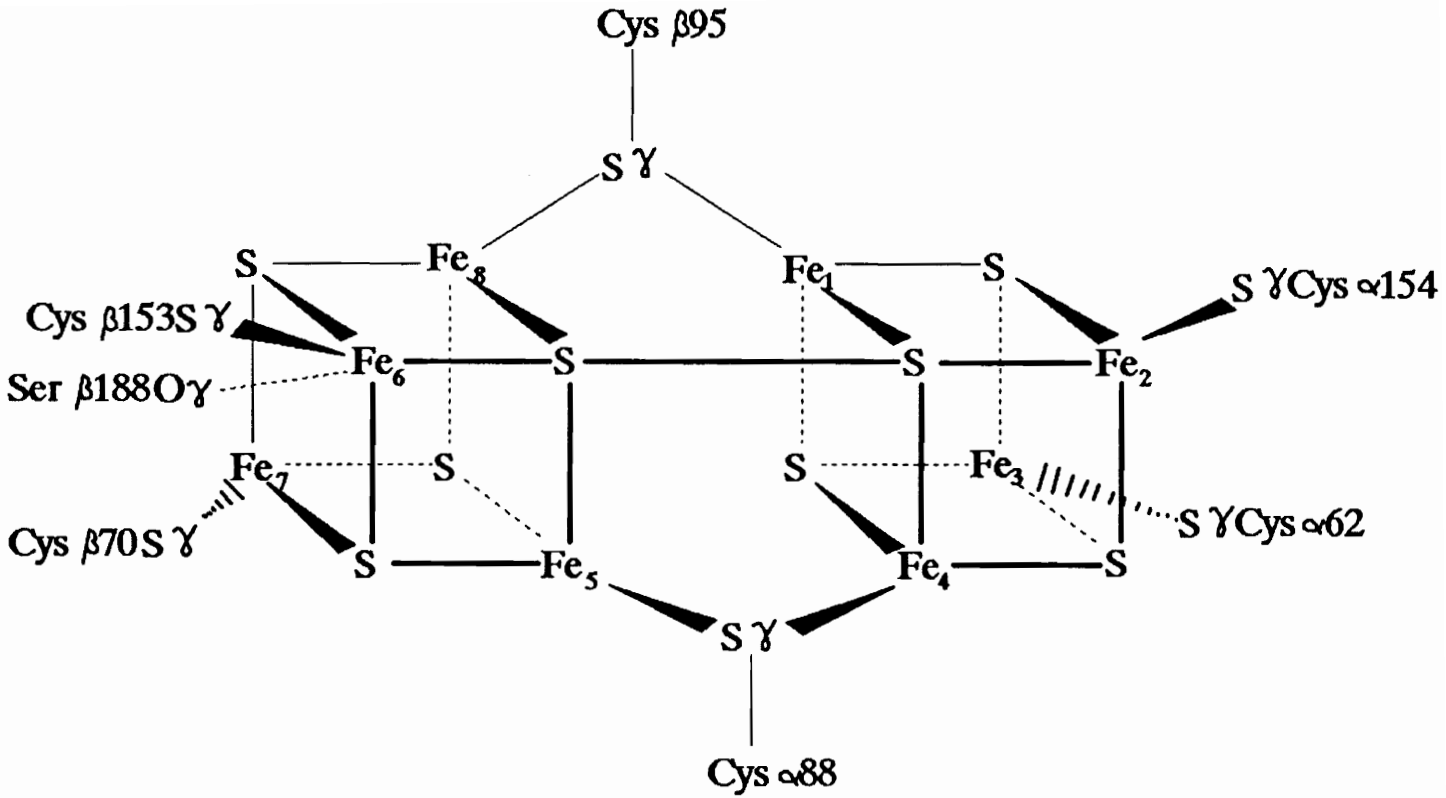

Figure 4. Schematic representation of the P-cluster model (Adapted from Kim and Rees, 1992a).

reconstituted by the simple addition of FeMoco clearly indicates that the P-clusters and FeMocos are separate entities (Shah *et al.*, 1977).

There are two copies of FeMoco per MoFe protein. The FeMoco can be extracted by *N*-methylformamide (NMF) following the acid denaturation of the MoFe protein (Shah & Brill, 1977). The FeMoco almost certainly provides the site for substrate binding and reduction of nitrogenase (Hawkes *et al.*, 1984; Scott *et al.*, 1990). Each FeMoco contains two sub-clusters of composition 4Fe:3S and 1Mo:3Fe:3S that are bridged by three non-protein sulfide ligands as is shown in Figure 5. Homocitrate, which is an essential component of FeMoco (Hoover *et al.*, 1987-1989; Madden *et al.*, 1990), is coordinated directly to the Mo through hydroxyl and carboxyl oxygens (Kim & Rees, 1992a; Chan *et al.*, 1993). The cofactor is buried $\sim$10 Å beneath the protein surface, in an environment primarily provided by the α-subunit. There are only two direct protein ligands to the FeMoco: α-275-Cys coordinates Fe1, whereas the Mo is ligated by the side chain of α-442-His. This model confirms the mutagenesis studies which suggested that the α-275-Cys is a likely ligand to the FeMoco (Kent *et al.*, 1989, 1990; Dean *et al.*, 1990a). The α-442-His residue was indicated as important prior to the crystal structure, through gel electrophoresis studies of a variety of mutants (Govezensky & Zamir, 1989). There are hydrogen bonds to sulfurs in the cluster provided by the side chains of residues α-96-Arg, α-195-His, α-359-Arg, and the NH groups of residues α-356-Gly and α-358-Lys (α-358-Ser in *Cp* sequence). These hydrogen bonds may provide a mechanism for funneling protons to substrate bound to the FeMoco (Howard & Rees, 1994). α-195-His and α-191-Gln are within 5 Å of Fe2 and Fe6 respectively, again confirming predictions that these residues are involved in the binding of FeMoco to MoFe protein (Scott *et al.*, 1990; Thomann *et al.*, 1987 & 1991). Homocitrate is hydrogen bonded to the amide side chain of α-191-Gln and is also surrounded by a pool of buried waters,

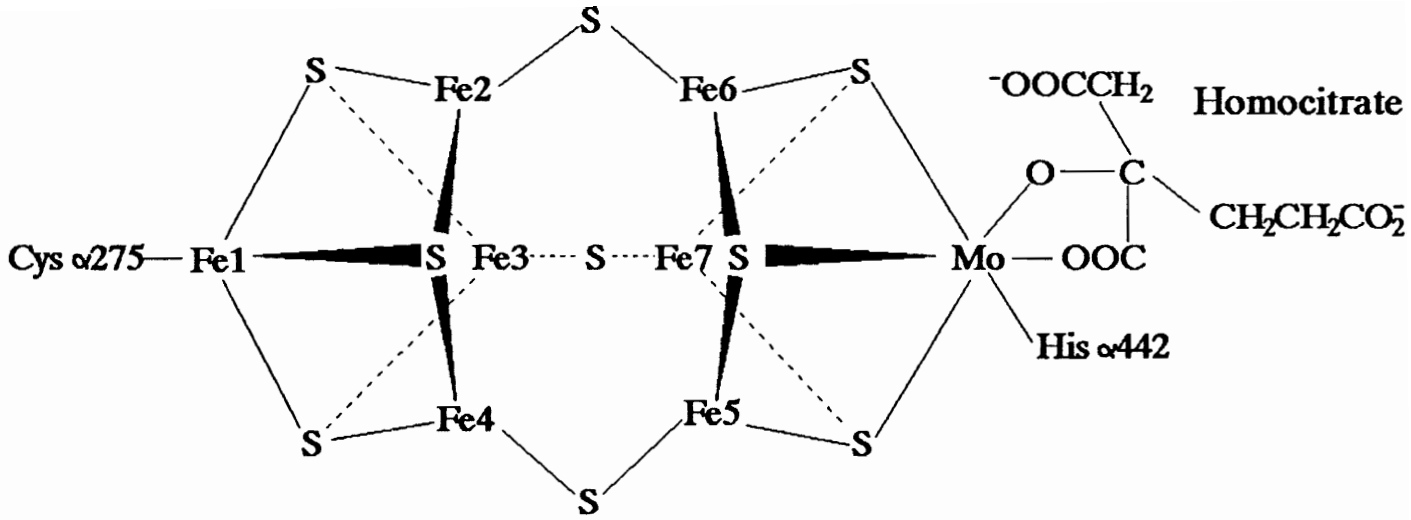

Figure 5. Schematic representation of the FeMoco model (Adapted from Kim and Rees, 1992a).

which could conceivably function as a proton source for substrate reduction. This arrangement supports the proposal that α-191-Gln interacts with homocitrate (Scott *et al.*, 1990). The uniqueness of the FeMoco structure, especially with six of the Fe atoms being three-coordinated, has led to the speculation of them providing suitable substrate-binding sites (Howard and Rees, 1994 and the references cited therein).

FeMoco is the source of the biologically unique electron paramagnetic resonance (EPR) spectrum, which is characteristic of an $S=3/2$ spin system, of nitrogenase. As shown in Figure 6, the $S=3/2$ EPR signal of the FeMoco in the MoFe protein shows apparent g values of 4.3, 3.65 and 2.0; while those of the isolated FeMoco are 4.7, 3.3 and 2.0, at temperature of 13 K. The broadening of the EPR signal upon FeMoco extraction was attributed to the change in its ligation (Shah *et al.*, 1977).

There is no direct evidence for the function of the P cluster. However, mutagenesis, spectroscopic and structural studies all indicate that the P clusters are mostly likely involved in electron transfer to the FeMoco during the catalytic cycle (May *et al.*, 1991; Lowe *et al.*, 1993; Chan *et al.*, 1993; Rees *et al.*, 1993; for more details see section 1.5). The distance of closest approach between metal sites in the P cluster pair and the FeMoco is $\sim$14 Å, which suggests that the electron transfer rate between these centers should be faster than the rate of nitrogenase turnover (Wuttke *et al.*, 1992; Farid *et al.*, 1993). Potential electron-transfer pathways between the P clusters and the FeMoco centers have been described (Kim & Rees, 1992b; Bolin *et al.*, 1993). In particular, the helices α63 - α74 and α88 - α92, adjacent to the P cluster ligands α-62-Cys and α-88-Cys, are directed towards the FeMoco. The locations of homocitrate and the Mo on the side of the FeMoco closest to the P cluster pair suggest that these groups might also participate in electron transfer between these two redox centers (Howard &

Figure 6. Comparison of $S = 3/2$ EPR signals of protein-bound FeMoco ($g = 3.65, 4.34$) (top); and of isolated FeMoco ($g = 3.3, 4.7$) (bottom) at 13 K (Adapted from Newton and Dean, 1992).

Rees, 1994).

1.2.4 FeMoco is the Substrate-reduction Site

The minimum requirements for *in vitro* FeMoco biosynthesis were shown to include the *nifB* product (Shah & Brill, 1977; Roberts *et al.*, 1978; Hawkes & Smith, 1983; Paustian *et al.*, 1990), the *nifEN* products (Roberts *et al.*, 1978; Brigle *et al.*, 1987a), a factor (homocitrate) whose accumulation requires the *nifV* product (Hawkes *et al.*, 1984), Fe protein (Filler *et al.*, 1986; Robinson *et al.*, 1987; Shah *et al.*, 1988), ATP and Mo (Shah *et al.*, 1986). It is believed that the FeMoco is, contains or is part of the substrate-reduction site. Evidences that FeMoco is directly involved in substrate reduction are summarized as follows.

(1) Certain mutant strains, which are incapable of synthesizing FeMoco, produce a FeMoco-deficient inactive and EPR-silent MoFe protein (Shah *et al.*, 1977). Such inactive MoFe protein can be reconstituted by the addition of FeMoco that has been extracted from native MoFe protein. MoFe protein reconstituted in this way regains not only its enzymatic activity but also the biologically unique $S=3/2$ EPR signal characteristic of semi-reduced MoFe protein. Isolated FeMoco also exhibits an $S=3/2$ EPR signal similar in g value to MoFe protein but it has a considerably broadened lineshape (see Figure 6).

(2) Certain mutant strains, those having a defective *nifV* gene, produce an altered form of FeMoco (Hawkes *et al.*, 1984). MoFe protein from such mutants exhibits dramatic changes in its substrate-reduction properties. When FeMoco prepared from the *nifV*$^-$ mutant is used to reconstitute a FeMoco-deficient, inactive MoFe protein, the newly reconstituted MoFe protein exhibits the catalytic properties of the MoFe protein isolated from the *nifV*$^-$ mutant strain. Thus, the altered catalytic properties of the *nifV*$^-$ mutant are the consequence of a defective FeMoco. The *nifV* gene product is involved with the synthesis of homocitrate (Hoover *et al.*,

1987; 1989). The *nifV*⁻ mutant produces an altered FeMoco which has citrate replacing homocitrate as the organic constituent (Liang *et al.*, 1990).
(3) Altered MoFe proteins from mutant strains, each having a single substitution for a certain amino-acid residue targeted as either providing or being located near FeMoco-binding sites, simultaneously exhibit altered substrate-reduction properties and changed EPR spectra (Scott *et al.*, 1990).

Furthermore, FeMoco accumulates on a protein in bacterial strains completely lacking the MoFe protein (Shah *et al.*, 1984; Ulgalde *et al.*, 1984), suggesting that intermediates in FeMoco biosynthesis are likely bound to FeMoco biosynthetic enzymes. In support of this concept, no such accumulation occurs in *nifB*⁻, *nifE*⁻ or *nifN*⁻ mutant strains. Also, the sequencing of the *nifEN* genes revealed considerable identity of their putative products when compared to the α- and ß-subunits of the MoFe protein, respectively, suggesting that the *nifEN* products form a template on which FeMoco is built before insertion into the MoFe protein (Brigle *et al.*, 1987). Support for this idea was obtained through purification of a tetrameric *NifEN* protein complex (Paustian *et al.*, 1989).

1.3 The Genetic Organization of *nif* Genes

Because of its genetic amenability to using the classical bacterial genetic manipulations developed for *E. coli*, the facultative anaerobe *K. pneumoniae* was used in early work of identifying genes that are involved in N_2 fixation. There are a total of 20 *nif*-specific genes found in *K. pneumoniae*, whose nucleotide sequences are available: *nifJ, nifH, nifD, nifK, nifT, nifY, nifE, nifN, nifX, nifU, nifS, nifV, nifW, nifZ, nifM, nifF, nifL, nifA, nifB,* and *nifQ*. As shown in Figure 7, these 20 genes are organized into eight transcriptional units. At least two of the transcriptional units, those contained within the *nifUSVWZM* and *nifM* gene clusters, appear to overlap. A diagram of the physical organizations of *nif* and *nif-*

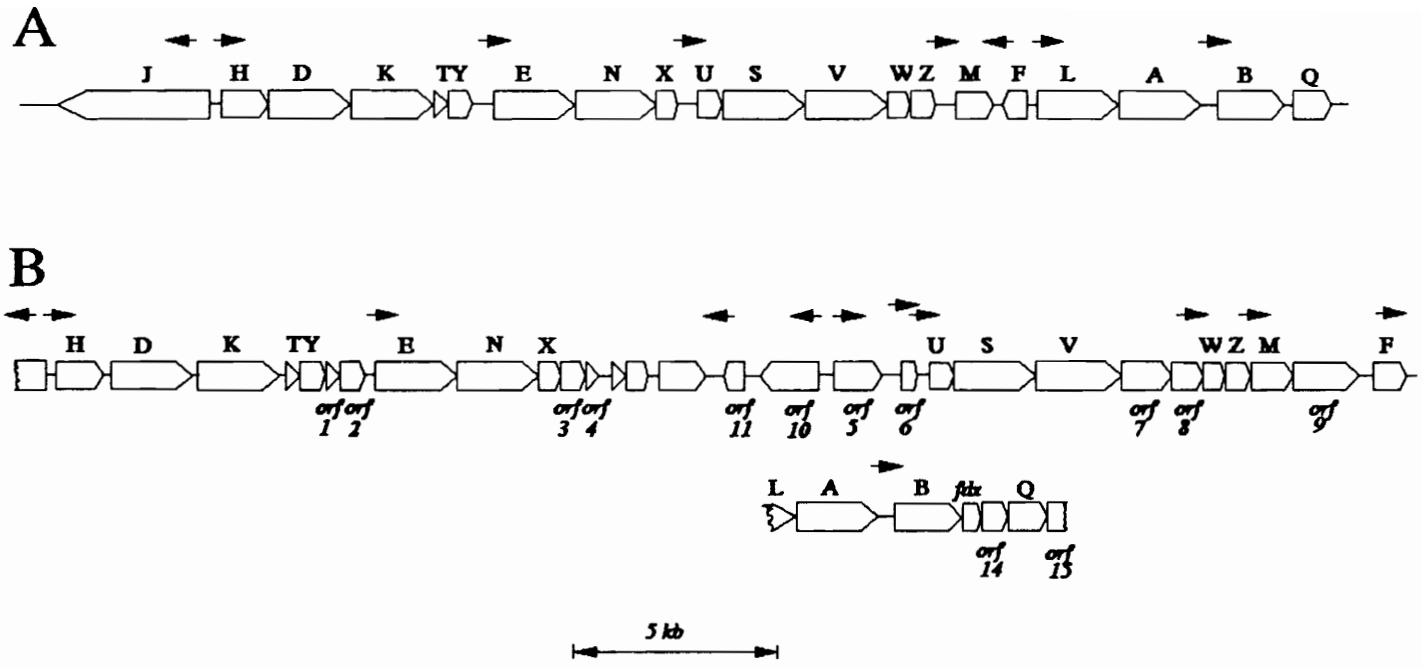

Figure 7. Comparison of the physical organizations of *nif* genes from (A) *K. pneumoniae* and (B) *A. vinelandii* (Adapted from Dean and Jacobson, 1992).

associated genes from both *K. pneumoniae* and *A. vinelandii* is shown in Figure 7. In *Azotobacter vinelandii*, *nifJ* has not been identified, resulting only 19 of 20 *K. pneumoniae*-like *nif* genes. There are, however, about a dozen more open reading frames scattered within the *Azotobacter nif* cluster whose functions are not clear (designated as *orf1* and so on, refer to Figure 7 for details). It has been found that *nifJ* is required for nitrogen fixation in *Klebsiella pneumoniae*. Because it is absent in *Azotobacter vinelandii*, there must be another *nif* gene product that serves as part of the *in vivo* electron donor system to the *Azotobacter* nitrogenase. However, one of the likely candidates, *nifF*, is found to be unnecessary for nitrogenase activities in *Azotobacter vinelandii* (Martin *et al.*, 1989).

Various aspects of the structure and function of *nif*-specific genes as revealed by DNA sequence analysis and biochemical studies are briefly summarized in Table 1 (for a recent review, refer to Dean & Jacobson, 1992; Dean *et al.*, 1993).

1.4 Site-directed Mutagenesis Studies

1.4.1 Effect of Amino Acid Substitutions in the P Cluster Environment

A detailed study of individually substituting Ser for α-62-Cys, α-154-Cys, β-70-Cys, and β-95-Cys residues of *A. vinelandii* MoFe protein, the ligands for the P clusters, revealed that these residues were essential for activity (Dean *et al.*, 1990b). Independent studies using Ala or Ser for the corresponding residues from *Klebsiella pneumoniae* produced mutants displaying the same phenotype (Kent *et al.*, 1989). Further mutagenesis studies involved substituting α-88-Cys with Thr or Asp and these resulted in strains retaining their capability of diazotrophic growth, although at a slower rate (Setterquist, Newton, and Dean, unpublished results). Also, for both *A. vinelandii* and *K. pneumoniae*, substitution of β-153-Cys with Ser does not significantly reduce diazotrophic growth rates (Dean *et al.*,

Table 1. *nif* gene products and their known or proposed functions in *A. vinelandii*

Gene	Product and Known or Proposed Function
nifH	Fe protein subunit, forms homodimer (M_r=63,000), has a single [4Fe-4S] cluster bridged between the two subunits, required for FeMoco biosynthesis
nifD	MoFe protein α-subunit, forms the MoFe protein holoprotein with β-subunit as $\alpha_2\beta_2$ tetramer (M_r=230,000), 2 P clusters and 2 FeMocos
nifK	MoFe protein β-subunit, forms the MoFe protein apoprotein with α-subunit as $\alpha_2\beta_2$ tetramer (M_r=230,000), 2 P clusters and 2 FeMocos
nifF	Flavodoxin, physiological reductant of the Fe protein
nifE	Required for the FeMoco biosynthesis, forms $\alpha_2\beta_2$ tetramer (M_r=210,000) with the *nifN* gene product, exhibits a fair level of sequence identity when compared to the MoFe protein α-subunit
nifN	Required for the FeMoco biosynthesis, forms $\alpha_2\beta_2$ tetramer (M_r=210,000) with the *nifE* gene product, exhibits a fair level of sequence identity when compared to the MoFe protein β-subunit
nifB	Required for the FeMoco biosynthesis
nifQ	Involved in the FeMoco biosynthesis, possibly in forming the $MoFe_3S_3$ in the FeMoco, the *nifQ*⁻ (defective in FeMoco synthesis) can be suppressed by elevated levels of Mo, cysteine or cystine[a]
nifU	Stabilization of the Fe protein, possibly involved in providing Fe for nitrogenase metallocluster synthesis[b]
nifS	L-cysteine desulfurase, involves in donating inorganic sulfide for nitrogenase metallocluster synthesis[b]
nifV	Homocitrate synthase, synthesis of the organic component of FeMoco
nifW	Function not known, might be involved in processing homocitrate[c]
nifZ	Function not known, required for full activity of the MoFe protein, might have a function related to FeMoco formation or insertion[c]
nifM	Required for Fe protein activation[d]
nifA	Positive regulatory element
nifL	Negative regulatory element
nifX	A possible negative regulatory element[e]
nifT	Function not known, not required for diazotrophic growth[e]
nifY	Function not known, not required for diazotrophic growth, possibly involved in stabilizing the conformation of apo-MoFe protein for FeMoco insertion[e]

[a] Ugalde *et al.*, 1985; Joerger & Bishop, 1988..

[b] Jacobson *et al.*, 1989b; Miller & Orme-Johnson, 1992; Zheng *et al.*, 1993.

[c] Jacobson *et al.*, 1989b; Paul & Merrick, 1989.

[d] Howard *et al.*, 1986; Jacobson *et al.*, 1989b; Paul & Merrick, 1989.

[e] Gosink *et al.*, 1990; White *et al.*, 1992; Homer *et al.*, 1993.

1988; Kent *et al.*, 1989). More recently, the altered β-153^{ser} MoFe protein was found to have preserved an intact FeMoco as well as retaining the same component protein interaction as in the wild-type protein. Rather, the result of this substitution is a disruption in electron transfer within the MoFe protein, which further demonstrated a role for this residue and the region at the P clusters (May *et al.*, 1991).

1.4.2 Effect of Amino Acid Substitution around the α-183-Cys Residue of MoFe Protein

As mentioned above in section 1.2.4, based on sequence identity, there is considerable similarity between the FeMoco environment of the MoFe protein α-subunit and its putative site in the *nifE* gene product (Brigle *et al.*, 1987a). Using this identity as a guide (see Figure 8), appropriate substitutions were placed within the MoFe protein α-subunit region involving the conserved α-183-Cys residue. The resulting altered MoFe proteins have been characterized with respect to catalytic and spectroscopic competence in order to understand the role of this part of the FeMoco's polypeptide environment (reviewed by Newton and Dean, 1993).

Two such mutant strains in which one or the other of α-191-Gln and α-195-His in the MoFe protein α-subunit were replaced by lysine and asparagine residues, respectively, were constructed based on the occurrence of these residues at the corresponding position in the *nifE* gene product. Both strains lost their diazotrophic growth capability and so indicated the importance of the region in which these two residues are located in FeMoco binding (Scott *et al.*, 1990; Scott *et al.*, 1992).

Upon substitution of α-191-Gln with lysine, the altered MoFe protein from the Nif$^-$ mutant strain was able to reduce acetylene not only to ethylene but also ethane, a characteristic previously thought to be unique to the V-nitrogenase

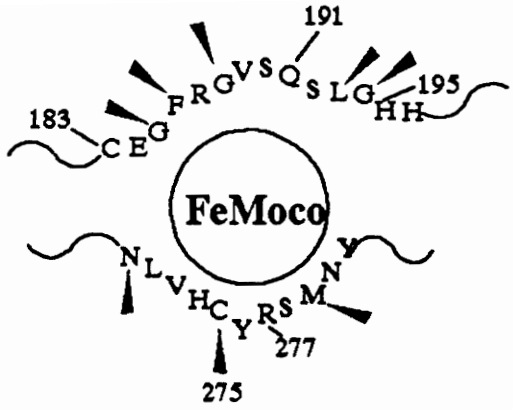

MoFe Protein α-subunit

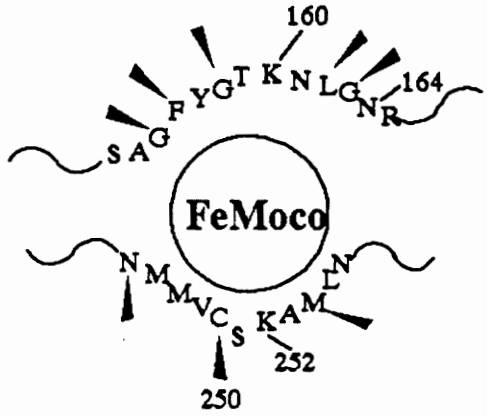

nifE Product

Figure 8. Schematic representation of FeMoco binding within the proposed α-subunit (α-183-Cys and α-275-Cys region) and the corresponding region in the *nifE* gene product which is proposed for FeMoco biosynthesis (Adapted from Dean and Jacobson, 1992). Arrow heads indicate the conserved residues within the corresponding area of both *nifE* gene product and the MoFe protein α-subunit. Numbers indicate the residues of particular interest.

system (Dilworth *et al.*, 1987). However, ethane formation by the altered Mo-nitrogenase occurs by a different mechanism. Furthermore, the altered MoFe protein also exhibited CO sensitivity of its H_2 evolution activity, which was observed in the *nifV*⁻ nitrogenase but not wild type (McLean *et al.*, 1983), and was interpreted to indicate that α-191-Gln might well interact with the homocitrate moiety of FeMoco. This change in catalytic properties was accompanied by a changed $S = 3/2$ EPR signal, which is a signature of FeMoco. Therefore, because both changes occurred with a single amino-acid substitution, this is strong evidence that FeMoco is involved in substrate binding. The mutant strain resulting from substitution of α-195-His by Asn was also able to reduce acetylene to both ethylene and ethane and exhibited an altered EPR spectrum.

The crystallographic structure confirmed that α-195-His and α-191-Gln are within 4 Å of Fe2 and Fe6, respectively, of FeMoco. The side chain of α-191-Gln interacts with one of the carboxyl groups of homocitrate and α-191-Gln is hydrogen bonded to a central S that bridges FeMoco's two sub-clusters (Figure 5).

More recent work has shown that the altered α-195^{Gln} MoFe protein can bind, but not reduce N_2 (Kim *et al.*, 1994). The binding of N_2 is indicated by its ability to inhibit effectively both H^+ and C_2H_2-reduction activities. The binding of N_2 in the altered α-195^{Gln} MoFe protein was inhibited by the addition of H_2 or D_2. Under a N_2/D_2 atmosphere, the α-195^{Gln} MoFe protein produces HD (Kim, Newton and Dean, unpublished data) as had been found previously for wild type (Hoch *et al.*, 1960; Newton *et al.*, 1977; Burgess *et al.*, 1981; Guth & Burris, 1983). This last observation indicates that binding of N_2 at the active site of the altered MoFe protein is necessary, but its reduction is not required, for the formation of HD. The altered α-195^{Gln} MoFe protein exhibited hypersensitivity to CO inhibition of both acetylene reduction and nitrogen binding which suggests that the imidazole group of the α-195-His residue might be involved in protecting an

Fe atom on the FeMoco from attack by CO (Kim *et al.*, 1994).

Previous work using the ESEEM spectroscopy technique, which is a pulsed version of the EPR experiment designed to probe the immediate environment of the FeMoco paramagnetic center, first identified an N-modulation of the $S = 3/2$ EPR signal of the wild-type MoFe protein from *Clostridium pasteurianum* nitrogenase (Thomann *et al.*, 1987). This N-modulation of the signal was assigned to the nitrogen atom of a ligand to the FeMoco, most likely from a histidine residue, because the N-modulation was not observable in isolated FeMoco. This hypothesis was further explored by using whole cells of a series *Azotobacter vinelandii* mutant strains in which various conserved histidine residues were individually substituted by a variety of other residues (Thomann *et al.*, 1991). The results of these experiments indicated that only substitution at the α-195-His residue (in this case, by Asn) caused the disappearance of the N-modulation of the signal. Other mutants with substitutions at residues α-83-His, α-196-His, α-274-His or β-90-His showed no change in the signal. This result led to the conclusion that α-195-His was required for, but not necessarily responsible for, providing the proposed N-ligand to the FeMoco. Further, because only the α-195-His-substituted mutant was Nif$^-$, this N-coordination was proposed to be essential for nitrogen fixation. Structural studies revealed that the α-195-His does not provide a direct N-ligand to the FeMoco, but is hydrogen-bonded to a central sulfide, thus the N-modulation arises elsewhere. This work was later complemented by another ESEEM probe (DeRose *et al.*, 1994) in which altered MoFe proteins from mutant strains α-195^{asn} and α-195^{gln} were used. In contrast to the α-195^{asn} MoFe protein, the α-195^{his} MoFe protein inhibited the N-modulation and was able to bind, though not reduce N_2. Thus, the N-modulation was proposed as a signature for N_2 binding and as an indicator that the hydrogen bond to sulfide was retained by the glutamine.

1.4.3 Effect of Amino Acid Substitutions around α-275-Cys Residue of MoFe Protein

Shortly after the original extrusion protocol for releasing FeMoco from the MoFe protein was reported (Shah & Brill, 1977), it became clear that isolated FeMoco was reactive to a variety of chemical reagents, including thiols, EDTA, *o*-phenanthroline, α,α'-bipyridyl and CN^- (Rawlings *et al.*, 1978; Burgess *et al.*, 1980; Yang *et al.*, 1982; Smith *et al.*, 1985). A 1:1 binding stoichiometry of phenylthiol to the isolated FeMoco (Burgess *et al.*, 1980) indicated that FeMoco is bound to its polypeptide matrix by only one cysteinyl residue (Brigle *et al.*, 1985). Using nuclear magnetic resonance (Masharak *et al.*, 1982) and x-ray absorption spectroscopy (Newton *et al.*, 1985) on isolated FeMoco, the site of thiol binding was clearly shown to be on Fe and not at the unique Mo. The most likely candidate cysteinyl for the binding of FeMoco to the polypeptide was suggested to be the strictly conserved α-275-Cys residue because: (1) it is surrounded by a concentration of conserved residues with amide functions, unmatched elsewhere in the primary sequence, which might be simulated by NMF; and (2) α-subunit Cys residues 62, 88 and 154 and β-subunit Cys residues 70, 95 and 153 appeared more likely to be P cluster ligands (Brigle *et al.*, 1985; Brigle *et al.*, 1987).

This early prediction was supported by biochemical-genetic evidence. An important experiment concerning the possibility that the MoFe protein α-Cys-275 provides an essential thiol ligand to FeMoco was the finding that its substitution by Ala in *K. pneumoniae* dramatically increased the pool of accessible FeMoco in crude extracts of the mutant strain (Kent *et al.*, 1989). This was shown by mixing extracts of the $\alpha\text{-}275^{ala}$ mutant strain with an extract of a *nifB*$^-$ mutant (*nifB*$^-$ mutants accumulate an inactive apo-MoFe protein devoid of FeMoco) to reconstitute more active nitrogenase than with extracts of other mutant strains. Also, the elevated pool of the FeMoco in these extracts was detected by EPR

spectroscopy with broadened EPR signal which indicated the existence of free FeMoco in the mutant extract. The simplest interpretation of these results is that, in the absence of the proposed thiol ligand (α-275-Cys), FeMoco is only loosely associated with the altered MoFe protein and is, thus, available for reconstitution of wild-type apo-MoFe protein. Support for this hypothesis comes from the observation that the $\alpha 275^{ala}$ MoFe protein exhibits a native electrophoretic mobility characteristic of apo-MoFe protein (Kent *et al.*, 1990). Based on fluorine-19 chemical shifts, used as a probe of the reactivity of isolated FeMoco, it was further suggest that, if α-275-Cys does provide a thiol ligand to FeMoco, formation and breaking of such a linkage could be in dynamic equilibrium and related to substrate binding or reduction (Conradson *et al.*, 1988). The recent x-ray crystallographic structure of MoFe protein proves that α-275-Cys is indeed a mercaptide ligand to FeMoco by direct ligation to Fe1 (Figure 5, Kim *et al*, 1992a).

A second mutagenesis-based study of the involvement of α-275-Cys in FeMoco binding is based on the assumption that the differences in the catalytic and spectroscopic properties of MoFe proteins from different organisms may arise from the different constraints placed on their FeMoco by variations in their respective polypeptide matrixes (Dean *et al.*, 1990a). Both *A. vinelandii* and *C. pasteurianum* MoFe protein have an identical FeMoco as shown by reconstitution (Shah & Brill, 1977) and the x-ray crystal structure (Kim & Rees, 1992a; Kim *et al.*, 1993). A reported spectroscopic difference (Morgan, *et al*, 1988) was the temperature relaxation patterns for the S=3/2 EPR signal from MoFe protein isolated from *Clostridium pasteurianum* when compared to MoFe protein isolated from *Azotobacter vinelandii*. If such spectroscopic differences arose from the different FeMoco polypeptide environment in these proteins, differences in their primary sequence within FeMoco-binding domains should be observable. As a

matter of fact, a comparison of primary sequence around the α-275-Cys residue of the *Clostridium pasteurianum* and *Azotobacter vinelandii* MoFe proteins does reveal significant differences in primary sequence. Of particular interest are the residues immediately flanking α-275-Cys, which is directly ligated to the FeMoco, as shown below.

	275
	↓
A. vinelandii	-NLVHCYRSMNY-
C. pasteurianum	-NLVQCHRS I NY-

The *Azotobacter vinelandii* sequence around α-275-Cys, His-Cys-Tyr, is replaced with the sequence Gln-Cys-His in *Clostridium pasteurianum*. Thus, it was reasoned that, because α-275-Cys is a direct ligand to FeMoco, the position of a histidine residue on the opposite sides of the cysteine ligand in the two MoFe proteins may place different constraints upon FeMoco's environment. To examine this possibility, this portion of the *A. vinelandii* sequence was replaced with the corresponding *Clostridium pasteurianum* sequence.

Substitution by Gln for α-274-His and His for α-276-Tyr together does not have any significant effect on its diazotrophic growth capability of the mutant strain. Thus, FeMoco's functional environment has not been compromised in the resulting mutant strain (DJ386). This result is consistent with the observation that both *A. vinelandii* and *C. pasteurianum* MoFe proteins are functionally equivalent with respect to catalysis. However, the FeMoco environment within the MoFe protein from DJ386 is clearly altered because a significant change in EPR spectrum of the MoFe protein from DJ386 was observed (for details, see Chapter 4). Although the x-ray crystal structure shows that these two residues do not interact directly with FeMoco, these results and related studies (Kent *et al.*, 1989) indicated that these residues could be involved in maintaining a polypeptide pocket in the proper orientation for the binding of the FeMoco.

This dissertation research concerns the functions of three residues: α-274-His, α-276-Tyr and α-277-Arg that are located in the vicinity of the essential α-275-Cys residue. Figure 9 is a schematic representation of their orientation relative both to FeMoco and to other catalytically or structurally critical residues around FeMoco.

1.5 Complex Formation between the Nitrogenase Component Proteins and P Cluster Function

Nitrogenase isolated from *K. pneumoniae* (Smith *et al.*, 1973; Thorneley, 1975), *A. vinelandii* (Orme-Johnson *et al.*, 1972; Hageman *et al.*, 1980) and *C. pasteuranium* (Zumft *et al.*, 1974) were used to define the direction of electron flow through nitrogenase and to demonstrate that one electron is transferred from the Fe protein to the MoFe protein where substrate reductions take place.

It is known that complex formation between the component proteins is essential for nitrogenase turnover (Hageman & Burris, 1978; Thorneley & Lowe, 1983) and that higher salt concentrations have an inhibitory effect on enzyme activity (Deits & Howard, 1983; Burns *et al.*, 1985; Wolle *et al.*, 1992). As mentioned in section 1.2.1, ADP-ribosylation of the Arg-100 residue blocked the binding of Fe protein to the MoFe protein (Pope *et al.*, 1985; Murrell *et al.*, 1988). Together with the site-directed mutagenesis (Lowery *et al.*, 1989) and the post translational modification studies of ADP-ribosylation of Arg-100, plus the chemical crosslinking that occurs between Glu-112 on the Fe protein and the β-300-Lys on the MoFe protein (Willing *et al.*, 1989; Willing & Howard, 1990), these results support the idea that ionic interactions contribute to the formation of the active complex. Specifically, the three-dimensional structure (Georgiadis *et al.*, 1992) shows that Glu-112 and Arg-100 are located within two patches of

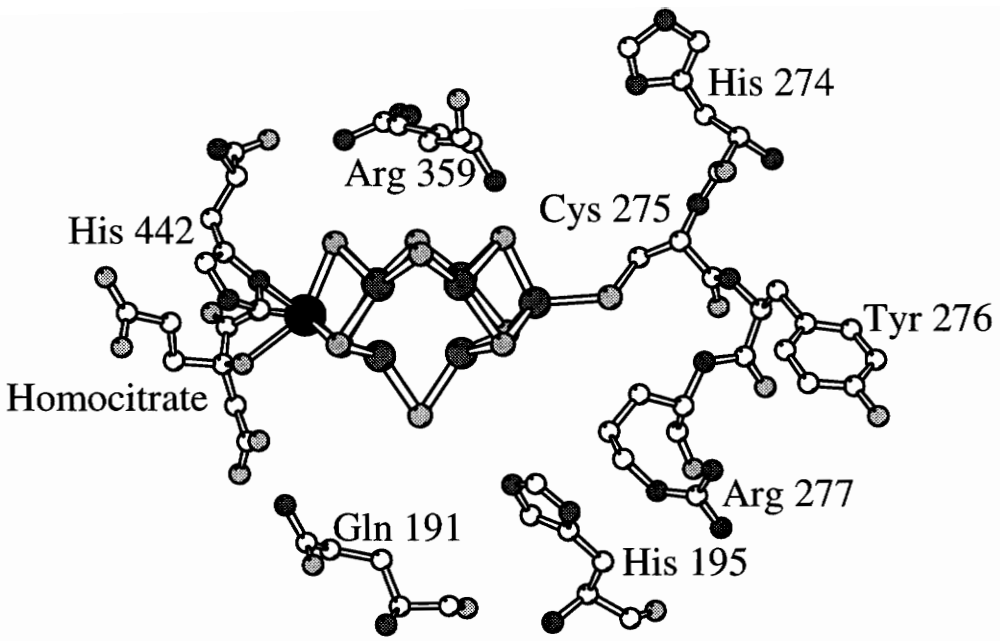

Figure 9. Structural relationship of the α-274-His, α-276-Tyr and α-277-Arg and other residues around the FeMoco. This graph was generated using the program MOLSCRIPT (Kraulis, 1991) and data kindly provided by Dr. Jeff Bolin at Purdue University.

significant ionic character, which are on the same surface as the 4Fe:4S cluster on the Fe protein and so could be involved in ensuring the closest possible approach of this cluster to the MoFe protein.

The minimum requirements for formation and turnover of a kinetically competent complex must include the following conditions. Intimate and precise orientation of the two nitrogenase components should precede electron transfer. Some differences must exist in component protein complexes before and after the electron transfer from Fe protein to the MoFe protein to ensure appropriate alignment and unidirectional electron transfer. In the complex, there could be some signal sent from the MoFe protein to the Fe protein nucleotide site and, during the transition between the ATP-bound and ADP-bound states, the protein components must undergo conformational changes that lead to the correct alignment of the respective electron donor and acceptor pair. On the other hand, binding of Fe protein could induce the necessary conformational changes in MoFe protein to allow electron transfer from the P cluster pair to the FeMoco. Thus, both component proteins are likely to undergo some conformation changes during electron transfer within the complex. After electron transfer to the MoFe protein, the complex must relax sufficiently so that electron transfer back to the oxidized Fe protein is rare. The overall reaction leads to the reduction of FoMoco and the oxidation of the Fe protein 4Fe:4S cluster by one electron each, while the P-cluster pair remains in the same oxidation state at the beginning and the end of the redox cycle (reviewed by Howard & Rees, 1994).

As mentioned above, it seems likely that the ionic interactions contribute to the component protein complex, and the complex-formation sites are on the same surface as the cluster (Howard & Rees, 1994 and the references therein). Besides the ionic interaction, there are potentially important hydrophobic interactions between the component proteins. β-125-Phe residue is in a highly conserved

region in the MoFe protein between β-95-Cys and β-154-Cys, which are shown to be P-cluster ligands. It was shown to be located on or close to the surface of the *K. pneumoniae* MoFe protein first by a single cleavage site at this residue using chymotrypsin and second by the three-dimensional crystal structure. Further, site-directed mutagenesis at this position subsequently showed its involvement in MgATP-dependent electron transfer from the Fe protein (Fisher, *et al.*, 1993). Computer-based protein docking studies indicate both α-125-Phe and β-125-Phe residues can interact with the hydrophobic residues 102-109 that are part of the two surface helices on the Fe protein. Figure 10 is a α-carbon backbone diagram of both MoFe protein and Fe protein in which, at van der Waal's contact, the Fe-protein cluster and the P cluster are separated by >16 Å.

During the component protein complex formation, an electron is being transferred from the Fe protein 4Fe:4S cluster through P cluster to the FeMoco of the MoFe protein, where substrates are reduced. In order to address the question of a possible role of the P-cluster in the nitrogen-reduction reaction, stopped-flow spectrophotometric studies as well as the EPR data on turnover samples were used in the successful simulation of the sequential reduction of the MoFe protein from state E_0 through E_1 and E_2 to the N_2 binding states E_3 and E_4 (for detailed descriptions, refer to the following section 1.6.2). The conclusion, reached from these studies was that oxidation of the P clusters occurs and is required to increase the electron density at, and so irreversibly bind N_2 to, FeMoco. This oxidation is proposed to be a crucial step in the catalytic cycle of nitrogenase that irreversibly couples electron transfer to the protonation of bound N_2 (Lowe *et al.*, 1993).

1.6 The Lowe/Thorneley Kinetic Model of Nitrogenase

Nitrogenase is one of the slowest enzymes present in bacteria and it has a turnover time of approximately 1.5 s at 23°C for the reduction of dinitrogen to

Figure 10. α-carbon backbone diagram of both MoFe and Fe protein from *A. vinelandii* nitrogenase. The graph was generated using the program MOLSCRIPT (Kraulis, 1991) and data kindly provided by Dr. Jeff Bolin at Purdue University.

ammonia and the concomitant evolution of one equivalent of dihydrogen. Its slowness is compensated by its relative abundance which constitutes up to 10% of the total soluble protein of free-living diazotrophs. The long turnover time has made it possible to study partial reactions and the pre-steady state phase of the functioning enzyme using kinetic techniques, such as, stopped-flow spectrophotometry, rapid freeze EPR measurements and rapid chemical quench with product analysis, and so on (Thorneley & Lowe, 1983; Gutteridge *et al.*, 1978).

Hageman and Burris first proposed that only one electron-transfer event occurs before dissociation of the Fe-protein/MoFe-protein complex. The Lowe/Thorneley model was derived from a pre-steady-state kinetic study of *K. pneumoniae* nitrogenase activity at 23°C, pH 7.4 (Lowe & Thorneley, 1984a,b; Thorneley & Lowe, 1984a,b). This model was developed in terms of two main processes, the Fe protein cycle and the MoFe protein cycle.

1.6.1 The Fe-protein Oxidation-reduction Cycle

The Fe-protein cycle is a redox cycle during which one electron is transferred from the Fe-protein to the MoFe-protein in a series of reactions that involves the hydrolysis of MgATP. It can be represented by the partial reactions shown in Figure 11. These partial reactions are discussed in detail below.

1. Reduced Fe protein and MoFe protein complex formation (k_1) and dissociation (k_{-1})

Before electron transfer from the Fe-protein to the MoFe-protein can occur, the protein complex is formed. Evidence for formation of such a protein complex is provided by an extensive series of kinetic studies (Thorneley *et al.*, 1975; Hageman & Burris, 1980; Thorneley & Lowe, 1984a, b; Lowe & Thorneley, 1984a, b). Using *Klebsiella pneumoniae* nitrogenase and monitoring the MgATP-

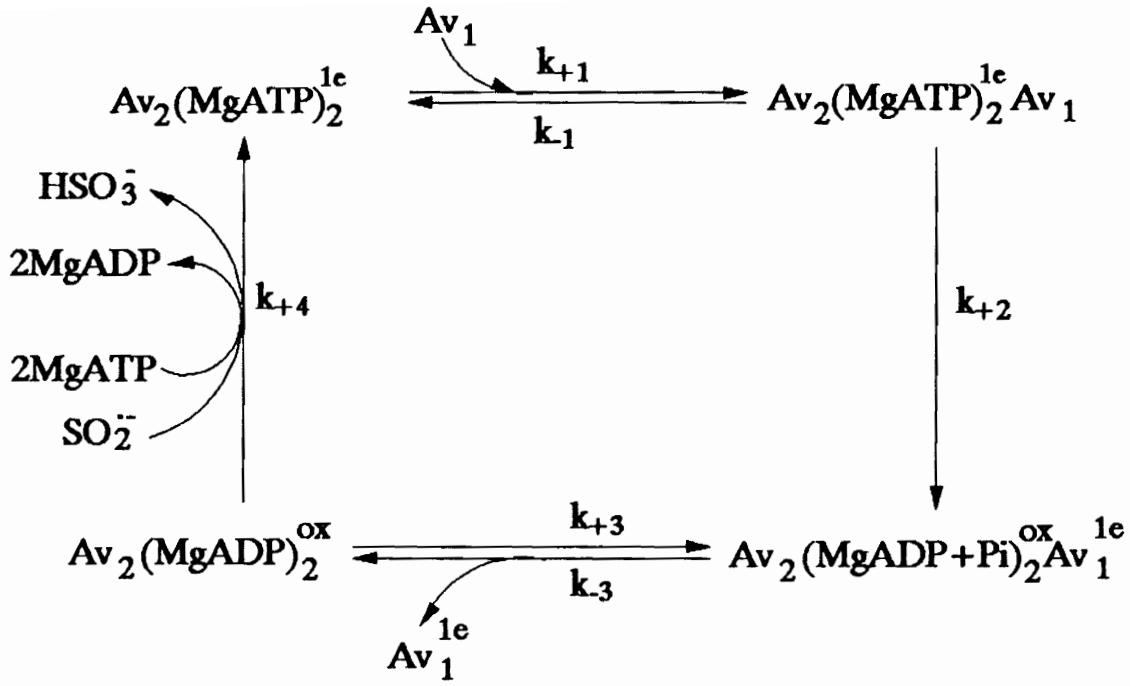

Figure 11. Oxidation-reduction cycle for the Fe protein from *A. vinelandii* (Adapted from Thorneley & Lowe, 1985). In the diagram, Av_1 represents the MoFe protein from *A. vinelandii* and Av_2 represents the Fe protein.

induced electron transfer from Fe protein to MoFe protein as a function of the component protein concentrations at 23°C using stopped-flow spectrophotometry, k_1 was estimated to have a lower limit of 5×10^7 $M^{-1}s^{-1}$ (Lowe and Thorneley, 1984b), which is close to the diffusion limit. A high value of k_1 was proposed to increase the efficiency of nitrogenase for N_2 reduction relative to H_2 evolution, particularly under conditions of low electron flux (Thorneley and Lowe, 1985). k_{-1} was estimated to be $15s^{-1}$ assuming the association-dissociation rates of the nitrogenase protein complex are independent of the MoFe protein oxidation level (Thorneley and Lowe, 1985).

2. Electron transfer from Fe-protein to MoFe-protein coupled to MgATP hydrolysis (k_2)

Stopped-flow experiments with spectrophotometric monitoring at 420 or 430 nm of the absorbance change in the Fe protein that occurs on its oxidation as it transfers one electron to the MoFe protein, have accurately measured the rate constant for electron transfer and its dependence on MgATP and MgADP concentrations. k_2 has been measured as 320 s^{-1} at 30°C (pH 7.4) (Hageman *et al.*, 1980) for *A. vinelandii* Fe protein, and 200 s^{-1} at 23°C, and 24 s^{-1} at 10°C for *K. pneumoniae* Fe protein (both at pH 7.4) (Thorneley, 1975; Eady *et al.*, 1978). The coupling of the hydrolysis of two molecules of MgATP with each electron transfer between the complexed proteins has been studied by a number of investigators. Early work suggested that MgATP hydrolysis and electron transfer occurred simultaneously (Eady *et al.*, 1973). Stopped-flow calorimetry at 5°C suggested that ATP hydrolysis precedes electron transfer (Thorneley, 1989). And stopped-flow spectrophotometry studies at 20°C indicates that protons (detected by a pH-sensitive dye) are released slower than, and therefore, after electron transfer (Mensink *et al.*, 1992). Probably the 20°C data better reflect the actual physiological situation.

3. The dissociation of oxidized Fe-protein from reduced-MoFe protein (k_{-3}): the rate-limiting step in the catalytic cycle for substrate reduction

Thorneley and Lowe (1983) used stopped-flow spectrophotometry and EPR spectroscopy to study the kinetics of the reduction by dithionite of oxidized Fe-protein in the presence of MgADP. The inhibition of the reaction by MoFe protein enabled the rate constant to be determined ($k_{-3} = 6.4 \pm 0.8\ s^{-1}$) for the *K. pneumoniae* system at 23°C and pH 7.4. Thus, the dissociation of oxidized Fe-protein from the MoFe-protein is the rate limiting step in the catalytic cycle of nitrogenase. k_3 was determined to be $4.4 \times 10^6\ M^{-1}s$ for *K. pneumoniae* nitrogenase and it was proposed to be responsible for inhibition of catalytic activity at high protein concentration (Thorneley & Lowe, 1983).

4. Reduction of oxidized Fe protein by $SO_2^{\bullet-}$ (k_4)

The reduction of oxidized *K. pneumoniae* (Lowe & Thorneley, 1983) and *A. chroococcum* (Thorneley *et al.*, 1976) Fe protein, for example in the form of $(Kp_2)_{ox}(MgADP)_2$ (Kp_2 represents Fe protein from *K. pneumoniae*, $(Kp_2)_{ox}$ represents the oxidized state of the Fe protein) by $SO_2^{\bullet-}$ can be described by a single exponential ($k_{obs} = 10.3\ s^{-1}$ with 10 mM $Na_2S_2O_4$). A linear dependence of k_{obs} on $[S_2O_4^{2-}]^{1/2}$ confirms that $SO_2^{\bullet-}$, from the pre-dissociation of $S_2O_4^{2-} \rightleftarrows SO_2^{\bullet-}$, is the active reductant, and a value of $k_4 = 3 \times 10^6\ M^{-1}s^{-1}$ was obtained at 23°C. Uncomplexed by MgATP, $(Kp_2)_{ox}$ is reduced approximately 30 times faster than $(Kp_2)_{ox}(MgADP)_2$ at 23°C ($k > 10^8\ M^{-1}s^{-1}$) (Thorneley *et al.*, 1976). It is likely that MgADP induces a conformation change in Kp2 that results in slow electron transfer from $SO_2^{\bullet-}$ to the 4Fe-4S cluster (Ashby and Thorneley, 1987). Thus, the limiting conformation change or release of MgADP was suggested to happen before Fe protein's rapid reduction by $SO_2^{\bullet-}$ (Thorneley & Lowe, 1983).

1.6.2 The MoFe-protein Cycle

After the completion of one Fe-protein cycle, one electron is transferred from the Fe protein to the MoFe protein. Because the reduction of dinitrogen to ammonia is an eight-electron process, the Fe-protein cycle has to operate eight times to give the MoFe protein reduction cycle (Figure 12). During this cycle, the MoFe-protein is progressively reduced, binds and reduces substrates, and finally returns to its highest oxidation state, E_0. Because each Fe protein cycle is a single-electron transfer, the MoFe protein cycle is simplified by considering an $\alpha\beta$ dimer and its associated one FeMoco, rather than the complete $\alpha_2\beta_2$ tetramer which apparently operates as a dimer of dimers. Therefore, in the MoFe protein cycle the species E_n represents one of two independently functioning halves of the tetrameric MoFe protein; and n refers to the number of times MoFe protein completes the Fe-protein cycle. Designating structures such as E_2H_2 is not intended to imply the exact level of protonation of a metal site nor the existence of specific metallo-hydride intermediates. The initial E_0 state is that of MoFe protein isolated in the presence of dithionite ion. The three reactions represented by the arrows linking E_n with E_{n+1} are reactions (1), (2) and (3), respectively, of the Fe protein cycle shown in Figure 11.

The scheme was devised to explain the lag and burst phases of product appearance during substrate reduction and the slowness of the overall process. By monitoring the time courses of product appearance and from the determination of the rate constants of the individual reactions, the following conclusions were reached.

(1) The rate-limiting step was the protein-protein dissociation of the complex $(Av_2)_{ox}(MgADP)_2(Av_1)_{red}$ rather than ATP hydrolysis, electron transfer, or substrate reduction.

(2) Only free MoFe protein could bind substrates and release products.

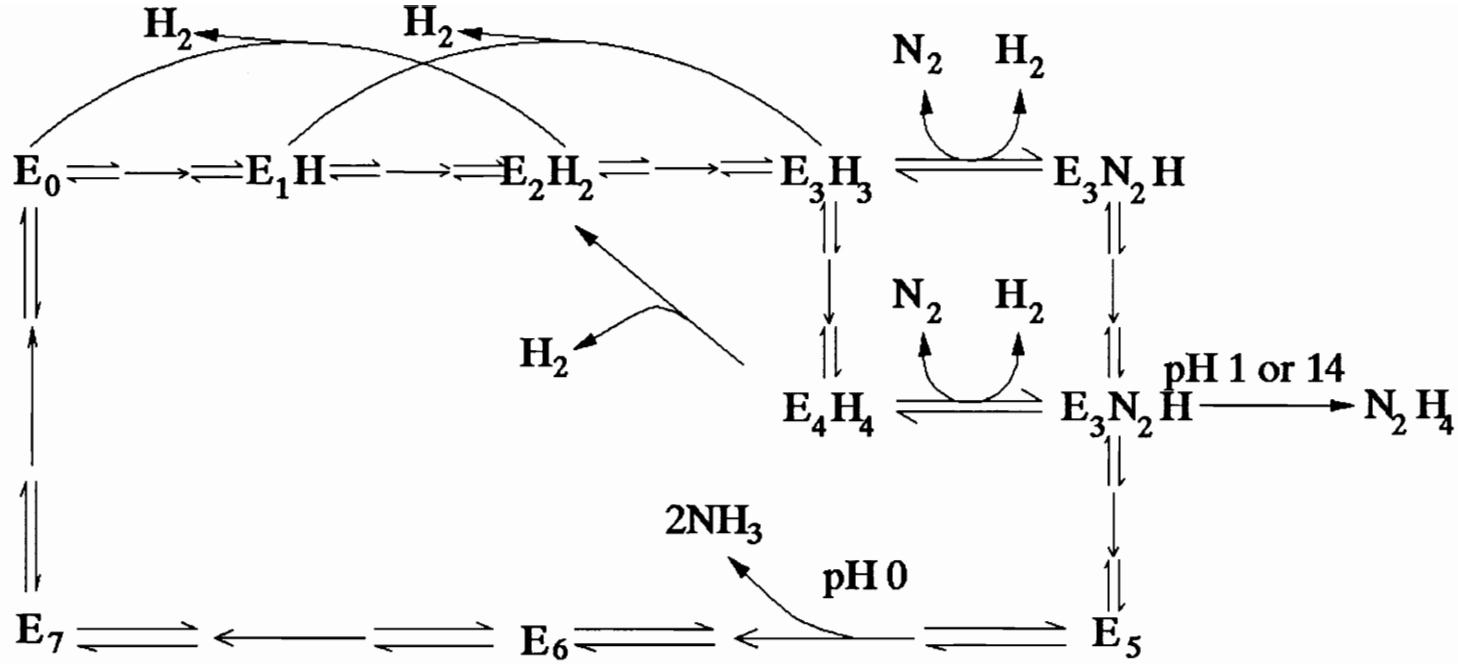

Figure 12. MoFe-protein cycle. E_n represents Av_1 ($\alpha\beta$ dimer of the MoFe protein), and n refers to the number of times Av_1 completes the Fe protein cycle, which is indicated by the three arrow reactions linking the E_n and E_{n+1}.

(3) N_2 is bound to a more reduced form of MoFe protein (probably E_3) than that which could release H_2 (E_2). Its reduction intermediate, the hydrazido (2-) group ($=N\text{-}NH_2$), is probably bound to oxidation state E_4, which releases hydrazine on quenching with acid or alkali. NH_3 may be released at oxidation state E_5.
(4) Competition between H_2 evolution and the binding of reduced Fe protein to MoFe protein determines the distribution of electrons into N_2 reduction and H_2 evolution.
(5) If the electron flux is low, then oxidation state E_2H_2 will lose H_2 and revert to state E_0. However, because nitrogenase is a slow enzyme, the rate-limiting step being the dissociation of component proteins, its high concentration in the cell helps to suppress H_2 evolution and maximize its N_2-reduction activity.

It has been proposed that acetylene binds to the E_1 and E_2 states and ethylene is released from the E_3 state in the MoFe-protein cycle (Ashby *et al.*, 1987; Fisher *et al.*, 1990). In more recent studies, by using both stopped-flow spectrophotometric and EPR methods, it was found that H_2 can be evolved from E_2, E_3 and E_4 independently from N_2 binding, because the spectrum associated with the E_4 state in the MoFe-protein cycle can only be observed in nitrogenase under either an Ar or N_2 atmosphere, and not under a C_2H_2 atmosphere (Lowe *et al.*, 1993).

1.7 Substrate Reactions of Nitrogenase

1.7.1 General Requirements for Nitrogenase

Mo-nitrogenases reduce N_2 to ammonia with the concomitant production of H_2, in the presence of MgATP, an electron source and anaerobic conditions. In the absence of an added reducible substrate, nitrogenase catalyzes an MgATP-dependent H_2-evolution reaction (Bulen *et al.*, 1965) because nitrogenase reactions are run in aqueous solution and H^+ is always available to the enzyme. Apart from

N_2 and the proton, a number of alternative substrates have been discovered.

Nitrogenase turnover requires the hydrolysis of MgATP to MgADP and inorganic phosphate (Mortenson *et al.*, 1964). Because of the inhibition effect of MgADP on nitrogenase catalysis (Moustafa & Mortenson, 1967), an ATP-generating system was developed for use with nitrogenase to avoid ADP accumulation and this system consists of creatine phosphate, creatine phosphokinase, $MgCl_2$ and ATP (Bulen & LeComte, 1966). Nitrogenase *in vitro* assays are usually carried out in small anaerobic vials containing the ATP-regenerating system as described above, MoFe protein, Fe protein, dithionite, buffer and added substrates. It is known that both pH and temperature can affect nitrogenase reactivity. Ionic strength may be an important factor in substrate studies because nitrogenase activity exhibits salt inhibition (Burns *et al.*, 1985).

When $S_2O_4^{2-}$ is added to a nitrogenase assay system it disproportionates to $2SO_2^{\bullet-}$ and on reducing nitrogenase becomes oxidized

$$SO_2^{\bullet-} + H_2O \rightarrow HSO_3^- + H^+ + e^-$$

with the Fe protein serving as the electron acceptor (Mortenson & Thorneley 1979). During nitrogenase turnover, the rate of MgATP hydrolysis to MgADP and inorganic phosphate (Mortenson *et al.*, 1964) is often expressed as ATP/$2e^-$ ratio which represents the number of ATPs hydrolyzed per electron pair used by nitrogenase to reduce substrate. Although for many nitrogenase reactions this ratio is constant at 4 ATP/$2e^-$ (Winter & Burris, 1968; Kennedy *et al.*, 1968), this value does not hold true for all reactions and, thus, the rate of MgATP hydrolysis is not necessarily a measure of the rate of electron flow.

1.7.2 MgATP and Reductant

The reaction between N_2 and H_2 to form NH_3 is exergonic and therefore should proceed spontaneously. However, the reaction is restricted kinetically

because of the high activation energy of the N_2 molecule. Industrially, the reaction is accelerated by a metal catalyst, high temperature and pressure. Biologically, the catalyzed reduction of N_2 by nitrogenase depends upon a source of low-potential electrons. These are supplied by the reduced form of the nitrogenase Fe protein, in a process that requires the concomitant hydrolysis of MgATP. Although MgATP hydrolysis is known to be coupled with the electron transfer from Fe protein to MoFe protein, unanswered questions remain on how they are coupled. There is no inherent thermodynamic requirements for MgATP hydrolysis in substrate reduction. Consequently, it appears that ATP must be required for kinetic reasons, such as controlling a conformational gate that ensures quasi-unidirectional electron transfer. The conformational changes associated with MgATP binding and hydrolysis might be utilized in two possible alternative ways: (i) to introduce conformational changes in the MoFe protein required for intramolecular electron transfer from the P cluster pair to the FeMoco; or (ii) to induce conformational changes in the Fe protein required for intermolecular electron transfer to the P cluster pair of the MoFe protein.

The electrons needed for nitrogenase substrate reduction reactions are supplied by sodium dithionite *in vitro*, as mentioned above, or ferredoxin or flavodoxin *in vivo*. In *K. pneumoniae*, the gene encoding flavodoxin (*nifF*) is located within the Mo-nitrogenase *nif* gene cluster, as well as a pyruvate flavodoxin oxidoreductase (*nifJ* gene product) (Shah *et al.*, 1983; Hill & Kavanagh, 1980; Thorneley & Diestung, 1988). Pyruvate is an electron source for *K. pneumoniae* nitrogenase, this is not so for the *A. vinelandii* nitrogenase as no *nifJ* has been found in this organism, although flavodoxin is produced.

1.7.3 Nitrogenase Substrates, Products and Proposed Intermediates

All the nitrogenase-catalyzed substrate-reduction reactions require reductant

and the hydrolysis of MgATP. Among the substrates for wild-type Mo-nitrogenase, proton reduction is the only reaction that is not inhibited by CO. This property of the nitrogenase H_2-evolution reaction distinguishes it from H_2 evolution via conventional hydrogenases (Hardy & Knight, 1975).

1.7.3.1 Dihydrogen Evolution

Nitrogenase catalyzes an ATP-dependent H_2-evolution reaction (Bulen *et al.*, 1965) that has all the same requirements as N_2 fixation. Studies of the ratios of H_2:HD:D_2 evolved from mixed H_2O-D_2O solutions of turning-over nitrogenase (Jackson *et al.*, 1968) demonstrated that hydronium ions are the ultimate source of nitrogenase-catalyzed H_2 evolution as shown in the following equation.

$$2H_3O^+ + 2e^- \rightarrow H_2 + 2H_2O$$

At present, both the chemical mechanism and site of H_2 evolution by nitrogenase is unknown, although, like all other substrates, the protons are almost certainly reduced at FeMoco. One possibility is that of a metal hydride or dihydride, which can produce H_2 either by reaction with protons or by reductive elimination, respectively, although it is currently unknown which metal atom it is on the FeMoco.

$$E + H^+ + 2e^- \rightarrow E\text{-}H \xrightarrow{+H^+} E + H_2$$

$$E^{2-} + 2H^+ + 2e^- \rightarrow E{<}\begin{matrix}H\\H\end{matrix} \rightarrow E^{2-} + H_2$$

In the absence of other substrates, proton is reduced by nitrogenase to evolve H_2 in aqueous solution. In the Lowe-Thorneley MoFe-protein cycle, H_2 is first evolved at the E_2 state, so a low flux condition favors H_2 evolution. Further, this scheme suggests that N_2 binding occurs via H_2 displacement. The reduction of N_2 is, thus, always accompanied by H_2 evolution. Although evolution has made nitrogenase a slow enzyme, its presence at high concentrations in the cells help

minimize H_2 evolution, a 25% total electron flux is apparently mandatory (Simpson & Burris, 1984).

1.7.3.2 Dinitrogen Reduction

Dinitrogen is reduced by nitrogenase to ammonia and dihydrogen as shown below.

$$N_2 + 8H^+ + 8e^- \rightarrow 2NH_3 + H_2$$

Reported K_m values for this reaction as measured *in vitro* using purified or partially purified nitrogenases from a number of organisms are generally in the range of 0.1 - 0.2 atm N_2 (Hardy, 1979). Thus, under physiological conditions, the substrate N_2 should be present at saturating levels. However, N_2 is the only substrate whose reduction is competitively inhibited by H_2. Even at 50 atm N_2 pressure, a minimum of 25% of the available electrons go into H_2 evolution (Simpson & Burris, 1984). Although no free reduction intermediates have ever been observed during N_2 reduction, indirect evidence strongly suggests the formation of enzyme-bound intermediates during the 6-electron reduction of N_2 to ammonia. In 1978, the first unequivocal evidence was reported of such intermediates when hydrazine was produced after acid or base treatment of a turning-over nitrogenase under N_2 (Thorneley *et al.*, 1978).

Earlier reports clearly demonstrated that N_2H_4 is not a free product of N_2 reduction (Burris *et al.*, 1965), however, it is a substrate (Bulen, 1976). Because hydrazine reduction catalyzed by nitrogenase is not inhibited by H_2 and does not enhance HD formation under D_2 (Bulen, 1976), both of which occur during N_2 reduction catalyzed by nitrogenase, the possibility that HD formation and H_2 inhibition occur at an earlier stage in the N_2-reduction pathway than the hydrazine-level intermediate was proposed as evidence that bound intermediate likely occur and that the reduction occurs in steps of two electron or less (Thorneley *et al.*,

1978; Burgess *et al.*, 1981). The occurrence of bound diazene (N_2H_2) remains controversial.

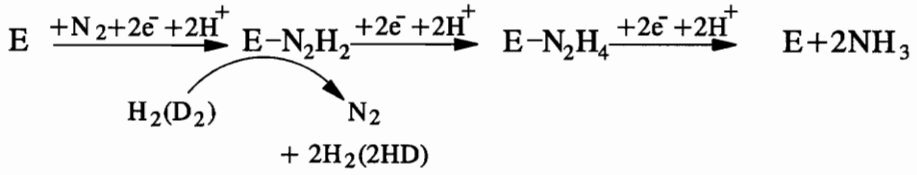

Recently, the altered α-195^{gln} MoFe protein which has been shown to bind, but not reduce N_2, also suffers H_2 inhibition of N_2 binding and produces HD from N_2/D_2 atmosphere (Kim *et al.*, 1994).

1.7.3.3 Hydrazine Reduction

Nitrogenase catalyzed reduction of hydrazine to ammonia was first demonstrated using an *A. vinelandii* nitrogenase complex (Bulen, 1976). The reaction is described in the following equation.

$$N_2H_4 + 2e^- + 2H^+ \rightarrow 2NH_3$$

That the free base N_2H_4, and not the protonated species $N_2H_5^+$, is the substrate has been shown by controlled pH studies (Bulen, 1976; Davis, 1980). N_2H_4 is a poor substrate because of its large K_m of ~20 - 30 mM (Davis, 1980), and it is the only known nitrogenase substrate which is not either a C or N multiple-bonded species.

1.7.3.4 Azide Reduction

Crude extracts of N_2-grown *A. vinelandii* and *C. pasteurianum* cells reduce azide by two electrons to N_2 and NH_3 (Schöllhorn & Burris, 1967a). Later, using purified *K. pneumoniae* nitrogenase proteins, a third product, hydrazine, was

demonstrated (Dilworth & Thorneley, 1981). The product ratio in that work was found to be $\sim 1N_2H_4{:}2N_2{:}5\text{-}6NH_3$ with azide as the presumptive substrate. More recently, by using *A. vinelandii* nitrogenase system, it was found that, in the nitrogenase-catalyzed azide-reduction reactions, both N_3^- and HN_3 are substrates (Rubinson *et al.*, 1985). The reactions are summarized below.

$$N_3^- + 2e^- + 2H^+ \rightarrow N_2 + NH_3$$

$$HN_3 + 6e^- + 6H^+ \rightarrow N_2H_4 + NH_3$$

$$N_3^- + 8e^- + 8H^+ \rightarrow 3NH_3$$

Using a mixture with $^{15}N_2H_4$ present, the results strongly suggest that N_2H_4 does not rebind to the enzyme for possible further reduction to NH_3 (Dilworth & Thorneley, 1981). HN_3 is an extremely good substrate with a K_m of 12 μM in the six-electron reduction reaction (Rubinson *et al.*, 1985). In the same report, it was suggested that HN_3 binds to and is reduced at a redox state of the enzyme more oxidized than the N_2-reducing state. N_3^- is the only anionic substrate known for nitrogenase. It may bind to and be reduced at a number of different redox states of the enzyme. N_2 from the two-electron reduction of N_3^- is probably produced in close proximity to the N_2-reduction site of the enzyme because the amount produced is well below the K_m for N_2 if it were to be distributed in the gas phase, and yet some N_2 is apparently further reduced to NH_3. The authors argued that N_2 must be produced close to the N_2-binding site which is in a receptive state (*i.e.* state E_3 of the Lowe/Thorneley model). At present, the details of the mechanism by which nitrogenase catalyzes the azide-reduction reactions are unknown.

1.7.3.5 Acetylene reduction

The first demonstrated reduction of C_2H_2 to C_2H_4 by nitrogenase as shown below used crude extracts of nitrogenase-derepressed *C. pasteurianum* cells (Dilworth, 1966).

$$C_2H_2 + 2e^- + 2H^+ \rightarrow C_2H_4$$

C_2H_2 inhibits N_2 reduction noncompetitively (Rivera-Ortiz & Burris, 1975). The acetylene-reduction reaction subsequently became the most commonly used assay for nitrogenase both *in vivo* and *in vitro* (Hardy *et al.*, 1973). Acetylene is a fairly good substrate, compared to other alternative substrates, with apparent K_m values ranging from about 0.003 to 0.02 atm (Hardy, 1979). The only product of this reaction is C_2H_4, with no ethane or methane produced by wild-type Mo-nitrogenases (Hardy, 1979; Dilworth, 1966), although some altered Mo-nitrogenases (Scott *et al.*, 1990, 1992) and the alternative nitrogenases do produce C_2H_6 (Dilworth, *et al.*, 1987, 1988). Reduction of C_2H_2 in D_2O has definitively established that *cis*-$C_2H_2D_2$ is the major product (Dilworth, 1966; Kelly, 1969; Hardy, *et al.*, 1969). This geometric specificity of this reaction and the retention of the acetylene protons has been used to support a concerted $2H^+/2e^-$ transfer mechanism involving side-on bonding to a metal atom in nitrogenase (Stiefel, 1973) and to argue against a mechanism involving acetylide-type bonding (M-C≡CH) (Dilworth, 1966; Hardy, 1979). C_2H_2 binds to two sites (or oxidation states) and C_2H_4 to only one with C_2H_4 released at oxidation state of E_3 of the MoFe-protein cycle (Ashby *et al.*, 1987; Fisher *et al.*,1990).

1.7.3.6 Cyanide Reduction

Cyanide reduction by nitrogenase was first demonstrated in 1967 (Hardy & Knight), but further studies (Li *et al.*, 1982) found that HCN actually served as substrate for nitrogenase. The cyanide reduction reactions can be summarized as follows.

$$HCN + 4e^- + 4H^+ \rightarrow CH_3NH_2$$

$$HCN + 6e^- + 6H^+ \rightarrow CH_4 + NH_3$$

$$HCN + 2e^- + 2H^+ \rightarrow CH_2NH$$

Upon hydrolysis, CH_2NH (methyleneimine) from the last reaction above gave NH_3 and possibly HCHO. The K_m for cyanide reduction is reported to be 4.5 mM HCN (Li *et al.*, 1982).

The proposed mechanism for HCN reduction is analogous to one of the proposed mechanisms for N_2 reduction.

$$E\text{–}HCN \xrightarrow{+2e^- +2H^+} E\text{–}CH_2NH \xrightarrow{+2e^- +2H^+} E\text{–}CH_3NH_2 \xrightarrow{+2e^- +2H^+} E + CH_4 + NH_3$$

There are, however, two differences concerning the reactivity of N_2 and HCN. One is that, unlike N_2, HCN reduction is not inhibited by H_2 and does not give rise to HD under D_2 (Newton *et al.*, 1977). The other is that, of the two proposed 4-electron reduced intermediates, N_2H_4 is a substrate but not a product of N_2 reduction, while CH_3NH_2 is a product of HCN reduction but not a substrate for the enzyme (Li *et al.*, 1982).

It was found that a higher Fe protein to MoFe protein ratio favors H_2 release rather than cyanide reduction, thus, it was suggested that cyanide binds to a more oxidized state of the MoFe-protein cycle than the H_2-releasing state (Li *et al.*, 1982). Pre-steady-state kinetics showed that the H_2 release time lag was the same with or without cyanide, but an unprecedented 3-sec lag occurred before CH_4 was released. Thus, it was proposed that this slow release was due to a slow, cyanide-induced modification of the binding site, necessary before either inhibition or product release can occur (Lowe *et al.*, 1989).

1.7.4 Inhibitors of Substrate Reduction

In Mo-nitrogenase, CO is a potent non-competitive inhibitor of N_2 reduction and all other alternative substrate reductions, except H^+ reduction (Hwang *et al.*,

1973; Hardy, 1979; Burris, 1979). However, mutants (such as, nifV$^-$ and substitution of α-191-Gln with Lys) have been constructed that display CO sensitivity of their H_2 evolution activities. Interestingly, this inhibition is not complete and at least $\sim$25% of the electron flow remains. This result may or may not be coincidental, but because this percentage is about the same as the percentage of remaining H_2 evolution at very high dinitrogen concentrations for wild-type nitrogenase (Rivera-Ortiz & Burris, 1975; Simpson & Burris, 1984), it may suggest more than one H_2-evolution site. Recently, there has been a suggestion of possible H_2 evolution from the P-cluster in the MoFe protein of nitrogenase (Kim *et al.*, 1993).

Spectroscopic studies have found a number of transient EPR signals during nitrogenase catalysis (Smith, 1983), two of which were interpreted as CO binding to the Fe_4S_4 clusters of at least two sites (Davis *et al.*, 1979). In the same report, only one of the signals was seen in the presence of C_2H_2, suggesting that C_2H_2 may also bind to an Fe_4S_4 cluster (Davis *et al.*, 1979).

1.7.5 Substrate Interactions and Potential Binding Sites

Nitrogenase-catalyzed substrate reductions have been studied extensively. For example, H_2 inhibits N_2-reduction activity competitively; C_2H_2 is a noncompetitive inhibitor for N_2 reduction while N_2 is a competitive inhibitor of C_2H_2 reduction (Rivera-Ortiz & Burris, 1975). In light of the Lowe-Thorneley model, the nature of the noncompetitive inhibition kinetics may reflect binding to different oxidation states of the enzyme during the MoFe protein cycle, rather than to different sites on the enzyme. A good example of this is the nitrogenase-catalyzed C_2H_2 reduction and N_2 reduction reactions. The non-reciprocal inhibition patterns between the two reactions correlate well with the different numbers of electron required for each of the reactions (2 for acetylene and 6 or 8

for nitrogen reduction) and therefore, could be better explained using the modified Lowe-Thorneley model (Fisher *et al.*, 1990). A similar situation exists when N_2 acts as the competitive inhibitor to azide reduction,

$$HN_3 + 6e^- + 6H^+ \rightarrow N_2H_4 + NH_3$$

where the K_i of N_2 as the inhibitor is ten times larger than the K_m for N_2 reduction to NH_3. The proposal of the same binding site at different oxidation levels on the enzyme for N_2 and HN_3 has been used to explain this situation.

Although a lot of research effort has been invested in kinetic probes of the substrate binding sites on the MoFe protein, no direct evidence has been forthcoming. Where and how the substrates bind and get reduced on nitrogenase thus still remain a mystery. The crystal structure model of the FeMoco within the MoFe protein has shed new light on this darkness and should help in the solution of this problem. Using the FeMoco structure of this model, possible N_2 binding modes on the FeMoco have been proposed recently. Nine theoretically possible motifs were examined and three of these proposed as the best candidates for activating N_2 for reduction (Deng & Hoffman, 1993). No unique best binding mode could be assigned demonstrating the complexity of the question of how and where FeMoco acts as the substrate binding and reduction site. It must be remembered that the MoFe protein x-ray crystal structure represents only a view of nitrogenase in its "resting state". What happens to the cofactor in the polypeptide pocket in the "turnover state" of the enzyme? How can the different types of substrates bind and be reduced at FeMoco? For example, unlike N_2, which could bind end-on to the one of the metal atoms on the FeMoco, C_2H_2 is a substrate that could only bind side-on. In summary, there are a lot of unanswered questions regarding substrate binding and reduction and to unravel this mystery awaits further work on the functional aspects with guidance from the x-ray crystal structure.

Chapter 2 Materials and Methods

2.1 Materials

All general chemicals were purchased from Fisher Scientific Company (Pittsburgh, PA) unless otherwise specified.

The following buffers, purchased from Sigma Chemical Co. (St. Louis, MO), were used in the studies: 50 mM Tris-HCl (pH 8.0), 25 mM Tris-HCl (pH 7.4), 25 mM Tes-KOH (pH 7.4), 25 mM Hepes-KOH (pH 7.4) and a three-buffer system containing 38 mM Hepps, 38 mM Ches and 75 mM Bistris. The desired pHs were attained through the addition of either HCl or KOH.

Sodium dithionite ($Na_2S_2O_4$) was purchased from Mallinckrodt Chemical Company (Berkeley, CA).

The DE-52 cellulose was purchased from Whatman Biosystems Ltd, Maidstone, Kent, England. The gel filtration media, Sephacryl S-200 and S-300, were purchased from Pharmacia Ltd, Uppsala, Sweden. Dowex AG1-X2 resin and Bio-Gel P-6DG desalting gel were purchased from BioRad, Hercules, CA.

Cylinder gases used, such as, nitrogen, argon, hydrogen, helium and air, were purchased from AirCo (Radnor, PA). Carbon monoxide was purchased from Matheson products, Inc. (East Rutherford, NJ). Cylinder argon gas was first passed through a heated ($\sim$120°C) BASF copper catalyst column to remove oxygen before being used as a flushing gas in the Schlenk line equipped with vacuum/gas manifolds. Acetylene gas was produced in the lab by the reaction of calcium carbide with water. The gas was collected over water in a 500 ml dropping funnel. Once the funnel was full the sampling port was capped with a suba-seal before removing the funnel from the water. A positive hydrostatic pressure was maintained by the attachment of a water reservoir.

2.2 Anaerobic Techniques

Because nitrogenase is extremely oxygen labile, all of the procedures were performed in anaerobic buffer under an argon atmosphere using the anaerobic Schlenk line that was designed to replace air with an inert gas such as argon, in a closed system. On the Schlenk line, a double manifold system one side of which is linked to a vacuum pump and the other side to an argon gas line are controlled by the two-way stopcocks. The negative atmospheric pressure generated by the vacuum line is monitored by a mercury manometer, whereas a bubbler is used to monitor the inert gas (Ar gas) flow into the system. A dry ice trap is also used in order to avoid the mixing of moisture generated by the vacuum with the pump oil. In order to replace air with argon, the buffer-containing flask was first degassed by applying vacuum over the closed system for 30 min to 60 min depending on the volume of the buffer contained in the flask, until rapid bubbling ceased, the flask was then flushed with argon followed by the addition of dithionite (1 mM $Na_2S_2O_4$ final concentration in the solution), finally the flask was evacuated and flushed with argon three times before being kept under a positive pressure of argon. If the atmosphere in an empty container was to be replaced, a repeated (at least three times) evacuation and flushing with argon were performed, and the duration of the evacuations was monitored by the mercury manometer attached to the vacuum line, before finally being kept under a positive pressure of argon.

When required, some of the procedures were carried out in an anaerobic glove box (Vac Vacuum Atmospheres Company, Hawthorne, CA) through which N_2 gas was circulated (100 l/min). The circulatory N_2 gas is continuously passed through heated BASF-copper-based catalyst filled columns to remove O_2. The O_2 concentration was continuously monitored, and always found to be less than 1 ppm, by a couloximeter (Vac Vacuum Atmospheres Company, Hawthorne, CA) sensor via an amplifier/meter with an accuracy of ± 0.2 ppm.

2.3 Cell Growth: Media and Nitrogenase Derepression

Growth of *Azotobacter vinelandii* wild-type and mutant strain cells were carried out on a modified Burk's medium (Strandberg and Wilson, 1968). Table 2 has a list of stock solutions used for making the Burk's medium. All mutant strains that do not grow (Nif^-) or grow slowly (Nif^{slow}) in nitrogen-free media were grown on urea-supplemented media and then derepressed for nitrogenase synthesis as described previously (Jacobson *et al.*, 1989).

Small batch cultures were grown at 30°C in Fernbach flasks with 500 ml Burk's medium per flask. The medium contains 10 μM Na_2MoO_4, which is sufficient to repress the alternative nitrogenase systems. Cultures were grown under air with shaking at 250 rpm using a New Brunswick Incubator Shaker (New Brunswick Scientific Company, New Brunswick, NJ). For growth of the Nif^+ strains, cells from a 2-day-old confluent culture on a 100 × 15 mm plastic petri dish (Fisher Scientific Co., Pittsburgh, PA) in Burk's medium, one dish per 500-ml culture, were scraped off and inoculated into the liquid Burk's media, and grown to midlog phase. The density of the *Azotobacter* cultures were monitored using a Klett-Summerson meter (Klett Mfg. Co. Inc., New York) equipped with a no.54 filter. The growth of the cells is considered to be at midlog phase when the cell density reaches 150-200 Klett. For Nif^- or Nif^{slow} strains, a fixed nitrogen source of filter-sterilized urea was added to a final concentration of 20 mM for growth of the culture to midlog phase. Then the medium was removed by the centrifugation at 10,400 × *g* for 10 min (DuPont Instrument, Wilmington, DE), the cell pellet resuspended in fresh Burk's nitrogen-free media and grown additional three hours for nitrogenase derepression. Final harvest of these small-scale cell cultures was achieved by centrifugation using a Sorvall RC-5B refrigerated superspeed centrifuge at 10,400 × *g* for 10 min, followed by resuspending the cell pellet in the 50 mM cold Tris-HCl (pH 8.0), and a second

Table 2. Composition of the Burk's medium

Chemical	Amount per liter
K_2HPO_4(dibasic)	0.8 g
KH_2PO_4(monobasic)	0.2 g
$MgSO_4 \bullet 7H_2O$	0.2 g
NaCl	0.2 g
Sucrose	20.0 g
$CaSO_4 \bullet 2H_2O$	0.05 g
Fe solution[1]	1.0 ml
Mo solution[2]	1.0 ml
Urea[3]	10 ml
Agar[4]	20.0 g

[1] Fe solution is made of 27.0 g of $FeCl_3 \bullet 6H_2O$ per 1 liter ddH_2O, filter sterilized and added separately after sterilization.

[2] Mo solution is made of 2.4 g of $Na_2MoO_4 \bullet 2H_2O$ per 1 liter ddH_2O, filter sterilized, and added separately after sterilization.

[3] Urea solution is made of 120 g of urea (NH_2CONH_2) per 1 liter ddH_2O, filter sterilized, used whenever is necessary by adding separately after sterilization.

[4] Agar is used in making plates and is added before the sterilization step.

centrifugation to remove the wash buffer as mentioned above. The wet cell paste was stored in a -80°C freezer (So-Low Environ. Equip. Co., Cincinnati, OH) until used.

Large-scale *Azotobacter* cultures were grown in a 28-liter fermentor (New Brunswick Scientific Company, New Brunswick, NJ) on modified Burk's medium. Cells from Fernbach midlog growth cultures were inoculated into the fermentor, usually 1 liter of inoculum per fermentor batch. Air flow in the fermentor was controlled with a flow meter at 35 ~ 40 liters/min; and the culture was vigorously stirred at 250 rpm with a built-in stirrer. All mutant strains with either a Nif^- or a Nif^{slow} phenotype were derepressed for nitrogenase expression by growing the culture on nitrogen-containing Burk's medium until its cell density reached 150-200 Klett units. The culture was then concentrated to 2 liter by filtration using a Watson-Marlow 601S/R peristaltic pump and a Millipore (Pellicon) cassette system fitted with 0.22 Å Pellicon filter in order to remove as much of the nitrogen source as possible. The two liters of culture were then reinoculated into 24 liters of Burk's nitrogen-free medium. After derepression for 3 hours in this nitrogen-free Burk's medium, the culture medium was removed and the cells isolated by centrifugation. Wild-type strains or Nif^+ strains were grown up on nitrogen-free Burk's medium in the fermentor directly, and concentrated to two liters as described above. Final harvest of all cells from the fermentor involved a wash with 6 liters of prechilled (4°C) 50 mM Tris-HCl (pH 8.0) by dilution of the 2 liters of concentrated culture, followed by filtration to reduce the volume to 2 liters again before the centrifugation step to ensure a maximum removal of the medium. Cells were stored at -80°C until used.

2.4 Mutant Strain Construction

Methods for site-directed mutagenesis, gene replacement, and the isolation

of mutant strains were performed as described or cited previously (Brigle *et al.*, 1987a, b). The strategy for making a number of substitutions at one specific amino-acid residue was to synthesize chemically an oligonucleotide on which the 3 nucleotides coding for the desired amino-acid residue have been degenerately replaced. For substitution at His-274, Tyr-276 or Arg-277 of the MoFe protein α-subunit, the oligonucleotide having the sequences respectively:

5'-AACCTGGTTXXXTGCTACCGCTCG-3' (for His-274)

5'-GTTCACTGCXXXCGCTCGATGAAC-3' (for Tyr-276)

5'-CACTGCTACXXXTCGATGAACTAC-3' (for Arg-277)

(where XXX represents the degenerate codon at the designated residue) were synthesized. Most of the mutants involved in the study were isolated using the degenerate oligonucleotide approach. A few of them were isolated using a specifically synthesized oligonucleotide, such as the ones with Leu, Phe or Lys substituting the Arg-277 residue. In those cases, CTC, TTC, AAG were used in the position of XXX respectively in the third oligonucleotide sequence listed above.

In this dissertation, each altered MoFe protein having a substitution within the MoFe protein α-subunit primary sequence is denoted by the subunit designation (α- in this case), a number representing the sequence of the amino-acid position substituted, followed by the substituting amino acid as superscript. For example, the altered MoFe protein having the α-subunit Arg-277 position substituted by Thr is designated as α-277^{thr} (the wild-type MoFe protein is denoted as α-277^{arg}). Strains are designated by their correspondent DJ numbers. DJ527 is a strain, which has mutations at the *hox*KG genes so as to abolish its uptake hydrogenase activity (Hup$^-$), whereas its *nif* genes remain intact. All the mutants used in this study are Hup$^-$ strains, which enables us to measure H_2-evolution activity accurately at the crude-extract level without the interference from uptake

hydrogenase activity. Although in the purified protein studies, the uptake hydrogenase is no longer a relevant concern, Hup$^-$ strains are used in order to keep the strains used in protein purifications consistent with the ones in the crude-extract studies.

2.5 Crude Extract Preparation

For small scale crude extract preparation, cells were thawed and diluted anaerobically at 4°C in degassed 50 mM Tris-HCl, pH 8.0, containing 2 mM sodium dithionite, at the approximate ratio of 1.0 g of cells to 2.0 ml of buffer. The cell suspension was broken with 3-min pulse sonication using a Heat System Sonicator model XL2015 in a 25-ml Rosette cooling cell (Heat Systems-Ultrasonics, Inc.) immersed in an ice water bath to offset increasing temperature. The extract was transferred anaerobically into centrifuge tubes and centrifuged for 60 min using a Beckman L5-50B Ultracentrifuge (Class H) at 98,000 $\times$ *g* at 4°C. The supernatant was removed from the centrifuge tubes anaerobically under blowing argon using a Hamilton syringe and pelleted into liquid nitrogen to store until used.

As the first step in protein purification procedures, crude extract was prepared on a large scale (500 g cells or more) by using a Manton-Gaulin homogenizer (Gaulin Corporation, Everett, MA) or on a medium-to-small scale (less than 500 g cells) using sonication in a 200-ml Rossette cooling cell as mentioned above. The cells were thawed under an Ar atmosphere and diluted approximately 1:2 with degassed 50 mM Tris-HCl (pH 8.0), 2 mM sodium dithionite, ruptured with either of the methods described above, transferred anaerobically to a degassed flask, an anaerobic DNase and RNase solution (10 mg/l) was added and stirred at room temperature for 30 min. A heat treatment at 56°C for 5 min was included as a standard step during the crude-extract

preparation of the heat-stable mutants. Use of the heat step requires a prior activity test of the temperature stability of the crude extract on a small scale (refer to section 2.9.2). The heated extract was then cooled down to 15°C or less using an ice bath before centrifugation at 98,000 × *g* at 4°C to separate the cell debris from the soluble protein supernatant. The supernatant was transferred from the centrifuge tubes to a previously degassed flask anaerobically, froze into liquid nitrogen and the frozen pellets stored until used.

2.6 Protein Purification

The crude extract was thawed anaerobically before being loaded onto a DE-52 cellulose column (5 cm diameter) which was equilibrated with 25 mM Tris-HCl (pH 7.4), 1 mM sodium dithionite. Usually, 1 ml of DE-52 resin was used for crude extract from 1 gram of *Azotobacter* cells. After the loading step, the column was washed first with 25 mM Tris-HCl (pH 7.4), 1 mM sodium dithionite and then with 0.1 M NaCl in 25 mM Tris-HCl (pH 7.4), 1 mM sodium dithionite for one-column volume each before a linear NaCl gradient from 0.1 M to 1.0 M in degassed 25 mM Tris-HCl (pH 7.4), 1 mM sodium dithionite, was applied. The MoFe protein eluted from the DE-52 cellulose column at ~0.2 M NaCl, and the Fe protein eluted from the DE-52 cellulose column at ~0.5 M, both the MoFe protein and the Fe protein eluted off the DE-52 column were almost devoid of the complementary protein activities. The MoFe protein fraction off the DE-52 column chromatography was concentrated using a ~300 ml amicon style concentrator (74 × 70 mm) fitted with a 100,000 Dalton membrane (Sigma Chemical Co., St. Louis, MO) in an ice water bath to reduce volume. Depending on the scale of the preparation, further purification of the MoFe protein was achieved by gel filtration over either a 5.0 × 50 cm (Spectrum) Sephacryl S-300 column or a 7.5 × 50 cm (Spectrum) Sephacryl S-200 column (Pharmacia LKB,

Sweden), using degassed 0.2 M NaCl in 25 mM Tris-HCl (pH 7.4), 1 mM sodium dithionite. Pure samples of MoFe protein, which migrated as the expected two bands on one-dimensional SDS-PAGE, were obtained in this way. The Fe-protein fraction off the DE-52 column chromatography was diluted ~1:4 with 25 mM Tris-HCl (pH 7.4), 1 mM sodium dithionite, before being applied to a 5.0 × 25 cm Q-sepharose column, which was previously equilibrated with 25 mM Tris-HCl (pH 7.4). A linear NaCl gradient from 0.1 to 1.0 M in degassed 25 mM Tris-HCl (pH 7.4), 1 mM sodium dithionite, was applied to separate the residual MoFe protein from the Fe protein. The protein fractions eluted off the Q-sepharose column at approximately 0.35 M NaCl for the MoFe protein fraction and 0.6 M NaCl for the Fe protein. The Fe protein at this stage was of sufficient purity for assays. Further purification of the Fe protein, which is necessary for protein component-ratio studies or stopped-flow spectrophotometric experiments was obtained by using gel-filtration column chromatography as described above.

It should be pointed out that the during column chromatography steps, the brown nitrogenase component proteins were monitored at 405 nm because of the interference of sodium dithionite ($Na_2S_2O_4$) in the solution with the conventional 280 nm protein absorbance.

2.7 Gel Electrophoresis

For sodium dodecyl sulfate-polyacrylamide gel electrophoresis (SDS-PAGE), samples and gels were prepared according to Laemmli (1970). The gels used were 12% polyacrylamide (1.35% cross-linker) with a 4% stacking gel. Electrophoresis was performed at 30 mA/gel in a Hoefer Mighty Small apparatus (Hoefer, San Francisco, CA), using 10,000 - 100,000 low molecular weight standards (Biorad Laboratories, Hercules, CA). The gels were stained with 0.1% Coomassie Blue (R-250), destained with 40% methanol/10% acetic acid/50%

water solution and preserved in 5% methanol/7% acetic acid/88% water solution. The SDS-PAGE was used extensively to monitor the nitrogenase purification progress, and was also used to evaluate the effectiveness of nitrogenase derepression during cell growth.

2.8 Protein Estimation

Protein concentrations of crude extracts and purified proteins were determined by the BCA method using bovine serum albumin (0 - 0.1 mg/ml) as a standard (Smith *et al.*, 1985). Dithionite is known to interfere with the BCA assay, therefore, protein samples that are used in the BCA assay are vortexed vigorously to consume their dithionite contents in order to eliminate the interference.

2.9 Steady State Assay for Nitrogenase Activity

2.9.1 Substrate Preparations

Prepared reaction mixture (see Table 3), which had been stored in the -20°C freezer was removed and thawed. An 0.3-ml aliquot of reaction mixture and distilled water (to give a final assay volume of 0.9 ml) were added to serum bottles (average volume = 9.25 ml). The bottles were capped with suba-seals and sealed with aluminum seals (Alltech Associates, Inc., Deerfield, IL). All reaction vials were subject to four cycles of evacuation and flushing using an automated machine (Corbin, 1978) to replace the air with either 100% Ar or 100% N_2 depending on the assays to be performed. The internal gas pressure inside each bottle was released by venting with a 3-ml disposable syringe barrel (Becton Dickinson and Company, Franklin Lakes, NJ) fitted with a 16-gauge needle filled with ~1 ml deionized water, before the assays or before the dilution of certain stock gases, such as, acetylene. For preparation of a C_2H_2/Ar gas mixture from

Table 3. Stock solutions for the reaction mixture

Stock solution	Volume used per 45 ml reaction mix
0.25 M Hepes-KOH buffer (pH 7.4)[1]	15 ml
0.1 M ATP[2]	3.75 ml
0.25 M $MgCl_2$[3]	3.0 ml
0.3 M creatine phosphate[4]	15 ml
creatine phosphate-kinase[5]	25,000 activity units
deionized water	0.75 ml

[1] 0.25 M Hepes-KOH buffer consisted of 5.96 g Hepes per 100 ml ddH_2O, pH adjusted to 7.4 using 2.0 M KOH solution. It was stored in the refrigerator.

[2] 0.1 M ATP consisted of 0.614 g ATP per 10 ml ddH_2O, pH adjusted to 7.0 using 2 M KOH. It was prepared cold and stored in the -20°C freezer.

[3] 0.25 M $MgCl_2$ solution consisted of 2.54 g $MgCl_2$ per 50 ml ddH_2O, store in the refrigerator.

[4] 0.3 M creatine phosphate solution consisted of 10.9 g creatine phosphate disodium salt, hexahydrate form per 100 ml ddH_2O, pH adjusted to 7.2 using 1 M HCl. It was stored in the refrigerator.

[5] Creatine phosphokinase solution consisted of 500 units per ml in 0.02 M Hepes buffer (pH 7.4), plus 10% more to compensate for activity loss during the preparation and/or storage. It was made fresh each time in assay mix preparations.

The reaction mixture is pre-prepared and stored in the -20°C freezer in 10 ml aliquots to avoid unnecessary freezing and thawing to ensure best performance.

100% C_2H_2 stock gas, an average gas volume (vol.) of 8.25 ml in each bottle was used in the calculation, using the following formula,

Desired vol. = 8.25 × (desired conc.) / (100% - desired conc.).

For example, a 10% C_2H_2/90% Ar atmosphere was achieved by dilution of 1 atm 100% Ar with 0.92 ml of 100% C_2H_2. The actual concentration (conc.) of the C_2H_2 in each vial was verified using gas chromatography (see later for details).

H^+-reduction assays were performed under a 100% Ar gas phase. N_2-reduction assays were performed under a 100% N_2 gas phase. For azide-reduction assays, appropriate aliquots of a 100 mM NaN_3 in 25 mM Hepes-KOH (pH 7.4) stock solution were added to each reaction vial before the atmosphere replacement step. For NaCN-reduction assays, a calculated amount of a 100 mM degassed NaCN in 25 mM Hepes-KOH (pH 7.4) stock solution was injected into each reaction vial during the pre-incubation period.

2.9.2 Nitrogenase Activity Assay

Assays were performed in 9.25-ml reaction vials fitted with butyl rubber stoppers and aluminum seals. Each 1.0-ml reaction volume, which consisted of the 0.9 ml starting volume (see section 2.9.1) plus 0.1 ml 20 mM $Na_2S_2O_4$ in 25 mM TES-KOH or Hepes-KOH (pH 7.4), contained 25 mM Tes-KOH or Hepes-KOH (pH 7.4), 2.5 mM ATP, 5.0 mM $MgCl_2$, 30 mM creatine phosphate, 0.125 mg creatine phosphokinase. For crude-extract activity assays, 50-μl of crude extract was used in each assay. Assays were performed on each extract alone or with an excess of each purified complementary protein to determine either maximum MoFe-protein or Fe-protein activity. In purified nitrogenase activity assays, a total of 0.5 mg of nitrogenase proteins in 1 ml was used to avoid complications introduced by both high and low protein concentrations, *i.e.* in most cases, 0.423 mg of purified Fe protein and 0.077 mg of purified MoFe protein,

resulting in an Fe-protein to MoFe-protein molar ratio of 20, were used. Each assay was started by the addition of the crude extract or the purified complementary protein to the otherwise complete reaction system in the reaction vial, which had been preincubated for 5 minutes at 30°C, and was terminated by the addition of 0.25 ml 0.5 M Na_2EDTA (pH 7.5) after 8 minutes. When required, CO was added by gas-tight Hamilton syringe (Reno, Nevada) to the appropriate assay vial during the preincubation period.

2.9.3 Product Analysis

2.9.3.1 Quantification of the Gases: C_2H_2, C_2H_4, CH_4 and H_2

C_2H_4, C_2H_2 and CH_4 were quantified by gas chromatography (GC-14A, Shimadzu, Tokyo, Japan) on a Poropak N column using a flame ionization detector (abbreviated as FID, Shimadzu, Tokyo, Japan). H_2 was quantified by gas chromatography (GC-8A, Shimadzu, Tokyo, Japan) on a molecular sieve 5 A column and a thermal conductivity detector (abbreviated as TCD, Shimadzu, Tokyo, Japan). All gas chromatographic apparatus must contain certain basic components as shown in Figure 13.

The flame ionization detector (FID) is the most commonly used detector in GC. Figure 14 represents a diagram of a flame ionization detector. The detector consists of a small H_2-air diffusion flame burning at the end of a jet formed at the tip of a length of capillary tubing. When organic compounds are introduced into the flame from the column, electrically charged species are formed. These are collected by applying a voltage across the flame. The resulting current is amplified by an electrometer. When hydrocarbons are introduced into this flame, ionization takes place, in strict proportion to the amount of compound, this is due to the radical reaction:

$$CH + O \rightarrow CHO^+ + e^-$$

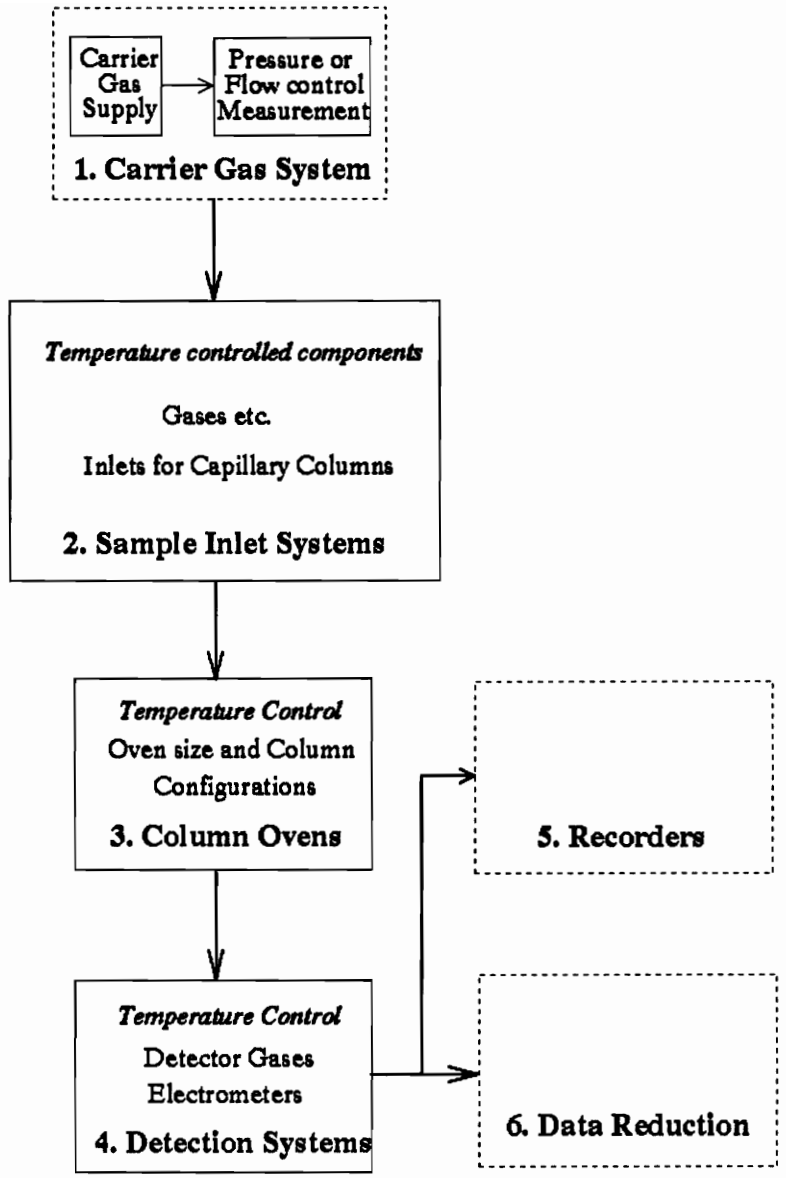

Figure 13. Basic requirements for gas chromatography (Adapted from Schill, 1977).

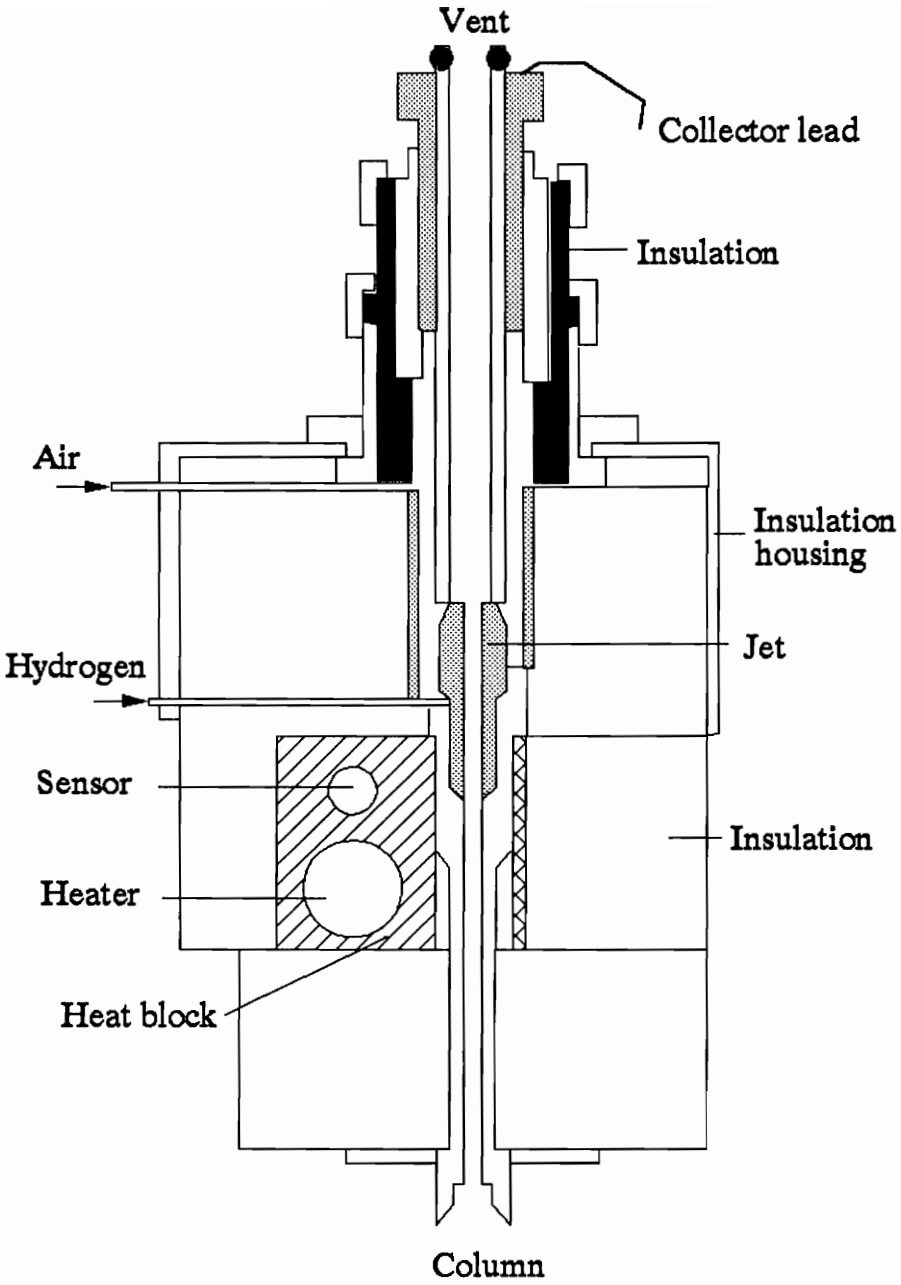

Figure 14. Schematic representation of GC with a Flame Ionization Detector (FID) (Adapted from Sullivan, 1977).

This reaction is an almost quantitative counter of carbon atoms being burned. In the GC-14A, the carrier gas, which is helium in this case, is set flow at 90 ml/min when operating. The column used here is of the dimensions 2 mm × 3 m (looped) whose temperature is maintained at 70°C. A H_2-air diffusion flame is burning with the constant flow of hydrogen and air gases. The temperature at the injection port and the detector are set at 180°C and 200°C respectively. The GC-14A is connected to a CR-5A chromatopac integrator (Shimadzu, Tokyo, Japan), where chromatographs are recorded and the area under each peak is calculated. Calibrations are performed using standard gases of 1 ppm C_2H_4/100% helium, 1 ppm C_2H_2/100% helium, 1 ppm CH_4/100% helium purchased from Scotty Specialty Gases (Plumsteadville, PA).

The TCD is a concentration dependent detector that is sensitive to some overall property of the effluent. The measured property is a physical parameter rather than a chemical one. The larger the difference between the thermal conductivities of the carrier gas and the sample, the greater the detector response. In our case, H_2 is the sample which has relative large thermal conductivity compared to Ar, thus making argon a good choice as a carrier gas (Schill, 1977). A flow rate of 60 ml/min argon is maintained while in use. A diagram describing the basis of a TCD is shown in Figure 15 which is composed of a four-cell bridge circuit. A current of 70 mA is used for the GC-8A TCD. The TCD requires strictly isothermal conditions and, in our case, 40°C is set for both column and injection/detection temperature. A CR-5A integrator is connected to the GC-8A to record chromatographs as well as performing calculations as mentioned above. Calibration is done by using the standard gas 1% H_2/100% N_2 purchased from Scotty Specialty Gases (Plumsteadville, PA).

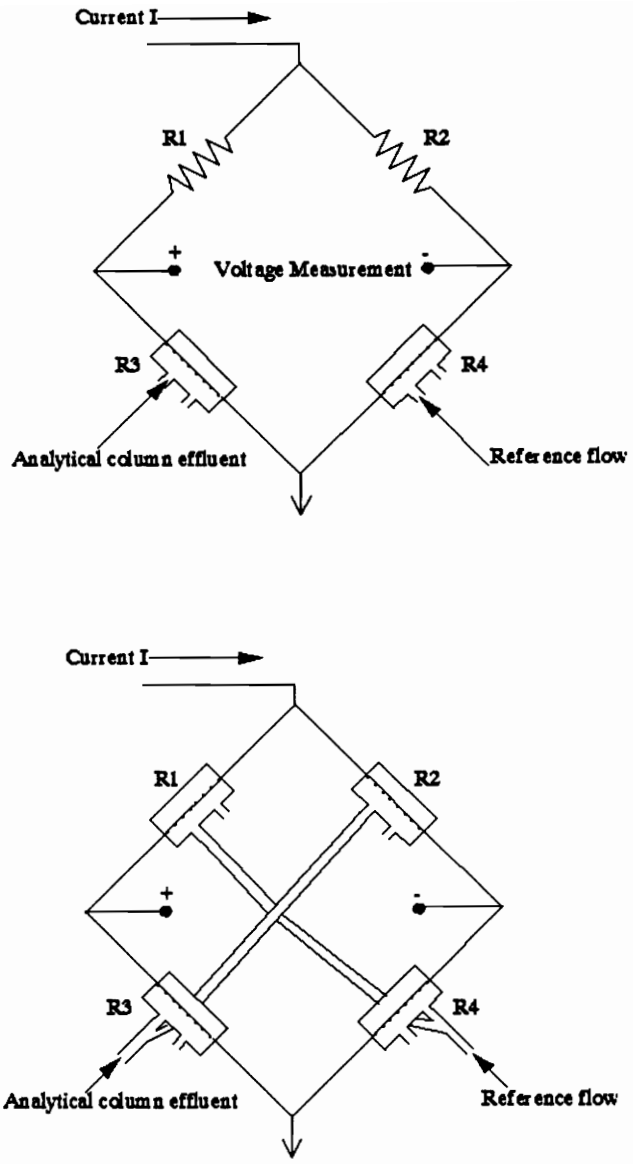

Figure 15. Schematic representation of bridge circuits in a Thermal Conductivity Detector (TCD) (Adapted from Sullivan, 1977).

2.9.3.2 Ammonia Assay

NH_3 produced from N_2-reduction and azide-reduction assays was quantified by the phenol/hypochlorite colorimetric determination using ammonium sulfate as standard as described previously (Dilworth *et al.*, 1992). In these assays, a Hepes-based reaction mixture was used because it interferes less with the color development of the ammonia assay used. In these assays, reactions were terminated with 0.25 ml of 0.5 M EDTA (pH 7.5) and, after all gas products were quantified using gas chromatography, the liquid mixture (0.5 ml) was removed from each reaction vial and applied to individually prepacked Dowex 1X2 ion exchange column (Cl^- form, 200-400 mesh, Biorad) to remove inhibitory components of the assay. The liquid flow-through plus the wash fraction with deionized water were combined (a total of 1.5 ml). An aliquot of 0.5 ml of each was used in the ammonia assay, which required the addition of 0.3 ml sodium phenolate (5% w/v phenol plus 2.5% w/v NaOH in deionized water), 0.45 ml sodium nitroprusside (0.02%, w/v in deionized water), and 0.45 ml sodium hypochlorite (10%, v/v in deionized water) in the stated order. After a 40-min incubation at room temperature, the absorbance of each solution was measured at 630 nm against $(NH_4)_2SO_4$ standards in the 0 - 0.2 μmole/ml range.

2.9.3.3 Hydrazine Assay

Enzyme-bound hydrazine (N_2H_4) was assayed by quenching the nitrogenase reaction with acid during nitrogenase turnover as described previously (Thorneley *et al.*, 1978). Assays were allowed to run for 5 min under N_2 and then quenched with 2 ml 95% ethanol containing 1 M HCl and 0.07 M *p*-dimethylaminobenzaldehyde (PMAB). The reaction mixture was centrifuged for 10 min to remove protein and N_2H_4 was measured as PMAB hydrazone at 458 nm using hydrazine sulfate (0 - 0.75 μM) as a standard. The hydrazine production in

the azide-reduction assays was measured using the PMAB colorimetric assay described previously (Dilworth and Thorneley, 1981). Aliquots of the Dowex 1X2 treated reaction mixture (as described above in the ammonia assay) were treated with 2 ml 95% ethanol containing 1 M HCl and 0.07 M PMAB, and absorbance was measured against hydrazine sulfate standard of 0 - 0.75 μM.

2.9.4 Measurement of ATP Hydrolysis

The ATP hydrolysis rates in nitrogenase activity assays were obtained by measurements of the creatine released from creatine phosphate upon the phosphorylation of the ADP produced in the reaction as catalyzed by creatine phosphokinase. The procedures were followed as mentioned in the ammonia assay. Aliquots from a Dowex 1X2 column were used in the creatine assay as described previously (Ennor, 1957). Samples (0.2 ml) were mixed with 2 ml 1% α-naphthol (w/v in deionized water) and 1 ml 0.05% diacetyl (v/v in deionized water). The volume was adjusted to 5 ml by the subsequent addition of deionized water. Absorbance was measured at 520 nm after a 20-min incubation at room temperature. The concentration of the creatine was determined using a creatine standard of 0 - 2.0 μmole/ml.

2.10 Pre-steady-state Kinetic Studies

Stopped-flow spectrophotometry was performed with a commercially available SF-61 instrument equipped with a kinetic data acquisition analysis and curve-fitting system (Hi-Tech, Salisbury, Wilts., UK). The SHU-61 sample handling unit was installed inside an anaerobic glove box operating at less than 1 ppm oxygen concentration, which was monitored with a Teledyne Analytical Instruments series 316 trace oxygen analyzer (Vacuum Atmospheres Co., Hawthorne, CA). Strict anaerobiosis must be ensured for studies with nitrogenase

and this was achieved by having the sample handling unit inside a high integrity glove box. The thermostatic control of the drive syringes, sample flow components and observation cell was achieved by closed circulation of water by a Techne C-85D circulator (Techne Ltd, Duxford, Cambridge, UK) attached to a FC-200 Techne flow cooler situated outside the glove box. The stopped-flow system consists of a pair of drive syringes, 2 × 1.0 ml "Hamilton" gas-tight syringes (Becton Dickinson and Company, Franklin Lakes, NJ) filled with the reacting species from two vertical 2.5 ml plastic reservoir syringes; a mixing device; observation cell and stopping syringe (500 μl "Hamilton syringe"), and a detecting and recording system. The light path length can be set to either 2 mm or 10 mm by altering the configuration of the mounting system. Simultaneous pushing of the drive syringe plungers, either manually or with the pneumatic ram, commences the reaction. The pneumatic ram was used where fast reactions were monitored since a higher reactant flow rate reduces the dead-time. The reacting solutions are forced through the observation cell into the stopping syringe. Each stopped-flow sample injection typically uses 0.1 ml from each syringe and yields a complete time course. A short movement of the plunger of the stopping syringe arrests the flow, which prevents further mixing and simultaneously activates the detection and recording system. The noise level of the amplified signal is sufficiently low that absorbance changes as low as $\Delta A = 0.005$ can be monitored over the wavelength range 350 to 700 nm.

This investigation is principally concerned with the absorbance changes that take place (430 nm) as the MoFe-protein is reduced to the various E_n states of the Lowe-Thorneley MoFe-protein cycle. Previous pre-steady-state stopped-flow spectrophotometric studies have been concerned with the primary electron transfer from Fe-protein$(MgATP)_2^{red}$ to the MoFe protein that is complete within 20 ms at 23°C, pH 7.5. A major assumption is that all reductions of the MoFe protein

occur at the same rate regardless of the redox state of the MoFe protein, *e.g.*, electron transfer to E^0 is at the same rate as for E_4. This has been confirmed only for the E_0 and E_1 states (Fisher *et al.*, 1991). Further, the absorbance changes (430 nm) that occur at longer times after the initial electron transfer reaction (Lowe *et al.*, 1992) are re-investigated in this study. These absorbance changes over the first 500 ms, as wild-type and altered MoFe proteins from *A. vinelandii* become reduced from E_0 through to possibly E_4, will be studied to determine if any of these states are associated specifically with N_2 binding and/or reduction. The oxidation of Av_2 (Fe protein from *A. vinelandii*) was monitored at 430 nm and fitted to a single exponential function. Monitoring of the absorbance change of the Fe-protein by stopped-flow spectrophotometry at 430 nm permits the accurate measurement of the rate constant for electron transfer between the component proteins. Single exponential functions are also used to analyze the complex absorbance changes that occur within the first 1 second of the reaction.

The details of experiments are presented in conjunction with the results in Chapter 6.

2.11 Electron Paramagnetic Resonance Spectroscopy

An electron possesses both charge and mass but also has angular momentum or spin. A spinning charge generates a magnetic field, so an electron may be thought of as a magnet orientated along the axis of spin (Knowles *et al.*, 1976; Palmer, 1985). The strength of the magnetic field is expressed as the magnetic moment. The magnetic moment of an electron can assume one of the two possible orientations with respect to an externally applied magnetic field. An unpaired electron has a spin of 1/2 and these two orientations are expressed as -1/2 (aligned with magnetic field) or +1/2 (aligned against the magnetic field). When electrons are paired, the spins oppose each other and are consequently

diamagnetic. Molecules containing one or more unpaired electrons are paramagnetic and therefore can be studied by EPR (Zavoisky, 1945). EPR spectroscopy gives information about the existence of an unpaired electron and about its immediate surroundings (as the g-values is affected by the environment surrounding the unpaired electron). For a free electron $g = 2.0023$, and the resonances in the $g = 2$ region are generally characteristic of non-metal, free radicals. EPR is particularly useful as a method of studying the Fe-S clusters in iron-sulphur proteins (Lowe, 1992). The single electron oxidation and reduction of these centers are very easily and strongly detected. Characteristic EPR spectrum of the nitrogenase MoFe protein is illustrated in Figure 6, that of the Fe protein is not discussed in this thesis because it is peripheral to the author's research. The spectra of whole cells and purified proteins were recorded on a Varian Associates E-line instrument at 9.22 GHz and 20 mW at 12 K maintained by liquid helium boil-off.

2.11.1 Preparation of Sample for EPR Analysis

The EPR tubes used were of 3 × 200 mm (Walmad Glass Co. Inc., Buena, NJ). The atmosphere in the EPR tubes was replaced using an automatic machine (refer to Corbin, 1978). Derepressed whole cells were prepared for EPR spectroscopy as described previously (Scott *et al.*, 1990). Samples of whole cells were prepared by thawing cells under argon and diluting 1:1 with 50 mM Tris-HCl (pH 8.0), 2 mM sodium dithionite. A mixture of 1 ml resuspended cells, 200 µl 20 mM sodium dithionite and 100 µl degassed methyl viologen was let sit at room temperature for 5 - 10 min to reduce the nitrogenase within the *Azotobacter* cells. A 200 µl aliquot was then transferred anaerobically into the argon-filled EPR tube and centrifuged at 600 × g for 5 min. The supernatant was removed and the cell pellet in the EPR tube was frozen in liquid nitrogen from the bottom

up to prevent cracking by gradually lowering the tube in the liquid nitrogen. Samples were stored in liquid nitrogen until ready to be examined.

Samples of crude extracts or purified proteins were taken into the anaerobic glove box for further concentration using the mini-amicon concentrator (Amicon Inc., Beverly, MA) until its concentration was estimated to be $\sim$60 mg/ml for the crude extracts and $\sim$30 mg/ml for the purified proteins. 200 μl of the samples were transferred into the EPR tubes inside the glove box using a syringe. The tubes were then capped and, upon removal from the glove box, frozen immediately in liquid N_2.

2.11.2 Preparations of Samples for Rapid-quench Experiments

The rapid-freeze apparatus is essentially that described by Gutteridge *et al.* (1978). The stepping motor is controlled electronically and delivers a pre-set volume of substrate/protein solution from each syringe at a defined velocity through a Perspex mixing chamber and along a variable length of thick walled nylon capillary tubing. The reaction solution emerges from a jet into an EPR tube that is partially immersed in a stirred iso-pentane bath, which is itself cooled by liquid nitrogen. The sample solution freezes immediately when it comes into contact with the iso-pentane-cooled tube. It has to be carefully packed down into the tube prior to performing the EPR spectroscopy.

Chapter 3 Catalytic Consequences of Substitution at the Nitrogenase MoFe Protein α-277-arginine Residue

This work represents a manuscript that is about to be submitted (Shen, J., Dean, D.R., & Newton, W.E.) solely based on the author's work. We thank Dick Dunham (University of Michigan) for performing some of the EPR spectroscopy and Jeff Bolin and Steve Muchmore (Purdue University) for computer modeling and helpful discussions.

3.1 Introduction

As part of our studies to map the catalytic surface of the nitrogenase FeMo-cofactor (FeMoco), we are substituting amino-acid residues in its polypeptide environment and analyzing the catalytic, redox and spectroscopic consequences (Newton and Dean, 1993). The FeMoco is one of the two prosthetic group types bound within the nitrogenase MoFe protein and there is substantial evidence that implicates FeMoco as the site of substrate reduction (Shah and Brill, 1977; Hawkes *et al.*, 1984; Scott *et al.*, 1990). Substrate reduction is accomplished by sequential associations and dissociations of the two component proteins of nitrogenase and, during each cycle, two molecules of MgATP are hydrolyzed and a single electron is transferred from the Fe protein component (a homodimer of ~63kDa, encoded by *nifH*) to the MoFe protein component (an $\alpha_2\beta_2$ tetramer of ~230kDa, encoded by *nifDK*) (Hageman and Burris, 1980; Lowe and Thorneley, 1984). Recently, the complete structure of both component proteins has been solved by x-ray crystallography (Georiadis *et al.*, 1992; Kim and Rees, 1992a; Kim and Rees, 1992b; Chan *et al.*, 1993; Kim *et al.*, 1993; Bolin *et al.*, 1993; for recent reviews, see Kim & Rees, 1994 and Dean *et al.*, 1993).

The MoFe protein contains 30 iron atoms and 32-34 sulfides distributed

among its two types of prosthetic groups: P-clusters and FeMoco (two copies each of both). Each FeMoco has the composition of Mo:Fe_7:S_9:homocitrate (Kim and Rees, 1992a; Chan *et al.*, 1993) and its properties have been reviewed (Smith and Eady, 1992; Burgess, 1990; Newton 1992). FeMoco is composed of a [4Fe-3S] unit and a [1Mo-3Fe-3S] unit that are bridged by three non-protein-derived inorganic sulfide ligands (Figure 5; Kim & Rees, 1992a; Bolin *et al.*, 1993). As isolated in its native state, the MoFe protein exhibits an S=3/2 electron paramagnetic resonance (EPR) signal that is unique among metallobiomolecules. This EPR signal is associated with the FeMoco because mutant strains, which fail to synthesize FeMoco (for example, *nifE*, *nifN*, or *nifB* mutants), produce an "apoMoFe protein" that has neither catalytic activity nor EPR signal (Shah *et al.*, 1973; Nagatani *et al.*, 1974; Roberts *et al.*, 1978; Hawkes and Smith, 1983; Brigle *et al.*, 1987a; Harris *et al.*, 1990; Paustian *et al.*, 1990). Such inactive apo-MoFe protein may be reconstituted to full catalytic activity and EPR competence by the simple addition of FeMoco extracted from the native MoFe protein.

In the presence of MgATP, a suitable source for reducing equivalents and an anaerobic environment, Mo-nitrogenase catalyzes the reduction of a variety of small molecule substrates. In addition to N_2, nitrogenase catalyzes, among others, the reduction of protons, nitrous oxide, acetylene, azide, hydrogen cyanide, alkyl cyanides, alkyl isocyanides, hydrazine, cyclopropene, and allene. Alternative substrates have often been studied as probes for the nature of substrate-enzyme interactions. Besides nitrogen, the reduction of proton, acetylene, cyanide and azide are the ones that have been studied mostly. Carbon monoxide (CO) is a commonly used inhibitor in the nitrogenase catalyzed reactions. Among the different substrates, proton reduction (Burns *et al.*, 1965) is the only nitrogenase-catalyzed reaction that is not inhibited by CO (Hardy *et al.*, 1965; Bulen *et al.*,

1965). It was reported that H_2 inhibited N_2 evolution, but it did not inhibit reductions of azide, acetylene, cyanide and H^+; and five sites or modified sites were proposed as (1) N_2 and H_2 site, (2) acetylene site, (3) azide, cyanide and methylisocyanide site, (4) CO site, (5) H^+ site (Hwang and Burris, 1972; Hwang, *et al.*, 1973). For the wild-type nitrogenase from *Azotobacter vinelandii*, acetylene or cyanide act as non-competitive inhibitors of nitrogen reduction; nitrogen is a competitive inhibitor of acetylene reduction, and it also inhibits azide and cyanide reductions noncompetitively; CO is non-competitive inhibitor of all of the commonly studied substrate reductions, except H^+ (Rivera-Ortiz and Burris, 1975). The results were interpreted such that nitrogenase serves as an electron sink and substrates and inhibitors bind at multiple modified sites on reduced nitrogenase (reviewed by Burgess, 1985). According to the Lowe/Thorneley model, during nitrogenase catalysis, the Fe protein delivers electrons one at a time to the MoFe protein where substrate reduction takes place. Each electron that the MoFe protein gets from the Fe protein per association/dissociation cycle reduces the enzyme to a more reduced state. The state to which N_2 is bound (probably E_3 and E_4) is more reduced than those states that usually release H_2. Ammonia may be released at the enzyme state of E_5. If the flux of electrons is low, then the oxidation state E_2H_2 will lose H_2 and revert to state E_0. Acetylene is reported to bind reversibly to species E_1H and E_2H_2 of the MoFe protein, whereas the product ethylene is released at enzyme state E_3 (Ashby *et al.*, 1987; Fisher *et al.*, 1990).

Of direct importance to the current studies, α-277-arginine is in a region of the α-subunit polypeptide that includes α-275-cysteine. α-275-cysteine was previously suggested, based on targeted mutagenesis, to provide a mercaptide ligand to the FeMoco (Kent, *et al.*,1989). This proposal has since been confirmed by the determination of the three-dimensional structure of the MoFe protein by x-ray methods (Kim and Rees, 1992a). From the crystallographic structure, it is

known that there is a putative hydrogen bond between the hydroxyl of α-278-serine and the mercaptide sulfur of α-275-cysteine, both of which are highly conserved among nitrogenases of different species (Kim & Rees 1992a; Dean *et al.*, 1993; Kim & Rees, 1994). The α-277-arginine residue is also highly conserved among different organisms, and together with α-192-serine and α-356-glycine, it may be involved in providing the entry/exit route for substrates and products as well as being a component of a channel for FeMoco insertion during biosynthesis of the MoFe protein (Kim & Rees, 1992b). Figure 16 shows the hydrogen-bonding interactions of α-277-arginine with other α-subunit residues located close to the FeMoco, namely the interaction with α-386-aspartate, α-281-tyrosine and α-195-histidine. Because of our previous studies on the altered MoFe proteins with substitutions at α-195-histidine residue (Kim *et al.*, 1994), we targeted α-277-arginine for these studies to determine whether its hydrogen-bonding network through α-195-histidine to FeMoco is important and, if disrupted, would result in similar changes in its properties.

In this report, we: (i) compare the characteristics of nine *Azotobacter vinelandii* mutants, each having a single amino-acid substitution at α-277-arginine in the α-subunit of the MoFe protein at the crude-extract level, with those from the wild-type; (ii) use spectroscopic methods to detect possible changes in the FeMoco polypeptide environment due to the substitutions; and (iii) analyze the N_2-, proton-, acetylene-, cyanide- and azide-reduction properties of the altered α-277^{his} MoFe protein purified from mutant strain DJ788 and compare it with those of the wild-type enzyme isolated from strain DJ527.

3.2 Experimental Procedures

3.2.1 Mutant Strain Construction

Methods for site-directed mutagenesis, gene replacement, and the isolation

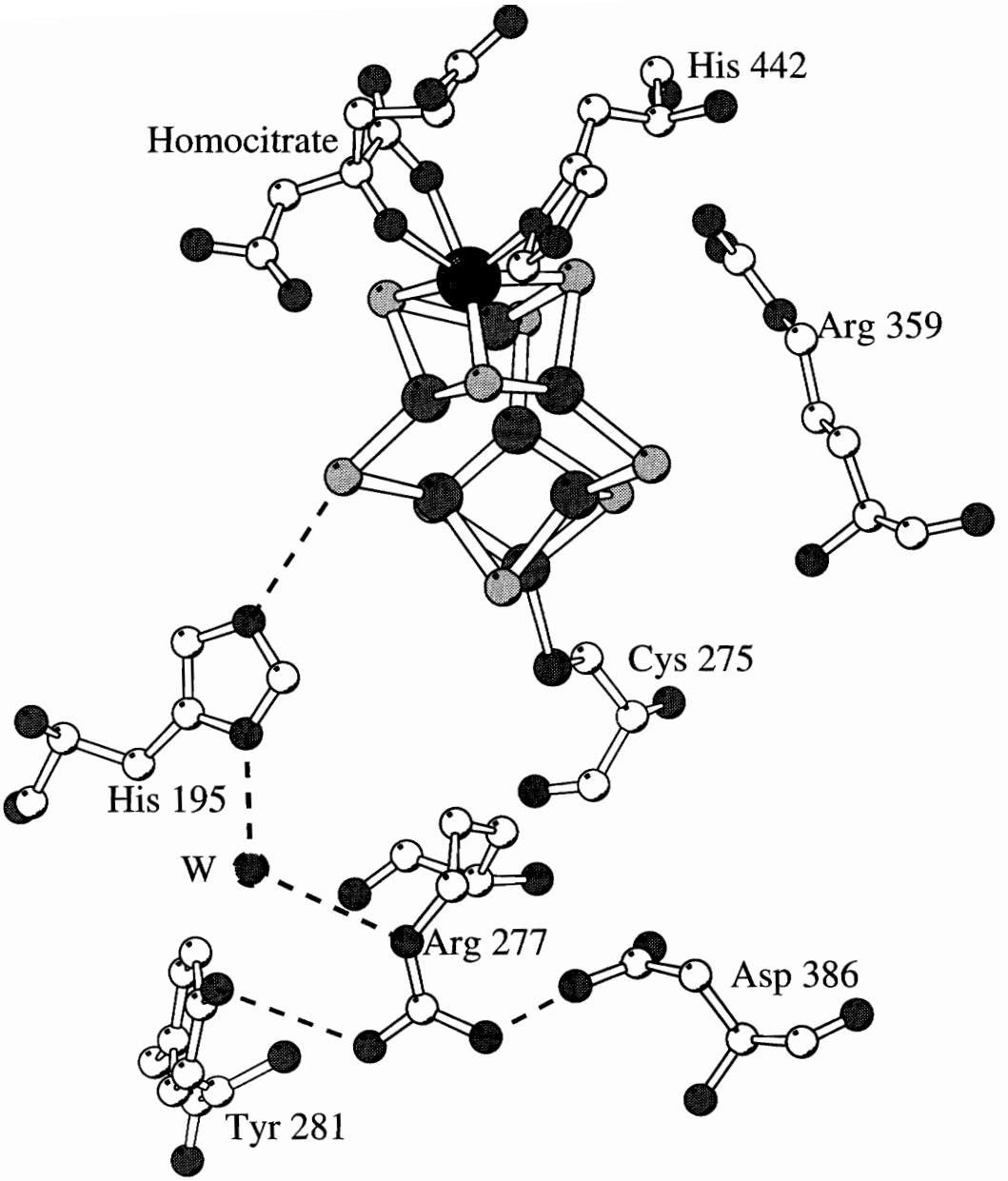

Figure 16. FeMoco and part of its surrounding environment (W: denotes water molecule). Prepared using MOLSCRIPT program with data kindly supplied by Dr. Jeff Bolin at Purdue University.

of mutant strains were performed as described or cited previously (Brigle *et al.*, 1987a, b). The strategy for making a number of mutants at one specific amino-acid residue site is to synthesize chemically an oligonucleotide on which the 3 nucleotides coding for the desired amino-acid residue have been degenerately replaced. For substitution at α-277-arginine of the MoFe protein, the oligonucleotide having the sequence:
5'-CACTGCGTACXXXTCGATGAACTAC-3' (where XXX represents the degenerate codon at the designated residue) was synthesized.

Each altered MoFe protein having a substitution within the MoFe protein α-subunit primary sequence is designated by the name of the subunit (α in this case), the number of the amino-acid position substituted, followed by the three letter code for the substituting amino acid in superscipt form. For example, the altered MoFe protein having α-277-arginine residue substituted by threonine is designated as α-277^{thr}. Strains are designated by their correspondent DJ numbers. DJ527 is a strain, which has mutations at the *hox*KG genes so as to abolish its uptake hydrogenase activity (Hup^-). Its *nif* genes remain intact. All the mutants used in this study are Hup^- strains, which enables us to measure H_2-evolution activity accurately at the crude-extract level without the interference from uptake hydrogenase activity.

3.2.2 Growth Conditions, Media, and Nitrogenase Derepression

Small batches of *Azotobacter vinelandii* wild-type and mutant strains were grown at 30°C in Fernbach flasks on a modified Burk's medium (Strandberg and Wilson, 1968) containing 10 μM Na_2MoO_4, which is sufficient to repress the alternative nitrogenase systems. All chemicals for media preparations were purchased from Fisher Scientific Company (Pittsburgh, PA), except sucrose which was purchased from the Kroger Co. (Cincinnati, OH). Cultures were grown under

Air with flask shaking at 250 rpm. A fixed nitrogen source of filter-sterilized urea was added to a final concentration of 20 mM when required. Large scale *Azotobacter* culture was grown in 28-liter fermentor (New Brunswick Scientific Company, New Brunswick, NJ) on modified Burk's medium as mentioned above. Air flow in fermentor was controlled with a flow meter at 35 ~ 40 liters/min; and the culture was vigorously stirred at 250 rpm with a built-in stirrer. Growth of *Azotobacter* cultures were monitored using a Klett-Summerson meter (Klett Mfg. Co. Inc., New York) equipped with a no.54 filter. All mutant strains that do not grow or grow slowly in nitrogen-free media were grown on urea-supplemented media and then derepressed for nitrogenase synthesis as described previously (Jacobson *et al.*, 1989). Culture was grown in nitrogen-containing Burk's medium until its density reached 150-200 Klett units. In Fernbach flask, the culture was centrifuged at 10,400 × *g* for 10 min to remove the medium and cell pellet resuspended in nitrogen-free medium; in fermentor, the culture was concentrated to 2 liter by filtration using a Watson-Marlow 601S/R peristaltic pump and a Millipore (Pellicon) cassette system fitted with 0.22 Å Pellicon filter in order to remove as much of the nitrogen source as possible, and then reinoculated into 24 liters of Burk's nitrogen-free medium. After derepression for 3 hours in nitrogen-free medium, culture medium was then removed and the cells isolated by centrifugation as before. *Azotobacter* cells were stored at -80°C until used.

3.2.3 Crude Extract Preparation

Cells were thawed and diluted anaerobically at 4°C in degassed 50 mM Tris-HCl, pH 8.0, containing 2 mM sodium dithionite, at the approximate ratio of 1.0 g of cells to 2.0 ml of buffer. The cell suspension was broken with 3-min pulse sonication using a Heat System Sonicator model XL2015 in a 25-ml Rosette cooling cell (Heat Systems-Ultrasonics, Inc.) immersed in an ice water bath to

offset increasing temperature. The extract was transferred anaerobically into centrifuge tubes and centrifuged for 60 min at 98,000 × *g* at 4°C. The supernatant was frozen dropwise to liquid nitrogen and the frozen pellets stored in liquid nitrogen until used.

3.2.4 Protein Purification

The altered α-277^{his} MoFe protein of the mutant strain, DJ788, and the wild-type (α-277^{arg}) MoFe protein from strain DJ527 were purified in parallel. Cells of both strains to be used for protein purification were grown up using a 28-liter fermentor (see Cell Growth Section). Crude extract was prepared on a large scale using a Manton-Gaulin homogenizer to break the cells which were thawed under Ar atmosphere and diluted 1:2 with degassed 50 mM Tris-HCl (pH 8.0), 2 mM sodium dithionite. A heat step at 56°C for 5 min was included before centrifugation at 98,000 × *g* at 4°C for 1 hour to separate the cell debris from the soluble protein supernatant. Partial purification of the MoFe protein was achieved by chromatography over DE52-cellulose (Whatman Biosystems Ltd, England) followed by a Q-sepharose column (Pharmacia LKB, Sweden), both of which were anaerobically equilibrated with 25 mM Tris-HCl (pH 7.4), 1 mM sodium dithionite. This resulted in ~70% recovery of MoFe-protein activity, that was devoid of Fe-protein activity. MoFe protein off the DE52-cellulose column was diluted 1:3 with 25 mM Tris-HCl (pH 7.4), 2 mM sodium dithionite, before loading onto the Q-sepharose column. On both DE52-cellulose and Q-sepharose columns, a linear NaCl gradient from 0.1 M to 1.0 M in degassed 25 mM Tris-HCl (pH 7.4), 1 mM sodium dithionite, was applied, and both wild-type (α-277^{arg}) and α-277^{his} MoFe proteins eluted at ~0.2 M NaCl off the DE52-cellulose column and at ~0.35 M NaCl off the Q-sepharose column. Further purification of the MoFe proteins was achieved by the Sephacryl S-300 gel filtration (Pharmacia

LKB, Sweden) chromatography using degassed 0.2 M NaCl in 25 mM Tris-HCl (pH 7.4), 1 mM sodium dithionite, to yield pure samples of both MoFe proteins. Wild-type (α-277^{arg}) MoFe protein purified in this way has specific activity of 1760 nmol of ethylene formed per minute per mg; while altered α-277^{his} MoFe protein has 1020 nmol of ethylene formed per minute per mg.

The wild-type Fe protein used in the assays was purified from *Azotobacter vinelandii* wild-type as described previously (Burgess *et al.*, 1980b) and had a specific activity of 2060 nmol of hydrogen formed per minute per mg.

3.2.5 Protein Estimation

BCA method was used for protein estimation with bovine serum albumin (0 - 0.1 mg/ml) as a standard (Smith *et al.*, 1985).

3.2.6 Nitrogenase Activity Assay

MoFe-protein and Fe-protein specific activities were measured in both crude extracts and purified proteins as described below in the presence of an optimal amount of purified complementary component protein. Assays were performed in 9.25-ml reaction vials fitted with butyl rubber stoppers and aluminum seals. Each 1.0-ml reaction volume contained 25 mM Tes-KOH, pH 7.4 (25 mM Hepes-KOH in the purified protein assays), 2.5 mM ATP, 5.0 mM $MgCl_2$, 30 mM creatine phosphate, 0.125 mg creatine phosphokinase, and 20 mM $Na_2S_2O_4$. All chemical reagents were purchased from Sigma Chemical Company (St. Louis, MO), except $Na_2S_2O_4$, which was from Mallinckrodt Chemical Company (Berkeley, CA). For crude-extract activity assays, 50-μl of crude extract was used in each assay. Three levels of titration assays were done on each extract using excess amount of purified complementary protein to determine its maximum MoFe or Fe protein activities. In assays with purified proteins, a total of 0.5 mg of

nitrogenase proteins in 1 ml was used to avoid complications introduced by both high and low protein concentrations. Usually, an Fe-protein to MoFe-protein molar ratio of 20 is used in the activity assays involving purified proteins. Protein concentrations were determined by the BCA method (Smith *et al.*, 1985). Each assay was started by the addition of either the crude extract or the purified protein to the otherwise complete reaction system in the reaction vial, which had been preincubated for 5 minutes, and was terminated by the addition of 0.25 ml 0.5 M Na_2EDTA (pH 7.5) after 8 minutes. When required, CO was added by gas-tight Hamilton syringe (Reno, Nevada) to the appropriate assay vial during the preincubation period.

3.2.7 Substrate Preparations

All reaction vials were subject to four cycles of evacuation and flushing using an automated machine (Corbin, 1978) to replace the air with either 100% Ar or 100% N_2 depending on the type of assay followed. In C_2H_2-reduction assays, dilution of 100% Ar with aliquots of C_2H_2 produced from calcium carbide (Fisher Scientific) was used to produce the desired C_2H_2 concentrations in each reaction vial. H^+-reduction assays were performed under a 100% Ar gas phase.

Appropriate aliquots of a 100 mM NaN_3 in 25 mM Hepes-KOH (pH 7.4) stock solutions were added accordingly into each reaction vial before the atmosphere replacement step. For NaCN-reduction assays, a known amount of a 100 mM degassed NaCN in 25 mM Hepes-KOH (pH 7.4) stock solution was injected into each reaction vial during the pre-incubation period. It was known that in NaN_3-reduction assays, HN_3 is actually the substrate. At pH 7.4, the concentration of HN_3 can be calculated by multiplying the NaN_3 concentration using a constant of 1.582×10^{-3} (Rubinson *et al.*, 1985). HCN, on the other hand, was proposed to be the substrate of NaCN (Li *et al.*, 1982), whose concentration

can be calculated using the formula of [HCN] = 0.981×[NaCN], at pH 7.4.

3.2.8 Product Analysis

C_2H_4 and CH_4 produced was quantified by gas chromatography on a Poropak N column using a flame ionization detector (Shimadzu, Tokyo, Japan). H_2 production was quantified by gas chromatography on a molecular sieve 5A column and a thermal conductivity detector (Shimadzu, Tokyo, Japan). Calibrations were performed using standard gases of 1 ppm C_2H_4/100% helium, 1 ppm CH_4/100% helium, 1% H_2/100% N_2 purchased from Scotty Specialty Gases (Plumsteadville, PA) respectively. Ammonia can be detected using a method of phenol/hypochlorite colorimetry (Dilworth *et al.*, 1992). Hydrazine (N_2H_4) production in the azide-reduction assays were measured using the p-dimethylaminobenzaldehyde colorimetric assay method (Dilworth and Thorneley, 1981).

3.2.9 Buffers Used in the Studies

Several buffers were used throughout these studies. Crude-extract preparation and protein purification were performed in 50 mM Tris-HCl (pH 8.0) and 25 mM Tris-HCl (pH 7.4) respectively. The purified protein was dialyzed into 25 mM Tes-KOH or 25 mM Hepes-KOH (pH 7.4) depending on the types of activity assays to be performed. For example, all crude-extract activity assays were performed in Tes-KOH buffer; all the assays on purified proteins that would involve ammonia determinations were done in Hepes-KOH buffer to minimize inhibition of color development (Dilworth *et al.*, 1992). The pH-profile studies of the activity of the purified protein were performed in a three-buffer system (containing 38 mM Hepps, 38 mM Ches and 75 mM Bistris, adjusted to the desired pHs by addition of either H^+ or OH^-) developed to maximize the buffer

capacity (Pham and Burgess, 1993).

3.2.10 Gel Electrophoresis

For sodium dodecyl sulfate-polyacrylamide gel electrophoresis, samples and gels were prepared according to Laemmli (1970). The gels used were 12% polyacrylamide (1.35% cross-linker) with a 4% stacking gel. Electrophoresis was performed at 30 mA/gel in a Hoefer Mighty Small apparatus (Hoefer, San Francisco, CA), using 10,000 - 100,000 low molecular weight standards (Biorad Laboratories, Hercules, CA) and the gels stained with Coomassie Blue (R-250).

3.2.11 Electron Paramagnetic Resonance Spectroscopy

Derepressed whole cells were prepared for EPR spectroscopy as described previously (Scott *et al.*, 1990). The spectra of whole cells and purified proteins were recorded on a Varian Associates E-line instrument at 9.22 GHz and 20 mW at 12 K maintained by liquid helium boil-off.

3.3 Results

3.3.1 Characteristics of Diazotrophic Growth and Nitrogenase Catalytic Activities in Crude Extracts

α-277-arginine of MoFe protein is a strictly conserved residue among molybdenum-dependent nitrogenases from different organisms (Dean and Jacobson, 1992). All of the mutant strains having a site-specific point mutation at residue α-277-arginine in the MoFe protein of *Azotobacter vinelandii* were produced using site-directed mutagenesis and gene replacement methods (for details, see Experimental Procedures). Table 4 summarizes the MoFe-protein and Fe-protein specific activities for crude extracts prepared from nitrogenase derepressed wild-type and the mutant strains along with their genotype and

Table 4. Diazotrophic growth rates of α-277-arginine mutant strains and their crude extract MoFe protein and Fe protein activities.

Strain[a]	Substitution at α-277	Codon	D.T.[b] (Hrs)	Under C_2H_2[c]		Under Ar[d]	
				C_2H_4	H_2	MoFe H_2	Fe H_2
DJ527	None (Arg)	CGC	2.0	78	6.4	78	40
DJ974	Lys	AAG	3.2	20	3.7	27	21
DJ679	Cys	TGC	4.0	51	2.6	51	30
DJ681	Thr	ACC	5.0	37	7.5	46	36
DJ978	Phe	TTC	6.0	21	5.3	32	34
DJ976	Leu	CTC	12.7	15	3.9	20	34
DJ788	His	CAC	N/G	27	16	46	37
DJ745	Gly	GGC	N/G	3.5	0.6	3.7	29
DJ747	Pro	CCT	N/G	5.8	0.1	4.0	19

[a] All strains are deleted for the uptake hydrogenase structural genes resulting in Hup$^-$ phenotype.

[b] D.T. denotes the doubling time of the corresponding *Azotobacter* strain grown in air on nitrogen-free Burk's medium. N/G indicates no growth under these conditions for the individual strain.

[c] MoFe-protein specific activity in the crude extract is listed as nmole of C_2H_4 and H_2 produced per minute per mg total protein under a 10% C_2H_2/90% Ar atmosphere in the presence of optimal amount of purified Fe protein.

[d] MoFe-protein and Fe-protein specific activities in the crude extract are listed as nmole of H_2 produced per minute per mg of total protein under a 100% Ar atmosphere. All assays were performed with optimal amount of purified complementary protein present.

diazotrophic growth behavior expressed as exponential growth doubling time. Also studied in the crude-extract assays were the carbon monoxide (CO) inhibition patterns for their acetylene- and proton-reduction activities. None of the α-277-arginine mutants displayed a different CO sensitivity pattern when compared to wild-type, *i.e.*, only acetylene- but not proton-reduction activities in the crude extracts were CO sensitive.

Mutations at residue α-277-arginine gave a complete range of phenotypes, from Nif^+ through Nif^{slow} to Nif^-. Only the substitution of α-277-arginine with lysine gave a Nif^+ strain; substitution with threonine, cysteine, leucine or phenalanine produced strains with a Nif^{slow} phenotype; while strains with proline, glycine or histidine substitution became Nif^-. The crude extracts from the mutant strains had lower acetylene- and proton-reduction activities compared to the wild type in line with their differences in diazotrophic growth behavior. Although the Nif^- strains cannot fix N_2 at a level sufficient to support diazotrophic growth, crude extracts prepared from the mutant strains exhibit various levels of acetylene- and proton-reduction activities ranging from 5% to 60% of the H_2-evolution activity of the wild-type, most of which correlated well with their diazotrophic growth capacity. The only extraordinary one is mutant strain DJ788 (α-277^{his}) whose MoFe protein acetylene- and proton-reduction activities are 50% ~ 60% of the corresponding wild-type (α-277^{arg}) activities despite the fact that the strain cannot grow diazotrophically. In addition, its electron distribution between ethylene and hydrogen production under a 10% C_2H_2/90% Ar atmosphere is very different from that of the wild-type, indicating that substrate specificity has changed in the α-277^{his} MoFe protein. No ethane was detected in any of the crude extracts assayed under an C_2H_2 atmosphere.

3.3.2 Whole-cell EPR Spectra

From the EPR-spectroscopic analysis of nitrogenase-derepressed whole cells, we found all of the altered MoFe proteins studied, except for α-277^{lys}, displayed significantly changed EPR signals in the $g = 4$ region. The EPR spectrum of the α-277^{lys} MoFe protein, as might be expected by the conservative nature of the substitution, contained only a very minor rhombic shift to $g = 4.35$ and $g = 3.63$ compared to the wild-type values of $g = 4.34$ and 3.65 with no change in linewidth or line shape of either resonance. A very similar situation holds for DJ679 (α-277^{cys}) cells, which also grow well on N_2 and have respectable H_2-evolution rates in crude extracts, because the EPR intensities are comparable ($\sim$65% of wild type) although a slight axial ($g = 4.30$ and 3.72) distortion is obvious here. The other substitutions that cause an increase in the rhombicity of the signal, are the hydrophobic residues, leucine ($g = 4.39$ and 3.57) and phenylalanine ($g = 4.57$ and 3.49), both of which also slightly broaden the resonances. Both substitutions produce diminished EPR intensity in the range 25-40% of wild type in line with their slower diazotrophic growth rates and their lower H_2-evolution activities. Cells of strains DJ745 (α-277^{gly}) and DJ747 (α-277^{pro}) exhibit very weak EPR-signal intensities ($<$10% of wild type), which is also consistent with their Nif$^-$ phenotypes and almost non-existent H_2-evolution activities. In contrast, EPR spectra from the α-277^{his} and α-277^{thr} MoFe-protein in strains DJ788 and DJ681 respectively, are dramatically altered. Both substitutions produce more than the expected two EPR lines in the $g = 4$ region, both have significant EPR intensities with DJ788 being $\sim$70% and DJ681 $\sim$50% of wild-type intensity, both have H_2-evolution activities of 50-60% of wild type, but only DJ681 (α-277^{thr}) cells are capable of diazotrophic growth. The EPR spectrum elicited from DJ681 cells has two resonances at $g = 3.76$ and 3.56, but three lines at $g = 4.50$, 4.30, 4.03. It is not certain which line pairs with which other

because of their similar intensities, but by comparison with the spectrum of DJ788 (see below), it is likely that the $g = 4.50$ line should be paired with $g = 3.56$ and the $g = 4.03$ line with the $g = 3.56$ line. The origin of the $g = 4.30$ resonance is then unclear, but may be due to contaminating ferric iron. For DJ788 (α-277^{his}) cells, two sets of signals are observed; the major pair of resonances at $g = 4.31$ and 3.64, which are close to wild-type values, account for $\sim 80\%$ of the signal intensity and the minor rhombically distorted pair at $g = 4.52$ and 3.57 account for the remaining $\sim 20\%$ of the intensity.

The considerable EPR intensity observed in whole cells for all these altered MoFe proteins (except α-277^{pro} and α-277^{gly}) indicates that each of these proteins has a full complement of FeMoco. The variety of changes in their EPR spectra elicited by these substitutions clearly indicates that the α-277-arginine residue impacts the properties of the bound FeMoco.

3.3.3 Purification of the Altered MoFe Protein from DJ788

Results from crude extract activities and EPR spectra promised an interesting phenotype for the MoFe protein with histidine replacing arginine at position α-277. Thus, the α-277^{his} MoFe protein from strain DJ788 was purified in order to further characterize its catalytic properties and to ask whether or not N_2 can bind to the protein and either be utilized as a substrate or act as an inhibitor of the reduction of other common nitrogenase substrates. MoFe proteins from both DJ788 and wild-type strains were purified in parallel to minimize any variation potentially introduced by different purification protocols. Table 5 is the purification table of MoFe proteins of wild-type (α-277^{arg}) and α-277^{his}. Similar levels of purification were achieved for both wild-type (α-277^{arg}) and α-277^{his} MoFe proteins as judged by their MoFe-protein activities and migration pattern on SDS- polyacrylamide gel electrophoresis (PAGE). At all stages of purification,

Table 5. MoFe Protein Purification Table from DJ527 (α-277^{arg}) and DJ788 (α-277^{his}).

Purification Step	Total Protein ($\times 10^2$) (mg)		Total Activity ($\times 10^6$) nmolH_2/min		Specific Activity (nmolH_2/min/mg)		Fold Purification		Yield (%)	
	WT	RH	WT	RH	WT	RH	WT	RH	WT	RH
Crude Extract[a]	120	134	1.26	0.78	105	58	1	1	100	100
DE-52 cellulose	18	20	1.00	0.59	546	291	5	5	79	76
Q-sepharose	8.9	11.5	0.88	0.53	978	451	9	8	69	67
Sephacryl S-300	2.6	3.4	0.63	0.33	2450	993	23	17	49	43

[a] Crude Extracts were obtained using a Manton-Gaulin homogenizer to break the cells followed by heat treatment of 56°C for 5 minutes, and centrifugation at 98,000$\times g$ for 1 hour to separate cell debris from the soluble protein supernatant.

the α-277^{his} MoFe protein exhibited ~40% of the activity of the wild-type MoFe protein. After Sephacryl S-300 gel filtration, these protein had specific activities of 2450 and 980 nmol H_2/min per mg, respectively. Analysis of the purified wild-type (α-277^{arg}) and α-277^{his} MoFe proteins using SDS-PAGE reveals two bands which correspond to the α- and β-subunits of the MoFe protein (Figure 17).

In addition, in crude extracts, we noted that the altered α-277^{his} MoFe protein allocated ~35% of total electron flow to hydrogen evolution under a 10% C_2H_2/90% Ar atmosphere. The same distribution was found for the purified α-277^{his} MoFe protein (see Table 5 & 8). In contrast, there was only 10% of total electrons going to hydrogen evolution under a 10% C_2H_2/90% Ar atmosphere in both wild-type crude extract and purified forms. The EPR spectrum of purified α-277^{his} MoFe protein also retained the same line shape and g-values in the $g = 4$ region as were observed in the whole-cell spectrum. The proportions of the major and minor set of FeMoco resonances remained at 4:1. These observations indicated that no changes were introduced catalytically after purification, and its FeMoco environment in the purified α-277^{his} MoFe protein remained the same as in the whole cell.

3.3.4 pH and Temperature Profile of the Altered α-277^{his} and Wild-type (α-277^{arg}) MoFe Proteins

When assays were performed at different pHs in order to probe the relationship between pH and electron allocation to proton reduction for the purified wild type and α-277^{his} MoFe proteins, a consistently higher percentage of electrons were used for H_2 evolution by the altered protein compared to that of the wild-type throughout the pH range from 6.0 to 9.0. However, changes in pH did not affect the electron distribution ratio between C_2H_4 and H_2 under 10% C_2H_2/90% Ar for either protein. At all pHs used from 6.5 to 8.5, the ratio of H_2:C_2H_4 production

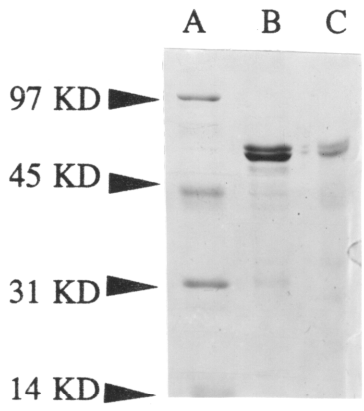

Figure 17. SDS-PAGE of purified MoFe proteins from DJ788 (α-277^{his}) and wild-type (α-277^{arg}). Lane A: Molecular weight marker; Lane B: purified α-277^{his} MoFe protein; Lane C: purified wild-type MoFe protein.

remained at 0.33 ~ 0.35:1 for α-277^{his} MoFe protein and 0.08 ~ 0.10:1 for wild type. For the more extreme pHs of 6.0 and 9.0, the ratio of H_2:C_2H_4 was 0.16:1 and 0.92:1 respectively for the α-277^{his} MoFe protein; and 0.04:1 and 0.52:1 for the wild type (α-277^{arg}).

We also performed experiments in which higher than usual concentrations of C_2H_2 were used in the assays to test if the higher concentrations of C_2H_2 would compete more effectively with H^+-reduction for the α-277^{his} MoFe protein. A parallel experiment was performed for wild-type MoFe protein. Results showed that C_2H_2-reduction activities from both α-277^{his} and wild-type (α-277^{arg}) MoFe proteins maximized at a 20% C_2H_2/80% Ar atmosphere. This agrees with the published optimal C_2H_2 concentration of 0.2 atm for the wild-type MoFe protein (Hwang & Burris, 1972). Concentrations higher than 0.2 atm C_2H_2 become self-inhibitory to its reduction catalyzed by both proteins. However, the percentages of electrons going to H_2 evolution for both MoFe proteins remain comparable with consistently higher numbers for α-277^{his} MoFe protein throughout the C_2H_2 concentrations tested in the study.

In order to test whether or not the altered α-277^{his} MoFe protein can reduce N_2 at a higher temperature, and to determine any changes in the electron distribution pattern at higher temperatures, we elevated assay temperatures from 30°C to 48°C in 5°C increments for individual experiments involving wild-type α-277^{arg} and α-277^{his} MoFe proteins under 100% Ar, 100% N_2 and 10% C_2H_2/90% Ar atmospheres. For the α-277^{his} MoFe protein, no detectable amount of C_2H_6 was produced in any of the C_2H_2-reduction assays; nor was there any NH_3 produced in N_2-reduction assays. Furthermore, a consistently higher ratio of electrons allocated to H_2 evolution versus C_2H_4 production with the α-277^{his} MoFe protein compared to that of wild-type remained throughout the temperature range. Although the MoFe protein from wild-type strain remained perfectly active, the α-

277^{his} MoFe protein lost 50% of its total catalytic activity under 10% C_2H_2/90% Ar at 48°C. However, both MoFe proteins showed higher levels of H_2-reduction activity under 100% Ar at 48°C. When both MoFe proteins were incubated at 48°C for 5 min before being cooled on crushed ice and used in the activity assays at 30°C, the results showed no denaturation effect on the proteins because both proteins retained their full H^+- and C_2H_2- reduction activities.

3.3.5 MoFe Protein from DJ788 (α-277^{his}) does not Bind or Reduce N_2

Unlike wild-type (α-277^{arg}) MoFe protein with which N_2 acts as an inhibitor to both hydrogen evolution and ethylene production (competitively) (Rivera-Ortiz and Burris, 1975), the α-277^{his} MoFe protein did not respond to the presence of N_2 in assays. We were unable to detect either NH_3 production from N_2 reduction catalyzed by the purified α-277^{his} MoFe protein or the formation of N_2H_4 by using the acid-quenched reaction assay (Thorneley *et al.*, 1978). In addition, neither proton- nor acetylene-reduction activities, which were assayed under 100% Ar and 10% C_2H_2/90% Ar atmospheres and compared to activities under 100% N_2 and 10% C_2H_2/90% N_2 atmospheres, showed any differences under any of the four atmospheres. Thus, N_2 is not an inhibitor of either substrate with the α-277^{his} MoFe protein. The MgATP hydrolysis rates remained constant at 4.4$\pm$0.2 ATP/2e$^-$ for both wild-type (α-277^{arg}) and α-277^{his} in all four experiments. The above evidence clearly demonstrates that N_2 neither binds nor is reduced by the altered α-277^{his} MoFe protein.

3.3.6 CO Inhibition Studies on C_2H_2-reduction Activities from Both Wild-type (α-277^{arg}) and α-277^{his} MoFe Proteins at High and Low Electron Flux

In the presence of saturating amounts of wild-type Fe protein (Fe protein to MoFe protein molar ratio of 20:1), the electron flux through either the wild-type

(α-277^{arg}) or α-277^{his} MoFe protein is constant and independent of the substrate (H^+, acetylene) being reduced. Under a 10% acetylene/90% Ar atmosphere, ethylene is the only hydrocarbon product. When 10% CO is present, the flux through either MoFe protein remains effectively unchanged and the only observable product is H_2. When 200 ppm of CO was added into the acetylene-reduction assay vials in order to partially inhibit the reduction of acetylene. The wild-type MoFe protein displayed a normal hyperbolic response on Michaelis-Menton plots, which gave linear Lineweaver-Burk plots under the same condition (Figure 18). Unlike wild-type protein, when 200 ppm CO was added to the acetylene-reduction assays catalyzed by the α-277^{his} MoFe protein, the production of ethylene responded sigmoidally to acetylene concentrations used. As is shown in Figure 19, for the altered α-277^{his} MoFe protein, the reciprocals of the ethylene production rates are not linear functions of the reciprocals of acetylene concentrations in the presence of smaller concentrations of CO, rather, these plots are curves. This result is consistent with the classic model of cooperativity and, from a Hill plot, we estimated $n = 1.6$ for the number of acetylene-binding sites on the enzyme. The plot of $1/v$ (here, v = specific activity of ethylene production) versus 1/[S] (here, [S] = acetylene concentration used in the assays) for the allosteric α-277^{his} MoFe protein in the presence of limiting amount of CO, is curved and approaches a horizontal line which intersects the $1/v$-axis at $1/V_{max}$. If the system is an $n = 2$ allosteric enzyme, we would expect to see a linear plot of $1/v$ versus $1/[S]^2$ (Segal, 1975). As expected, plots of $1/v$ versus $1/[S]^2$ in the α-277^{his} MoFe protein-catalyzed C_2H_4 production in the presence of CO yielded straight lines, as shown in Figure 20. However, on the same plot, in the absence of CO, the $1/v$ is not a linear function of $1/[S]^2$ indicating no cooperativity under this condition. Therefore, we conclude that the C_2H_4 production catalyzed by the altered α-277^{his} MoFe exhibits strong cooperativity among two sites in the presence

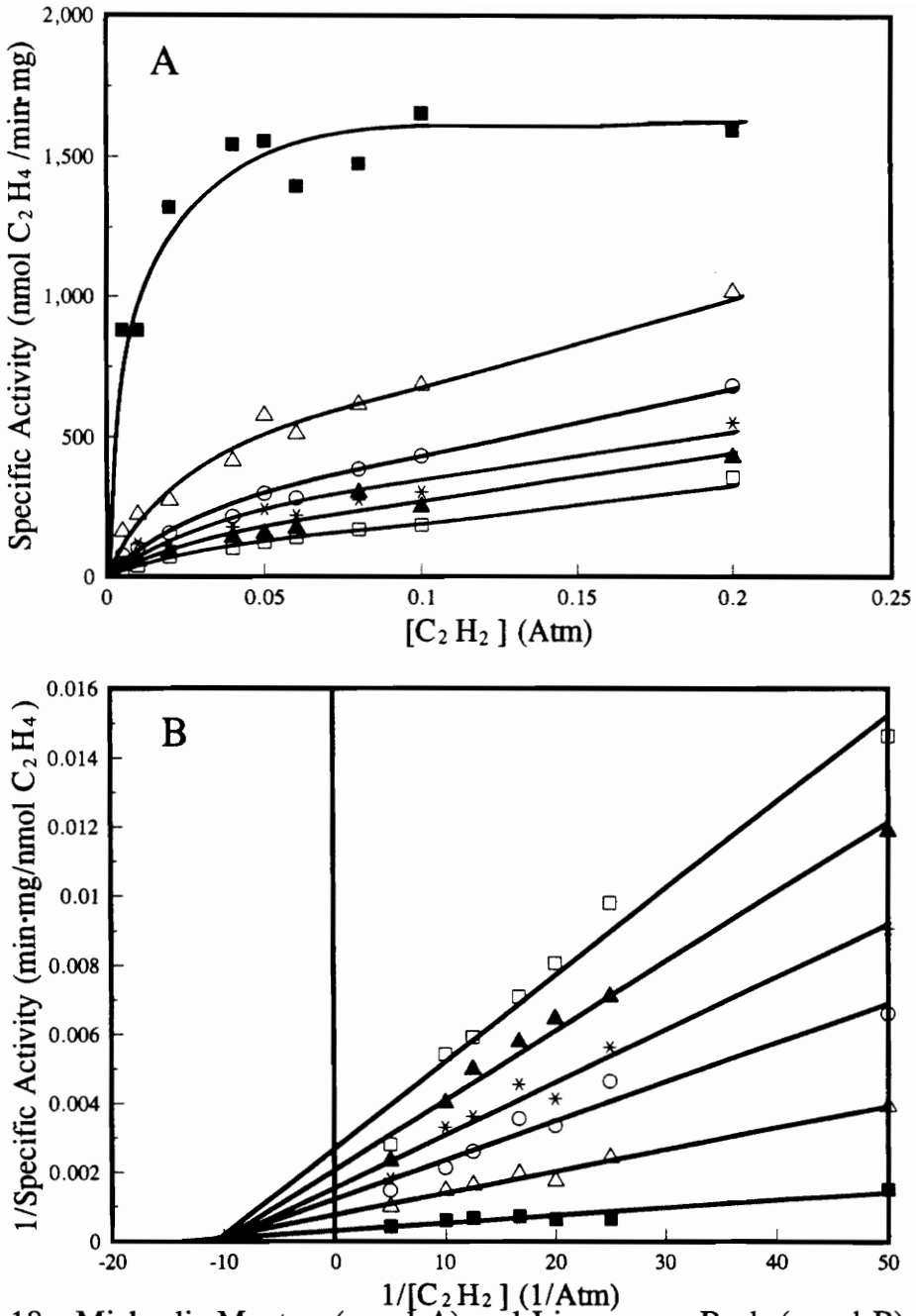

Figure 18. Michaelis-Menton (panel A) and Lineweaver-Burk (panel B) plots of wild-type MoFe protein C_2H_2-reduction reactions in the absence and presence of CO. Amount of CO used in the C_2H_2-reduction reactions are represented as, ■ (no CO); ▵ (6.25×10^{-4}atm CO); ○ (1.25×10^{-3} atm CO); * (1.9×10^{-3} atm CO); ▲ (2.5×10^{-3} atm CO); □ (3.1×10^{-3} atm CO).

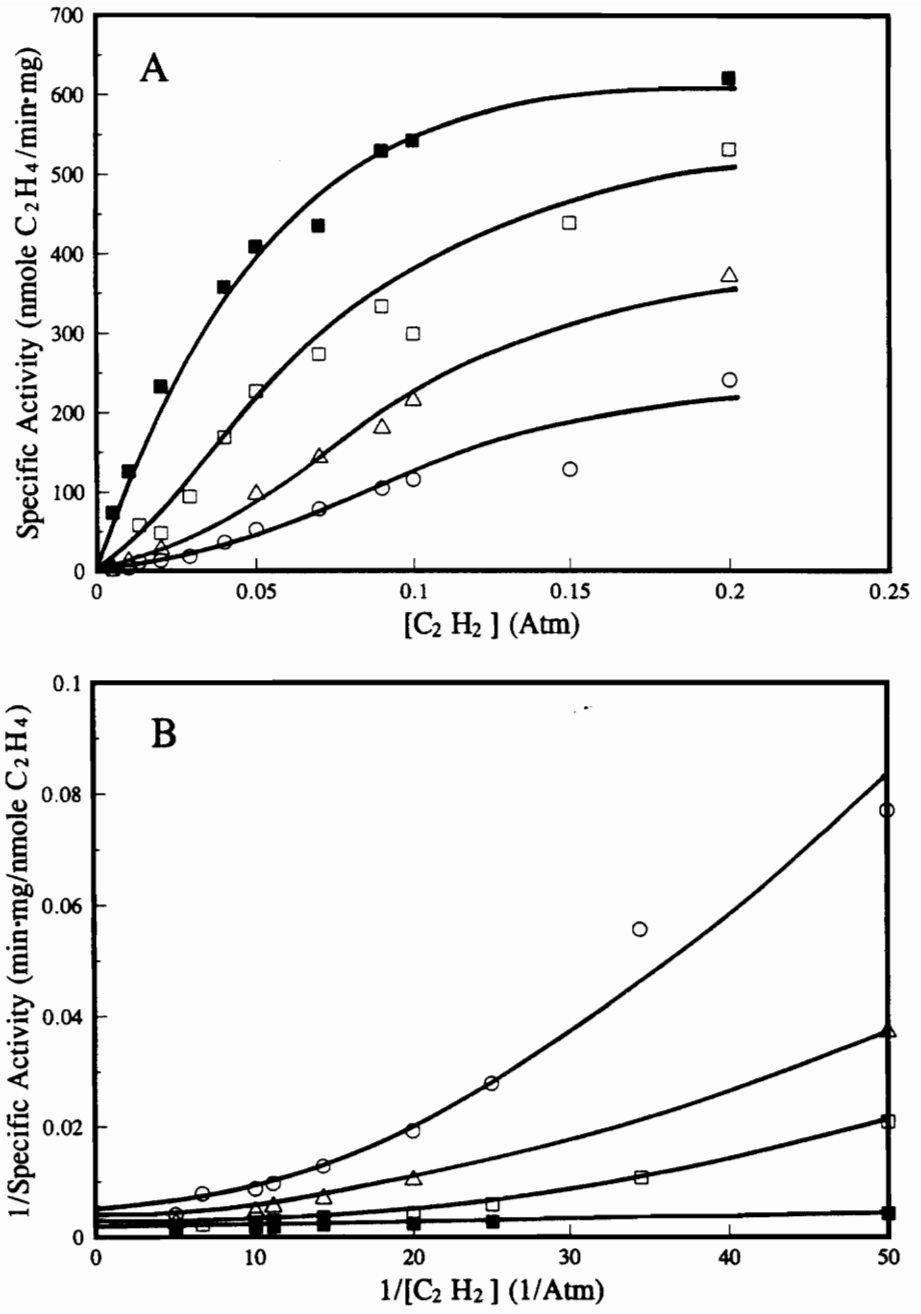

Figure 19. Michaelis-Menton (panel A) and Lineweaver-Burk (panel B) plots of α-277^{his} MoFe protein C_2H_2 -reduction reactions in the absence and presence of CO. Amount of CO used in the C_2H_2-reduction reactions are represented as, ■ (no CO); □ (2.5 × 10^{-4} atm CO); ▵ (6.25 × 10^{-4}atm CO); ○ (1.25 × 10^{-3} atm CO).

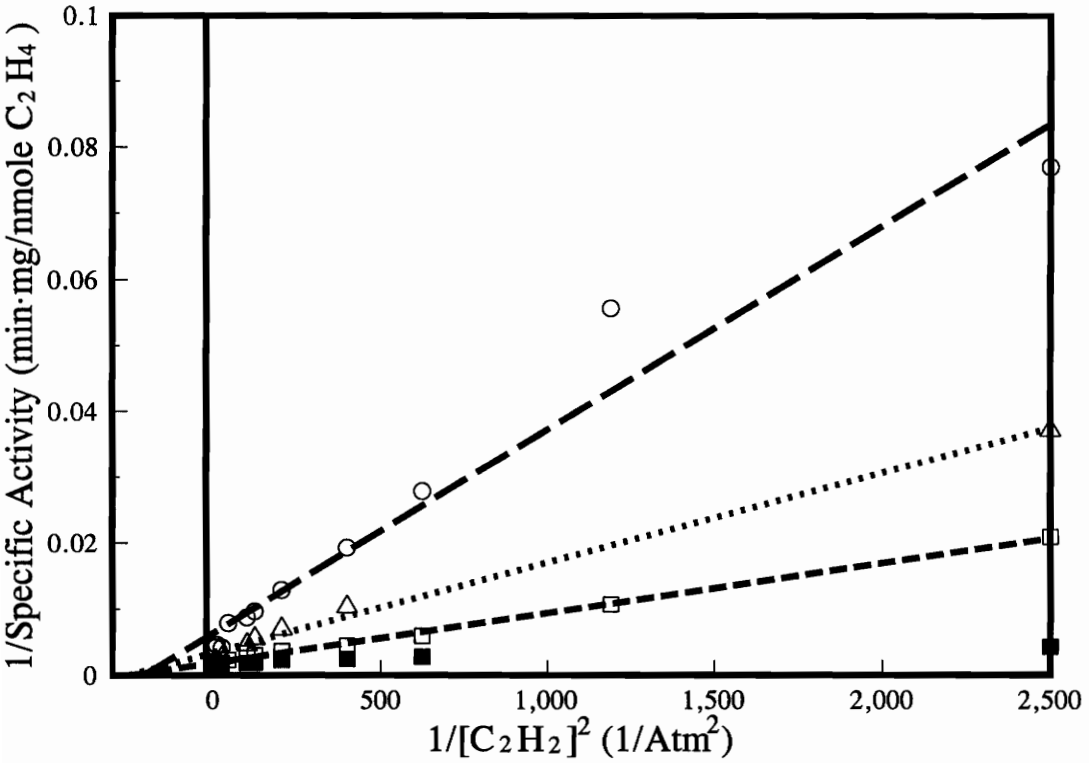

Figure 20. Plot of $1/v$ versus $1/[S]^2$ for the α-277^{his} MoFe protein exhibiting strong cooperative substrate binding ($n = 2$). Amount of CO used in the C_2H_2 reduction reactions are represented as, ■ (no CO); □ (2.5×10^{-4} atm CO); ▵ (6.25×10^{-4}atm CO); ○ (1.25×10^{-3} atm CO).

of CO.

For wild-type (α-277^{arg}) MoFe protein, a K_m of 0.005 atm C_2H_2 and a V_{max} of 1770 nmole C_2H_4/min/mg were calculated, with its K_i of 0.00015 atm of CO inhibition, using the Fig.P program (Biosoft, Ferguson, MO). These results fall within the range of values for these parameters reported previously (Hwang & Burris, 1972; Hwang *et al.*, 1973). For the α-277^{his} MoFe protein, a K_m of 0.051 atm C_2H_2 and a V_{max} of 870 nmole C_2H_4/min/mg were obtained using the same method and the K_i for CO was calculated to be 0.00014 atm (Table 6).

When assays were done under limiting amount of Fe protein (Fe protein to MoFe protein molar ratio of 2:1), *i.e.* low electron flux, the overall substrate reduction rates for both wild type and α-277^{his} MoFe proteins were lower than that at high flux. For wild-type MoFe protein, under an C_2H_2/Ar atmosphere and at low flux condition, there are fewer electrons going to C_2H_2 reduction than at high flux condition, and the loss of activity in C_2H_4 production can be partially compensated by the increase in H_2 evolution activity. Nevertheless, the sigmoidal behavior of C_2H_2 reduction by the α-277^{his} MoFe protein in the presence of CO was retained under low flux conditions.

Thus, the K_m values for C_2H_2 reduction by wild type (α-277^{arg}) and altered α-277^{his} proteins suggest that the altered MoFe protein has a lower affinity for C_2H_2, but the same K_i for CO inhibition for both MoFe proteins suggest that the affinity for CO is unchanged.

Table 6. Kinetic Parameters for purified MoFe proteins from DJ527 (α-277^{arg}) and DJ788 (α-277^{his}) for a variety of alternative substrates.

Substrate/ Product	DJ527 (α-277^{arg})		DJ788 (α-277^{his})	
	V_{max}[a]	K_m	V_{max}[a]	K_m
C_2H_2/C_2H_4	1770	0.005 atm C_2H_2	870	0.051 atm C_2H_2
H^+/H_2	2040	---	982	---
HCN/CH_4	135	2.6 mM[b] HCN	119	1.1 mM[b] HCN
HN_3/N_2H_4	158	7.1 μM[b] HN_3	113	24.2 μM[b] HN_3

[a] One unit of specific activity equals 1 nmole of product formed per minute per mg of total protein in each assay, which contained a saturating amount of wild-type purified Fe protein.

[b] The concentrations of HCN and HN_3 in the solution at pH= 7.4 were calculated from NaCN and NaN_3 concentrations respectively, according to the methods described in the Materials and Methods section.

3.3.7 Studies of Other Substrate-reduction Activities and the Effect of CO

We also used other substrates, namely azide and cyanide, to probe the substrate-reduction inhibitor-susceptibility patterns with the altered α-277^{his} MoFe protein and to compare them with CO as inhibitors of C_2H_2 reduction. Azide and cyanide were the ones used in the study. Another commonly used substrate hydrazine was not used in the study because it was found that the altered α-277^{his} MoFe protein could not reduce hydrazine nor was any hydrazine detected during turnover under N_2 atmosphere. It was reported in the previous studies (Li *et al.*, 1982; Rubinson *et al.*, 1985) that in solutions of NaCN and NaN_3, their HN_3 and HCN forms were the actual substrates for nitrogenase, respectively. Using aliquots of 100 mM solution of NaCN under 100% Ar atmosphere at pH 7.4 to produce the substrate, HCN, we measured a K_m of 2.6 mM HCN and a V_{max} of 145 nmoles CH_4/min•mg for wild-type MoFe protein and a K_m of 1.1 mM HCN and a V_{max} of 99 nmoles CH_4/min•mg for the α-277^{his} MoFe protein (Table 6) using the Fig.P program. For wild-type MoFe protein, the K_m value matches with the published value fairly well (Li *et al.*, 1981). CO acted as the expected noncompetitive inhibitor of CH_4 formation from HCN by both wild type and α-277^{his} MoFe proteins with no indication of a sigmoid response as occurred with acetylene reduction with the α-277^{his} MoFe protein. When NaN_3 was used as a source for HN_3 in the solution, which acted as a substrate, we measured the production of H_2 and N_2H_4 (Table 6). For wild-type (α-277^{arg}) MoFe protein, a K_m of 7.1 μM HN_3 was calculated which matches with the published number (Rubinson *et al.*, 1985); and for the α-277^{his} MoFe protein, a K_m of 24.2 μM HN_3 was found using the Fig.P program. We also used CO as an inhibitor in these studies, but again no sigmoidal response was observed. Neither was there any sigmoidal behavior when we attempted to use C_2H_2 as an inhibitor in place of CO in these substrate-reduction studies (data not shown).

In Table 7, activities from both MoFe proteins for different substrates are listed and also shown are the correspondent activities in the presence of CO whose presence causes partial inhibition of the activities. It is apparent CO inhibits all the substrate reduction activities except that of H_2 evolution for both proteins. It is necessary to point out that in general, the α-277^{his} MoFe protein has higher H_2 evolution activities in the presence of CO for all the substrates used in our study compared to the wild-type counterpart.

3.4 Discussion

Sequence comparison reveals that α-277-arginine is a strictly conserved residue among the MoFe proteins of Mo-nitrogenases from many different organisms (Jacobson and Dean, 1992). And it is a part of a patch of highly conserved residues within which the essential α-275-cysteine is located. Based on the x-ray crystallographic structure model (Kim and Rees, 1992) of the MoFe protein from *Azotobacter vinelandii*, α-277-arginine, together with α-192-serine and α-356-glycine, might be involved in providing possible entry/exit route for substrates and products. The structural diagram of FeMoco, α-277-arginine and the surrounding region (Courtesy of Dr. Bolin) is shown in Figure 16. According to the crystal structure, the closest distance from α-277-arginine to α-386-aspartate and α-281-tyrosine residues is measured to be 2.74 Å and 2.66 Å respectively. These lead to the proposal of putative hydrogen bonds between the α-277-arginine to α-386-aspartate and to α-281-tyrosine residues, both of which are highly conserved among nitrogenases from different organisms. α-277-arginine is also in proximity to another strictly conserved α-383-histidine (closest distance is 3.71 Å, and it is in a same helical structure where the α-381-Phe is located), and it is only 5.12 Å away from the α-195-histidine in an orientation which is likely to form hydrogen-bond though an intervening water molecule.

Table 7. Electron Distributions to products in the presence of different assay substrates.

Substrate	Product[a]	DJ527 (α-277^{arg})		DJ788 (α-277^{his})	
		SPA[b](-CO)	SPA[b](+CO)[c]	SPA[b](-CO)	SPA[b](+CO)[c]
10%C_2H_2/ 90% Ar	C_2H_4	1760 (87%)	767 (35%)	543 (68%)	202 (24%)
	H_2	266 (13%)	1396 (65%)	259 (32%)	652 (76%)
H^+/100% Ar	H_2	2230(100%)	2330(100%)	1070(100%)	1200(100%)
100% N_2	H_2	701	1870	1060	1120
15.8 μM[d] HN_3 100% Ar	N_2H_4	112	78	35	9
	H_2	584	973	597	852
9.8 mM[d] HCN 100% Ar	CH_4	105	55	111	28
	H_2	304	1070	119	573

[a] All products were detected for assays under 10% C_2H_2/90% Ar and 100% Ar; selective products were quantified for N_2, HN_3 and HCN reductions as indicated in the table.

[b] SPA denotes specific activity of purified MoFe protein activity from DJ527 (α-277^{arg}) or DJ788 (α-277^{his}) with 1 unit equals 1 nmole product formed per minute per mg of total protein in the presence of optimal complementary protein. All assays were performed in Hepes buffer, at pH 7.40, in 30°C water incubator shaker described in details (see Materials and Methods section) unless otherwise noted. n.d. stands for not determined in the table above.

[c] CO concentrations used in each studies were 0.06% except 0.025% in NaCN reduction assays. Such concentrations of CO were used in order to partially inhibit substrate reductions so as to visualize any unusual kinetic response to CO as an inhibitor.

[d] The concentrations of HN_3 and HCN were calculated from 10 mM NaN_3 and NaCN at pH=7.40 respectively, for details refer to the Materials and Methods section.

Thus, the α-277-arginine residue appears appropriately positioned to play an important structural role in orienting the FeMoco within its pocket so as to maintain its functionality.

We have previously suggested that the products of the *nifE* and *nifN* genes provide a scaffold upon which FeMoco is assembled prior to its donation to the apo-MoFe protein (Brigle *et al.,* 1987). Because FeMoco must escape from the *nifEN*-products complex during maturation of the MoFe protein, the respective FeMoco-binding sites within the MoFe protein and within the *nifEN*-products complex are likely to be structurally similar but functionally different. In the *nifE* gene-product, a lysine residue replaces arginine at the residue equivalent to the one in MoFe-protein α-277 position of *Azotobacter vinelandii*. Interestingly, in *Klebsiella pneumoniae*, it remains an arginine residue at the correspondent position in the *nifE* gene-product. This substitution could indicate that α-277-arginine is important in maintaining the correct FeMoco environment in MoFe protein, while a residue with a similar structure, like Lys, can still be functional at this position for the appropriate processing of FeMoco on the *NifEN* complex.

Substitutions at residue α-277-arginine gave variable Nif phenotypes, including Nif^{+} and Nif^{slow} which indicates that arginine at this position is not absolutely required for nitrogenase activity. Although only two of the eight mutants studied grow comparatively well diazotrophically, *i.e.* have doubling times of twice of wild type or less. Crude extracts prepared from six of the eight mutant strains, the exceptions being those with proline or glycine at residue α-277, exhibit different, but significant levels of both acetylene- and proton-reduction activity. Thus, substitution of α-277-arginine by amino acid residues other than lysine and cysteine changes the FeMoco environment variably but sufficiently so that the delicate balance required for enzymatic activity has been disturbed. Some substitutions, e.g., $\alpha\text{-}277^{thr}$ and $\alpha\text{-}277^{phe}$, retain slow diazotrophic growth and

~50% of wild-type C_2H_2- and H^+-reduction activity, while with α-277^{his}, the C_2H_2- and H^+-reduction activity remains, but diazotrophic growth is lost. Because the molecular sizes of C_2H_2 and N_2 are not very different, substitution of α-277-arginine residue should not affect substrate entry as a means of allowing the altered MoFe protein to discriminate among these two substrates.

In addition, DJ788 (α-277^{his}) MoFe protein distributes electron flux between the ethylene (65%) and hydrogen (35%) produced under 10% C_2H_2/90% Ar atmosphere very differently from that of the wild-type (<10% H_2) and the other mutant strains. These changes in substrate specificities by the altered α-277^{his} MoFe protein are consistent with the dramatic changes in its FeMoco-derived S=3/2 EPR spectrum; all suggest that the FeMoco orientation in the altered polypeptide matrix may be different than in the wild type.

By substitution of α-277-arginine with other amino acid, such as, histidine, threonine, it is unlikely that a global structural change was introduced into the altered MoFe protein. This is supported by the variety of phenotypes of the mutants resulting from single amino acid substitutions at the α-277-arginine residue, with most of them retaining some level of diazotrophic growth capacity. It was found in our study that the altered α-277^{his} MoFe protein could withstand a 56°C temperature during the heat treatment comparable to the wild type, and this is yet another indication of its intact global, but altered local, structure caused by the substitution of α-277-arginine by histidine. Other than the substitutions by proline and glycine, which are known to disturb protein secondary structure dramatically, the α-277^{his} is the only one that resulted in Nif$^-$ phenotype. The fact that most of them (except α-277^{pro} and α-277^{gly}) have EPR signals comparable in intensity to wild type indicates the presence of the protein-bound form of the FeMoco. Most of these altered MoFe proteins gave slightly shifted EPR signals compared to that of the wild type indicating that changes of their FeMoco

environment have been introduced by the individual substitution. This phenomenon is particularly striking in the cases of α-277^{his} and α-277^{thr}, each of which has two sets of signals of its EPR spectrum, which suggests that the environment of the FeMoco in the altered proteins has been changed sufficiently such that the cofactor may be oscillating between two major orientations within its polypeptide pocket. The second set of EPR signals (g = 4.52 and 3.57 for α-277^{his}; g = 4.50 and 3.56 for α-277^{thr}) is more rhombic than the normal one (g = 4.31 and 3.64 for α-277^{his}; g = 4.30 and 3.76 for α-277^{thr}), which is close to the wild-type values (g = 4.34 and 3.65). However, although both α-277^{his} and α-277^{thr} have similar EPR spectra, they are not at all similar in their abilities to reduce N_2.

According the Lowe-Thorneley model, N_2 is reduced at a more reduced form of MoFe protein (E_4 and higher), while C_2H_2 and H^+ are reduced at the more oxidized forms of E_2 and E_1. Maybe what happens in the altered MoFe proteins, especially α-277^{his} because it can reduce C_2H_2 and H^+ but not N_2, is that the less reduced forms (E_2 and E_1) are well populated but the more reduced E_4 state cannot be reached for N_2 binding and reduction. This would explain the observation that N_2 does not change the total electron flow when replacing argon for reactions under either 10% C_2H_2/90% Ar or 100% Ar atmospheres for the altered α-277^{his} MoFe protein. Its inability to reach E_4 may reflect a significant change in the redox properties of the protein-bound FeMoco. The preliminary data obtained from our stopped-flow spectrophotometry experiments suggests that the E_4 state is not achieved in α-277^{his} MoFe protein (for details, see Chapter 5).

Previous studies showed that C_2H_2 is a good substrate for wild-type nitrogenase with apparent K_m values ranging from 0.003 to 0.02 atm (Hardy, 1979). Our data of a K_m = 0.005 atm C_2H_2 for wild-type MoFe protein falls within the range of the published results. For the α-277^{his} MoFe protein, a K_m of

0.051 atm C_2H_2 was measured, which is 10-times higher than that for wild type. This likely poorer affinity for C_2H_2 is reflected in the higher percentage of electron flux producing H_2 (37%) compared to wild type (8%) under 10% C_2H_2. C_2H_2 has been suggested to bind to two sites or oxidation states on the enzyme, presumably at the E_1 and E_2 states (Ashby *et al.*, 1987) and C_2H_4 is likely to be released at oxidation state E_3 of the MoFe protein cycle. All nitrogenase catalyzed substrate reduction activities are inhibited by CO except the H^+-reduction activity, when the total electron flux is reflected solely in the H_2-evolution activity. This is true for MoFe proteins from both wild type and DJ788 mutant strain. Similarly, when CO is present in an amount sufficient only to partially inhibit C_2H_2 reduction activity, this is compensated by an elevated H_2-evolution activity for both wild-type and α-277^{his} MoFe proteins.

According to Segal's (1975) definition, if the binding of one substrate molecule induces structural or electronic changes that result in altered affinities for the vacant sites, the velocity curve will no longer follow Michaelis-Menton kinetics and the enzyme will be classified as an "allosteric" enzyme. Generally, allosteric enzymes yield sigmoidal velocity curves. The binding of one substrate molecule facilitates the binding of the next substrate molecule by increasing the affinities of the vacant binding sites. This phenomenon is called cooperative binding. When C_2H_2 reduction assays were performed in the presence of CO, we observed that the α-277^{his} MoFe protein gave sigmoidal Michaelis-Menton kinetics which produced curved lines when plotted as 1/v *vs.* 1/[S], indicating it behaved as an allosteric enzyme. By using the Hill plot, we were able to calculate an n = 1.6, which suggests that there are at least two sites involved in the inhibitor-induced cooperativity behavior for the α-277^{his} MoFe protein ethylene production in the presence of CO. This was confirmed by 1/v *vs.* $1/[S]^2$ plots, which were lines.

Because the two FeMoco prosthetic groups are 70 Å apart and the α-subunits in which they are bound are "insulated" from each other by the intervening β-subunits, we believe it very unlikely that the observed cooperativity is due to the classical Monod mechanism of induced α-subunit conformational changes. More satisfying is a mechanism in which two sites for C_2H_4 evolution exist in the vicinity of each FeMoco. In this model, the enzyme forms the complex E(CO)-(C_2H_2), which gives rise to product (C_2H_4) more rapidly than E(CO)-(C_2H_2). Thus, we propose:

a) Without CO

$$E + (C_2H_2) \overset{k_1}{\rightleftarrows} E\text{-}(C_2H_2) \overset{k_3}{\rightarrow} E + (C_2H_4)$$

b) With CO

$$E(CO) + (C_2H_2) \overset{k_1}{\rightleftarrows} E(CO)\text{-}(C_2H_2) \overset{k_2}{\rightarrow} E(CO)\text{-}(C_2H_2)_2 \overset{k_3}{\rightarrow} E(CO) + (C_2H_4) + (C_2H_4)$$

Implicit in this mechanism is the fact that the CO- and C_2H_2-binding sites are independent of one another. It might be that the two binding sites for C_2H_2 exist without CO (and also for wild-type MoFe protein) but they cannot be differentiated under the conditions used in our assays.

It is known that for wild-type MoFe protein, CO acts as a noncompetitive inhibitor of the reduction of C_2H_2 (Davis *et al.*, 1979), N_2 (Hwang *et al.*, 1973) and azide (Dilworth & Thorneley, 1981) catalyzed by nitrogenase (reviewed by Burgess, 1985), which suggests that CO binds at a different site or at a different oxidation level of the same site to that where C_2H_2 and N_2 bind (Lowe *et al.*, 1990). In the CO inhibition study of the α-277^{his} MoFe protein C_2H_2 reduction, we found the altered MoFe protein had a similar sensitivity to CO as for the wild-

type. We have followed up these effects by studying both NaN_3 and NaCN as alternative substrates to determine whether they also suffer from CO-induced cooperativity and also whether they might be used as inhibitors of C_2H_2 reduction and so induce cooperativity in C_2H_2 reduction. As part of this study, we measured a K_m= 4.5 mM HN_3 for wild type MoFe protein and a K_m= 15.3 mM HN_3 for the altered α-277^{his} MoFe protein in the production of N_2H_4. Thus, the altered MoFe protein has about 3.5-times less affinity for NaN_3 than does wild type. It was found (Dilworth & Thorneley, 1981) that N_2 acts as a competitive inhibitor to azide reduction ($HN_3 + 6e^- \rightarrow N_2H_4$), yet the K_i of N_2 as an inhibitor is ten-times larger than the K_m for N_2 reduction to NH_3. This led the authors to propose that the same binding site on the enzyme but at different oxidation levels is used for N_2- and HN_3-reduction. In line with this reasoning, although the altered α-277^{his} MoFe protein cannot reach the E_4 oxidation level resulting in its inability to reduce N_2, it can effectively reduce azide to hydrazine. Thus, we reasoned that the substitution of the α-277-arginine residue by histidine does not physically disturb the N_2-binding site on the enzyme, rather, it prevents the enzyme from successfully reaching the more reduced E_4 state necessary for N_2 binding and reduction. Thus, because we were able to detect both hydrazine and ammonia in the azide-reduction study using the altered α-277^{his} MoFe protein, our results are best explained by azide being reduced at a state more oxidized than E_4, which nicely complements the previous proposal (Dilworth & Thorneley, 1981).

Surprisingly, for NaCN reduction, we found that the altered α-277^{his} MoFe protein has higher apparent affinity for the substrate (K_m=1.1 mM) compared to the wild type (K_m= 2.7 mM). The K_m of wild-type MoFe protein was determined at an Fe protein to MoFe protein molar ratio of 20:1. At an Fe protein to MoFe protein ratio of 8:1, K_m was reported to be 4.5 mM which is expected to be higher than that measured at a high electron flux condition. Therefore, our number of

2.7 mM agrees reasonably well with the published number of 4.5 mM. When NaCN is used as the source of the substrate, both CN^- and HCN coexist in the solution. It was found previously that CN^- inhibits total electron flow (K_i=27 μM) and that this situation could be completely reversed by the presence of CO, thus implying a common binding site for both CO and CN^- (Li *et al.*, 1982). HCN is actually the real substrate for catalysis with over 99% in solution at pH 7.4. Further, it was found for the wild-type MoFe protein from *A. vinelandii* that the K_m of HCN increases with increased ratio of Fe-protein to MoFe-protein molar ratio (Li *et al.*, 1982), while the apparent K_m for N_2 decreases with increasing ratio (Wherland *et al.*, 1981). In studies on the *Klebsiella pneumoniae* $nifV^-$ mutant, HCN can be reduced under the usual assay conditions but N_2 can only be reduced when its Fe protein levels are greatly increased (McLean & Dixon, 1981). Thus, it appears that HCN is bound to and reduced at a state, which is more oxidized than the state responsible for N_2 reduction. For the α-277^{his} MoFe protein, the ability to reduce HCN but not N_2 is consistent with this situation.

CO acts as an inhibitor for both HN_3- and HCN-reduction activities of both α-277^{his} and wild-type (α-277^{arg}) MoFe proteins. However, none of the products from these substrate-reduction reactions showed any sigmoidal responses in the presence of partially inhibiting amounts of CO as observed for ethylene production by the α-277^{his} MoFe protein even though, these two substrates are likely bound to the same oxidation states as is C_2H_2. Thus, the failure to show sigmoidal velocity curves in the α-277^{his} MoFe protein when CO is present indicates that these two alternative substrates probably bind at a site distinct from that of C_2H_2. In addition, when we used cyanide or azide as inhibitors in the C_2H_2-reduction reactions catalyzed by the altered α-277^{his} MoFe protein, none of them showed the same inhibition pattern, *i.e.*, induced cooperativity in C_2H_4 production, as was observed in the presence of CO. We conclude that there is a unique interaction

between CO binding and C_2H_4 evolution, which does not exist with any other substrate-inhibitor combination used in the studies. The exact relationship among the CO-binding site(s) and C_2H_4- evolution site(s) remains unclear although it is possible that they are in close proximity in order to interact with each other.

In summary, by substituting α-277-arginine with histidine, we have constructed a mutant with its MoFe protein altered such that it is no longer able to reach an oxidation level of E_4, resulting in a lack of N_2-reduction activity. This altered MoFe protein displays cooperative C_2H_4-evolution behavior in the presence of CO. The result is consistent with the possible existence of two independent C_2H_4-evolution redox sites (or two states) on the altered MoFe protein. C_2H_2, NaN_3 and NaCN are unlikely to share same binding and reduction sites on the enzyme, although they may be reduced at the same oxidation state of the enzyme. All the information we have regarding the α-277-arginine residue suggests that it is important in enzyme functioning and upon its substitution by histidine, the FeMoco environment is changed in a way that destabilizes its E_4 oxidation state.

Chapter 4 Roles of MoFe Protein α-274-His and α-276-Tyr Residues in Nitrogenase Catalysis

This chapter forms the basis of a manuscript (Shen, J., Fisher, K., Setterquist, R.A., Dean, D.R., and Newton, W.E.). It describes the author's contributions to the manuscript. Dr. K. Fisher performed the rapid-quench turnover experiments and the mutant strains were constructed by R.A. Setterquist.

4.1 Introduction

Molybdenum-dependent nitrogenase (Mo-nitrogenase), the enzyme responsible for biological nitrogen fixation, is found in many free-living and symbiotic microorganisms. Although substantial differences exist among the species in which the nitrogenase is found, they function similarly to reduce atmospheric dinitrogen to ammonia at room temperature and under atmospheric pressure. Mo-nitrogenase is composed of an Fe protein (a homodimer, encoded by *nifH*), which serves as a one-electron donor to the MoFe protein (an $\alpha_2\beta_2$ tetramer, encoded by *nifDK*), which contains two types of prosthetic groups: FeMo-cofactor (FeMoco) centers and P clusters (two copies each per $\alpha_2\beta_2$ tetramer). Valid evidences (Shah *et al.*, 1977; Hawkes *et al.*, 1984; Scott *et al.*, 1990) support that substrates are reduced at the FeMoco within the MoFe protein α-subunit of Mo-nitrogenase. Each FeMoco in the MoFe protein is composed of 1 Mo, 7 Fe, and 8-9 inorganic S atoms. It is responsible for the characteristic EPR signal of nitrogenase due to its $S = 3/2$ spin system. The $S = 3/2$ EPR signal of FeMoco within the MoFe protein shows apparent g values of 4.34, 3.65 and 2.0; while those of the isolated FeMoco are 4.7, 3.3 and 2.0, all measured at 13 K (reviewed by Newton, 1992). The broadening of the EPR signal upon the FeMoco extraction is attributed to the change in its ligation resulting in a heterogeneous

population (Shah & Brill, 1977; Newton, 1992). The recent solutions of the three-dimensional crystal structure of the MoFe protein, with models for both prosthetic groups bound within the protein, from both *A. vinelandii* and *C. pasteurianum* has provided insights not only into the structure, orientation and relative location of these prosthetic groups but also into function and mechanism by indicating potential protein-protein interaction sites, electron transfer routes, *etc* (Kim & Rees, 1992a,b; Kim *et al.*, 1993; Chan *et al.*, 1993; Bolin *et al.*, 1993b; Howard & Rees, 1994).

Eight strictly conserved Cys residues occur in the α- and β-subunit of the MoFe protein. These are α-62-Cys, α-88-Cys, α-154-Cys, α-183-Cys, α-275-Cys, and β-70-Cys, β-95-Cys, β-153-Cys. Prior to the availability of structural data, it was proposed (Dean *et al.*, 1990) that α-62-Cys, α-88-Cys and α-154-Cys and the β-70-Cys, β-95-Cys and β-153-Cys provided two equivalent P-cluster environment, which led to the further proposal that the P-clusters would be distributed equally among the α- and β-subunits and might actually bridge the two subunits types. Further, it was proposed that the remaining two residues, α-183-Cys and α-275-Cys plus flanking residues that are located solely in the α-subunit of the MoFe protein, provide the polypeptide environment for the FeMoco. Site-directed mutagenesis studies showed that α-183-Cys is not essential (Brigle *et al.*, 1987b; Kent *et al.*, 1989, 1990), whereas the α-275-Cys is required for nitrogenase activity and was proposed to provide a mercaptide ligand to the FeMoco (Brigle *et al.*, 1987b; Kent *et al.*, 1989, 1990). Upon substitution of α-275-cysteine by alanine in *K. pneumoniae* MoFe protein, the enhanced, readily accessible pool of free FeMoco in the crude extract of the mutant strain could be detected by EPR spectroscopy by its characteristically broadened EPR signal. The crude extract from this mutant strain could also be used to reconstitute an extract from a mutant strain (*nifB*$^-$) deficient in FeMoco biosynthesis. Furthermore, it was

observed that the α-275^{ala} MoFe protein exhibited a native electrophoretic mobility characteristic of FeMoco-deficient MoFe proteins (Kent *et al.*, 1990). These proposals have been confirmed by the crystal structure, which shows that α-275-Cys provides one (to the Fe1 atom) of only two ligands from the protein environment to the FeMoco. In addition, the residue, α-442-His, which is ligated directly to the Mo atom of FeMoco (Kim & Rees, 1992a), was suggested to be functionally important from gel-electrophoresis studies of a series of point mutants (Govezensky & Zamir, 1989).

Reciprocal heterologous crosses of the *Clostridium pasteurianum* (*Cp*) and *Azotobacter vinelandii* (*Av*) nitrogenase component proteins are completely inactive (Emerich & Burris, 1976; Emerich *et al.*, 1978). The reasons for this incompatibility remain to be determined. The crystal structure of the MoFe proteins from both strains look very similar, except for a ~50 amino-acid long stretch in the *Cp* MoFe protein located on the outside of the α-subunit which makes its overall tetramer structure more symmetrical. The extra 50 amino acid stretch in the *C. pasteurianum* MoFe protein is by no means close to its FeMoco environment (Bolin *et al.*, 1993). Differences in the *Av* and *Cp* Fe-protein sequences and structures have also been suggested as the source of the incompatibility (Sundaresan & Ausubel, 1981; Chen *et al.*, 1986). Molecular genetic techniques have been used to construct "hybrid" *Av*/*Cp* Fe proteins, which replaced part of the *Av* Fe protein sequence with the *Cp* sequence, to investigate this possibility. Earlier studies using this strategy indicated that the difference in *Av* and *Cp* Fe protein sequences near the carboxyl termini did not contribute to the result of a tight, inactive complex between the *Av* MoFe protein and *Cp* Fe protein (Jacobson *et al.*, 1990). Recently, the Rees-Howard model revealed a potential component protein interaction site located at a loop involving residues 59 through 67 of the Fe protein (Howard & Rees, 1994). This suggestion was

supported by the observation of a tighter protein complex between the *Av* MoFe protein and an "hybrid" *Av* Fe protein in which the *Av* Fe protein sequence between residues 59 and 67 was replaced with that from the *Cp* (Peters *et al.*, 1994).

Other work showed similar optical and CD spectroscopic changes for both the *Av* and *Cp* MoFe proteins during oxidation-reduction but significantly different EPR spectra changes. Specifically, EPR measurements as a function of temperature demonstrated that the relaxation behavior of the $S = 3/2$ signal associated with FeMoco in the two MoFe proteins differed markedly. The EPR signal from the *Cp* MoFe protein only begins to undergo broadening above 65 K, whereas the *Av* MoFe protein signal is severely broadened at 25 K (Morgan *et al.*, 1988). The FeMoco centers of both MoFe proteins are identical (Shah & Brill, 1977), so this difference among species must arise from different constraints imposed on FeMoco by different polypeptide environments.

On examination of the amino-acid sequences of the MoFe proteins from both *A. vinelandii* and *C. pasteurianum*, one interesting difference was found in the residues flanking α-275-Cys. Although the sequence conserved in most organisms is His-Cys-Tyr, it is Gln-Cys-His only in *C. pasteurianum*. Around this sequence is a highly conserved region among which α-277-Arg has been identified as occupying a critical structural position. Figure-21 is a stereo view showing the relative positions of the α-274-His, α-276-Tyr residues with respect to the FeMoco in the *A. vinelandii* MoFe protein.

Previous research in this laboratory (Dean *et al.*, 1990a) has explored the importance of the residues flanking α-275-Cys by site-directed mutagenesis studies. It was found that on substituting α-276-Tyr by His together with α-274-His by Gln (DJ386), the resulting *A. vinelandii* mutant strain was not impaired in its diazotrophic growth ability (Nif^+). However, its considerably changed whole-

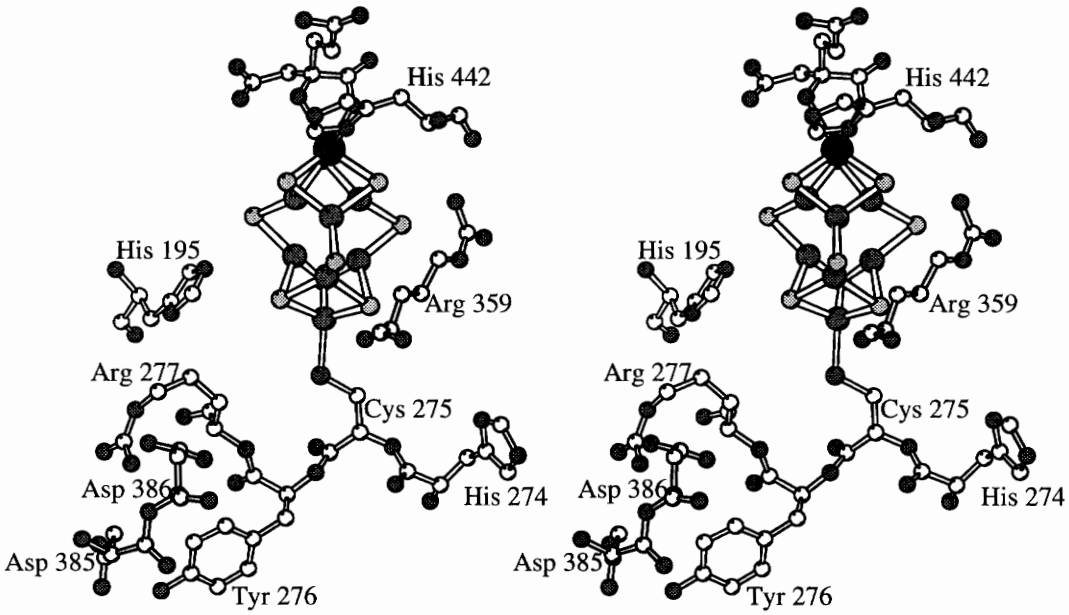

Figure 21. Stereo view of the α-274-His, α-276-Tyr and α-277-Arg residues and other residues in the vicinity of FeMoco. Prepared with MOLSCRIPT program, using data kindly supplied by Dr. Jeff Bolin (Purdue University).

cell EPR spectrum indicated that the environment of FeMoco within the altered *Azotobacter* MoFe protein had been affected by the substitutions. In this case, a second set of $S = 3/2$ signals was observed in addition to the normal wild type EPR signals at $g = 4.3$ and 3.65. The results were interpreted to indicate that the positioning of the His residue on opposite sides of the Cys ligand in the MoFe proteins from the different organisms is very likely to place different constraints upon FeMoco's environment. This evidence was proposed to support, prior to the crystal structure, the view that the region around the conserved α-275-Cys is involved in providing the polypeptide environment of the FeMoco. Later, mutagenesis studies in this region revealed similar patterns of double EPR signals from mutants with substitutions at the α-277-Arg residue, such as the α-277^{his} and α-277^{thr} MoFe proteins (see Chapter 3 for details).

Because it is not obvious that both sets of EPR signals represent active forms of FeMoco, the behavior of these EPR signals under turnover conditions should be informative. It is known that the $S = 3/2$ EPR signal arises from the presence of the paramagnetic FeMoco (s-r) center in the "semi-reduced" resting state of the MoFe protein. FeMoco within the MoFe protein can exist in at least three interconvertible oxidation states (Newton, 1992 and references therein), as shown in the following equation:

$$\begin{array}{ccccc} \text{FeMoco (ox)} & \Leftrightarrow & \text{FeMoco (s-r)} & \Leftrightarrow & \text{FeMoco (red)} \\ (S=0,\ \text{EPR silent}) & & (S=3/2,\ \text{EPR-active}) & & (S=\text{integer},\ \text{EPR silent}) \end{array}$$

When the MoFe protein is isolated during the normal purification protocol in the presence of excess dithionite, it contains FeMoco(s-r), which is denoted as the semireduced state (s-r) because it is both oxidizable and reducible by one-electron processes, as indicated in the above equation. In the operational nitrogenase system in the presence of Fe-protein, MgATP and dithionite, the FeMoco center is reduced to the functional state, FeMoco (red), during substrate reduction. This

state has integer spin and is, thus, EPR-silent. The FeMoco centers in the MoFe protein have an EPR signature signal with g = 4.34, 3.65 and 2.0. The disappearance of these EPR signals during nitrogenase turnover is a direct reflection of the reduction of the MoFe protein (Hageman & Burris, 1980) and, therefore, its effectiveness in substrate reduction. Once the nitrogenase reaction reaches its steady-state, the S = 3/2 EPR signal disappears. Thus, in order to determine whether both EPR-signal sets are equally active, the nitrogenase turnover reaction has to be frozen during its pre-steady state to determine the relative rates of disappearance of the two sets of EPR signals around g = 4.

In this report, we measured and compared with the wild-type MoFe protein: (i) the crude-extract level characteristics of the nitrogenase in twenty mutant strains, nine of which have a single amino-acid substitution at α-274-histidine, ten with single amino-acid substitution at α-276-tyrosine, and one double mutant with the *Clostridium* α-275-cysteine flanking sequence replacing the *Azotobacter* sequence (α-274-Gln / α-276-His); and (ii) the substrate-reduction pattern using purified $\alpha 276^{his}$ and α-274^{tyr}/α-276^{his} MoFe proteins from DJ609 and DJ610 strains. In addition, we apply freeze-quench EPR spectroscopic method to study the altered MoFe protein S = 3/2 signals during nitrogenase turn-over in order to determine their catalytic capabilities.

4.2 Experimental Procedures

4.2.1 Mutant Strain Construction

Methods for site-directed mutagenesis, gene replacement, and the isolation of mutant strains were performed as described or cited previously (Brigle *et al.*, 1987a, 1987b). The strategy for making a number of mutants at one specific amino-acid residue site is to synthesize chemically an oligonucleotide on which the 3 nucleotides coding for the desired amino-acid residue have been degenerately

replaced. For substitution at α-274-histidine of the MoFe protein, the oligonucleotide having the sequence: 5'-AACCTGGTTXXXTGCTACCGCTCG-3' (where XXX stands for the degenerate codon at the designated residue) was synthesized; similarly for substitution at α-276-tyrosine of the MoFe protein, the oligonucleotide having the sequence: 5'-GTTCACTGCXXXCGCTCGATGAAC-3' was synthesized.

Each altered MoFe protein having a substitution within the MoFe protein α-subunit primary sequence is designated by the subunit designator (α), the number of the amino-acid position substituted, followed by the three letter code for the substituting amino acid as superscipt form (see Table 8 and Table 9). For example, the altered MoFe protein having the α-274-histidine residue substituted by threonine is designated as α-274^{thr}. Strains are designated by their DJ numbers. DJ527 is a strain, which has mutations at the *hox*KG genes so as to abolish its uptake hydrogenase activity (Hup^-), while its *nif* genes remain intact. All the mutants used in this study are Hup^- strains, which enables us to measure H_2-evolution activity accurately at the crude-extract level without the interference from uptake hydrogenase activity. The DJ609 and DJ610 strains used in the studies are the Hup^- strains based on the previously constructed DJ384 and DJ386 strains (Dean *et al.*, 1990). Although uptake hydrogenase activity (Hup) does not interfere with the H_2-evolution activity of the purified MoFe proteins, the Hup^- strains were used in the purification as standard strains.

4.2.2 Growth Conditions, Media, and Nitrogenase Derepression

Small batches of *Azotobacter vinelandii* wild-type and mutant strains were grown at 30°C in Fernbach flasks on a modified Burk's medium (Strandberg and Wilson, 1968) containing 10 μM Na_2MoO_4, which is sufficient to repress the alternative nitrogenase systems. All chemicals for media preparations were

purchased from Fisher Scientific Company (Pittsburgh, PA), except sucrose which was purchased from the Kroger Co. (Cincinnati, OH). Cultures were grown under air with a shaking rate at 250 rpm. A fixed-nitrogen source of filter-sterilized urea was added to a final concentration of 20 mM when required. Large scale *Azotobacter* culture was grown in a 28-liter fermentor (New Brunswick Scientific Company, New Brunswick, NJ) on modified Burk's medium as mentioned above. Air flow in the fermentor was controlled with a flow meter at 35 ~ 40 liters/min, and the culture was vigorously stirred at 250 rpm with a built-in stirrer. Growth of *Azotobacter* cultures was monitored using a Klett-Summerson meter (Klett Mfg. Co. Inc., New York, NY) equipped with a no.54 filter. All mutant strains that do not grow or grow only slowly in nitrogen-free media were grown on urea-supplemented media and then derepressed for nitrogenase synthesis as described previously (Jacobson *et al.*, 1989). The culture to be derepressed was grown in urea-containing Burk's medium until its density reached 150-200 Klett units. In Fernbach-flask cultures, the culture was centrifuged at 10,400 × *g* for 10 min to remove the medium and the cell pellet resuspended in nitrogen-free medium. In the fermentor, the culture was concentrated to 2 liters by filtration using a Watson-Marlow 601S/R peristaltic pump and a Millipore (Pellicon) cassette system fitted with 0.22 Å Pellicon filter in order to remove as much of the nitrogen source as possible. It was then reinoculated into 28-liters of Burk's nitrogen-free medium. In both cases, after derepression for 3 hours, the culture medium was removed and the cells isolated by centrifugation as before. *Azotobacter* cells were stored at -80°C until used.

4.2.3 Crude Extract Preparation

Cells were thawed and diluted anaerobically at 4°C in degassed 50 mM Tris-HCl, pH 8.0, containing 2 mM sodium dithionite, at the approximate ratio of

1.0 g of cells to 2.0 ml of buffer. The cell suspension was broken with 3-min pulse sonication using a Heat System Sonicator model XL2015 in a 25-ml Rosette cooling cell (Heat Systems-Ultrasonics, Inc.) immersed in an ice water bath to offset increasing temperature. The lysate was transferred anaerobically into centrifuge tubes and centrifuged for 60 min at 98,000 × *g* at 4°C. The supernatant was frozen dropwise in liquid nitrogen in which the pellets were stored until used.

4.2.4 Protein Purification

The altered α-276^{his} and α-274^{gln}/α-276^{his} MoFe proteins of the mutant strains, DJ609 and DJ610 respectively, and the wild-type (α-277^{arg}) MoFe protein from strain DJ527 were purified in parallel. Cells of the three strains to be used for protein purification were grown up using a 28-liter fermentor (see Cell Growth Section 4.2.2). A crude extract was prepared on a large scale using a Manton-Gaulin homogenizer to break the cells which had been thawed under an Ar atmosphere and diluted 1:2 with degassed 50 mM Tris-HCl (pH 8.0), 2 mM sodium dithionite. A heat step at 56°C for 5 min was included before centrifugation at 98,000 × *g* at 4°C for 1 hour to separate the cell debris from the soluble protein supernatant. Partial purification of the MoFe protein was achieved by chromatography over DE52-cellulose (Whatman Biosystems Ltd, England) which had been anaerobically equilibrated with 25 mM Tris-HCl (pH 7.4), 1 mM sodium dithionite. This step resulted in ~70% recovery of the MoFe-protein activity, which was mostly free of Fe-protein activity. On the DE52-cellulose columns, a linear NaCl gradient from 0.1 M to 1.0 M in degassed 25 mM Tris-HCl (pH 7.4), 1 mM sodium dithionite, was applied. The wild-type (α-274^{his}/α-276^{tyr}), α-276^{his} and α-274^{gln}/α-276^{his} MoFe proteins all eluted at ~0.2 M NaCl off the DE52-cellulose column. Further purification of the MoFe proteins was

achieved by Sephacryl S-200 gel filtration (Pharmacia LKB, Sweden) chromatography using degassed 0.2 M NaCl in 25 mM Tris-HCl (pH 7.4), 1 mM sodium dithionite, to yield pure samples of three MoFe proteins. Wild-type (α-274^{his}/α-276^{tyr}) MoFe protein purified in this way has a specific activity of 1980 nmol of hydrogen evolved per minute per mg, while the altered α-276^{his} MoFe protein has a specific activity of 1190 nmol of hydrogen evolved per minute per mg and the α-274^{gln}/α-276^{his} MoFe protein has a specific activity of 830 nmole of hydrogen evolved per minute per mg.

The wild-type Fe protein used in the assays was purified from *Azotobacter vinelandii* wild-type as described previously (Burgess *et al.*, 1980b) and had a specific activity of 2060 nmol of hydrogen formed per minute per mg.

4.2.5 Protein Estimation

Protein concentrations were determined by the BCA method using bovine albumin serum (0 - 0.1 mg/ml) as standard (Smith *et al.*, 1985).

4.2.6 Nitrogenase Activity Assay

MoFe-protein and Fe-protein specific activities were measured both in crude extracts and with purified proteins as described below in the presence of an optimal amount of purified complementary component protein. Assays were performed in 9.25-ml reaction vials fitted with butyl rubber stoppers and aluminum seals. Each 1.0-ml reaction volume contained 25 mM Tes-KOH, pH 7.4 (25 mM Hepes-KOH in the purified protein assays), 2.5 mM ATP, 5.0 mM $MgCl_2$, 30 mM creatine phosphate, 0.125 mg creatine phosphokinase, and 20 mM $Na_2S_2O_4$. All chemical reagents were purchased from Sigma Chemical Company (St. Louis, MO), except $Na_2S_2O_4$, which was purchased from Mallinckrodt Chemical Company (Berkeley, CA). For crude-extract activity assays, 50-μl of crude

extract was used in each assay. Activity titrations were performed on each extract using appropriate amounts of purified complementary protein to determine the maximum MoFe-protein or Fe-protein activity. In assays with purified proteins, a total of 0.5 mg of nitrogenase proteins in 1 ml was used to avoid complications introduced by both high and low protein concentrations. Usually, an Fe protein to MoFe protein molar ratio of 20:1 was used in the activity assays involving purified proteins. Each assay was started by the addition of either the crude extract or the purified protein to the otherwise complete reaction system in the reaction vial, which had been preincubated for 5 minutes, and was terminated by the addition of 0.25 ml 0.5 M Na_2EDTA (pH 7.5) after 8 minutes. When required, CO was added by gas-tight Hamilton syringe (Reno, Nevada) to the appropriate assay vial during the preincubation period.

All reaction vials were subject to four cycles of evacuation and flushing using an automated machine (Corbin, 1978) to replace the air with either 100% Ar or 100% N_2 depending on the type of assay followed. In C_2H_2-reduction assays, dilution of 100% Ar with aliquots of C_2H_2 produced from calcium carbide (Fisher Scientific) was used to produce the desired C_2H_2 concentration in each reaction vial. H^+-reduction assays were performed under a 100% Ar gas phase.

C_2H_4 produced was quantified by gas chromatography on a Poropak N column using a flame ionization detector (GC-14A, Shimadzu, Tokyo, Japan). H_2 production was quantified by gas chromatography on a molecular sieve 5A column and a thermal conductivity detector (GC-8A, Shimadzu, Tokyo, Japan). Calibrations were performed using standard gases of 1 ppm C_2H_4/100% helium and 1% H_2/100% N_2 purchased from Scotty Specialty Gases (Plumsteadville, PA) respectively. For the determination of C_2H_2 concentration in each reaction vial, 1% C_2H_2 in helium was used as a standard.

4.2.7 Gel Electrophoresis

For sodium dodecyl sulfate-polyacrylamide gel electrophoresis, samples and gels were prepared according to Laemmli (1970). The gels used were 12% polyacrylamide (1.35% cross-linker) with a 4% stacking gel. Electrophoresis was performed at 30 mA/gel in a Hoefer Mighty Small apparatus (Hoefer, San Francisco, CA), using 10,000 - 100,000 low molecular weight standards (BioRad Laboratories, Hercules, CA) and the gels stained with Coomassie Blue (R-250).

4.2.8 Electron Paramagnetic Resonance Spectroscopy

Derepressed *Azotobacter* cells were prepared for EPR spectroscopy as described previously (Scott *et al.*, 1990). The spectra of whole-cells and purified proteins were recorded on a Varian Associates E-line instrument at 9.22 GHz and 20 mW at 12 K maintained by liquid helium boil-off.

4.3 Results

4.3.1 Characteristics of Diazotrophic Growth and Nitrogenase Catalytic Activities in Crude Extracts

Table 8 and Table 9 summarize the MoFe-protein specific activities for crude extracts prepared from nitrogenase-derepressed wild-type and the mutant strains with substitutions at α-274-His or α-276-Tyr along with their genotype and diazotrophic growth behavior expressed as exponential growth doubling time (D.T.). Also listed in the crude-extract assays were the carbon monoxide (CO) inhibition patterns for their acetylene- and proton-reduction activities. None of the α-274-His or α-276-Tyr mutants displayed a different CO sensitivity pattern when compared to wild-type, *i.e.*, only acetylene- but not proton-reduction activity in the crude extracts was CO sensitive. In addition, no ethane production was detected in any of the acetylene-reduction reactions at the crude extract level.

Table 8. Diazotrophic growth behavior of α-274-His mutant strains, their crude extract MoFe protein activities and CO inhibition pattern

Strains[a]	Substitution at α-274	Codon	D.T.[b] (Hrs)	Under C_2H_2[c]				Under Ar[d]	
				C_2H_4 SA		H_2 SA		H_2 SA	
				-CO	+CO	-CO	+CO	-CO	+CO
W-T	none (His)	CAC	2.0	78	0.7	6.4	81	78	83
DJ663	Ala	GCC	1.9	35	0.3	9.5	45	43	46
DJ661	Ser	TCG	3.3	33	0.3	9.0	46	42	41
DJ669	Thr	ACC	2.6	49	0.3	3.6	46	42	41
DJ651	Cys	TGC	2.1	27	1.1	6.2	38	28	36
DJ655	Tyr	TAC	2.1	95	3.7	9.4	124	91	101
DJ672	Gln	CAG	1.9	49	0.5	3.6	53	53	46
DJ659	Leu	CTG	2.6	31	0.2	4.2	33	28	22
DJ665	Asp	GAC	2.3	60	0.3	4.7	64	52	54
DJ683	Pro	CCT	5.7	27	0.4	7.8	36	39	46
DJ744	Arg	CGT	N/G	0.7	0.3	0.1	0.6	0.7	0.5

[a] All strains are deleted for the uptake hydrogenase structural genes resulting in Hup^- phenotype.

[b] D.T. denotes the doubling time of the corresponding *Azotobacter* strain grown in air in fixed nitrogen-free Burk's medium. N/G indicates no growth under these conditions.

[c] MoFe-protein specific activity in the crude extract is listed as nmole of C_2H_4 and H_2 produced per minute per mg total protein under a 10% C_2H_2 / 90% Ar atmosphere in the presence of an optimal amount of purified Fe protein. "+CO" under the same column denotes that the assays were performed in the presence of 10% CO under the otherwise same conditions as the "-CO" assays.

[d] MoFe-protein specific activity in the crude extract is listed as nmole of H_2 produced per minute per mg total protein under a 100% Ar atmosphere in the presence of an optimal amount of Fe protein. "+CO" under the same column denotes that the assays were performed in the presence of 10% CO under the otherwise same conditions as the "-CO" assays.

Table 9. Diazotrophic growth behavior of α-276-Tyr mutant strains, their crude extract MoFe protein activities and CO inhibition pattern

Strains[a]	Substitu-tion at α-276	Codon	D.T.[b] (Hrs)	Under C_2H_2[c]				Under Ar[d]	
				C_2H_4 SA		H_2 SA		H_2 SA	
				-CO	+CO	-CO	+CO	-CO	+CO
W-T	none (Tyr)	TAC	2.0	78	0.7	6.4	81	78	83
DJ649	Ala	GCC	2.2	21	0.1	3.9	18	19	14
DJ667	Gly	GGA	2.6	18	0	5.7	21	24	27
DJ635	Ser	TCC	2.2	27	0	6.9	30	31	27
DJ653	Thr	ACC	2.3	26	0	6.8	27	29	27
DJ657	Cys	TGC	2.3	22	0	6.3	27	22	17
DJ671	Asn	AAC	2.6	12	0.3	2.3	15	15	15
DJ674	Glu	GAA	2.1	26	0.2	10	28	31	29
DJ609	His	CAC	2.7	42	0	7.5	43	44	50
DJ687	Lys	AAG	3.8	10	5	1.2	12	13	13
DJ610	$Gln^{\alpha-274}$ /His[e]	CAG/ CAC[e]	1.9	22	0.1	4.2	26	28	29

[a] All strains are deleted for the uptake hydrogenase structural genes resulting in Hup$^-$ phenotype.

[b] D.T. denotes the doubling time of the corresponding *Azotobacter* strain grown in air in fixed nitrogen-free Burk's medium. N/G indicates no growth under these conditions.

[c] MoFe-protein specific activity in the crude extract is listed as nmole of C_2H_4 and H_2 produced per minute per mg total protein under a 10% C_2H_2 / 90% Ar atmosphere in the presence of an optimal amount of purified Fe protein. "+CO" under the same column denotes that the assays were performed in the presence of 10% CO under the otherwise same conditions as the "-CO" assays.

[d] MoFe-protein specific activity in the crude extract is listed as nmole of H_2 produced per minute per mg total protein under a 100% Ar atmosphere in the presence of an optimal amount of Fe protein. "+CO" under the same column denotes that the assays were performed in the presence of 10% CO under the otherwise same conditions as the "-CO" assays.

[e] DJ610 is a double mutant with α-274-His substituted by Gln and α-276-Tyr by His.

The crude extract characterization of the α-274-His mutants are shown in Table 8. Among all ten of the site-directed mutants made at this position, only two were either Nif^{slow} (α-274^{pro}) or Nif^{-} (α-277^{arg}). As is shown in Table 9, the α-276-Tyr residue position is similarly insensitive to substitutions than is α-274-His. Using a range of substitution from amino acid residues with an uncharged polar R group, through residues with a non-polar R group, to those negatively charged residues, only when α-276-Tyr was substituted by a positively-charged residue, Lys, did the resulting mutant grow significantly slower than the wild type. Thus, the conclusion so far is that the α-274-His and α-276-Tyr residues are not critical for nitrogenase catalytic activities, although the distribution of electrons among C_2H_4 and H_2 during the catalyzed reduction of acetylene is affected in some mutant strains.

4.3.2 Whole-cell Electron Paramagnetic Resonance (EPR) Spectroscopy Studies

From an EPR survey of these strains, it was found that the whole cell EPR spectra from mutant strains DJ609 (α-276^{his}), DJ610 (α-274^{gln}/α-276^{his}) were unlike that from the wild type. Shown in Figure 22, whole cell EPR spectra from the mutant strain DJ609 (α-276^{his}) has two sets of signals with *g* values of 4.35, 3.64 and 4.60, 3.45, the mutant strain DJ610 (α-274^{gln} / α-276^{his}) also has two sets of EPR signals with *g* values of 4.66, 3.24 and 4.47 and 3.52, while the wild-type cells have an EPR spectrum with *g* values of 4.34 and 3.65.

4.3.3 Purification of MoFe Proteins from DJ609, DJ610 and Wild-type

MoFe proteins from DJ609, DJ610 and wild type were purified in parallel. Purification procedures included crude extract preparation, DE-52 anion exchange chromatography, followed by Sephacryl S-200 column chromatography (see

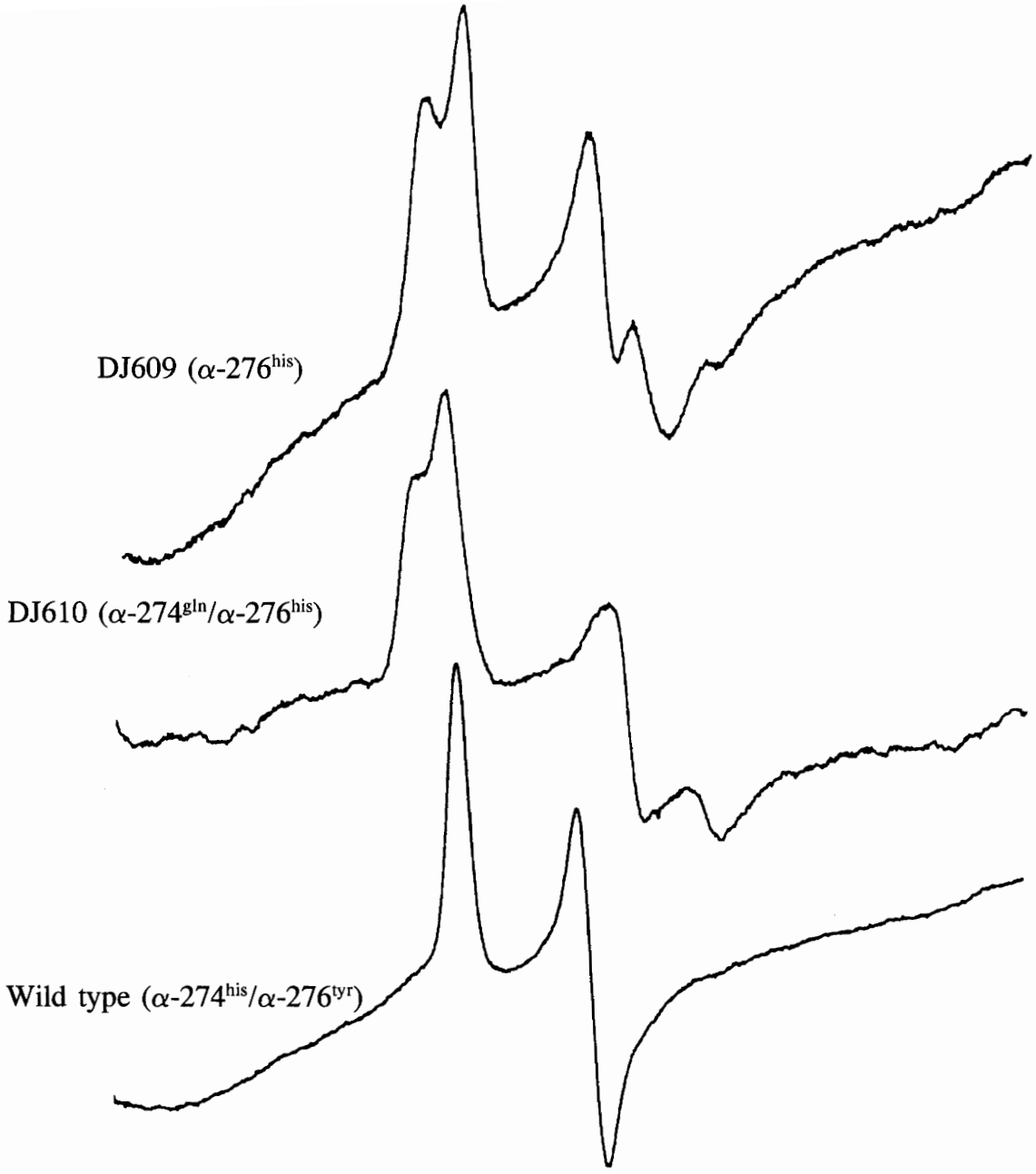

Figure 22. Whole cell EPR spectra from DJ609, DJ610 and wild type in the g = 4 region.

section 4.2.4 for details). The $\alpha 276^{his}$ and $\alpha 274^{gln}/\alpha 276^{his}$ MoFe proteins were heat stable at 56°C, thus, a heat step was included in making the crude extracts. The altered $\alpha 276^{his}$ and $\alpha 274^{gln}/\alpha 276^{his}$ MoFe proteins show lower C_2H_2- and H_2-reduction activities, which are ~60% and ~40% that of the wild-type respectively. Table 10 lists the purification steps and specific activities for all these MoFe proteins. Even so, the three MoFe proteins all behave similarly through this protocol as demonstrated by the similar increases in purity and activity achieved at each step, *i.e.*, all experience a ~3.5 times increase in activity after DE-52 treatment, followed by a ~2-fold increase on gel filtration. Figure-23 shows the MoFe protein α- and β-subunit from three of the strains on SDS-PAGE.

4.3.4 Determinations of the Kinetic Parameters Using α-276^{his}, α-$274^{gln}/\alpha$-276^{his} and Wild-type (α-$274^{his}/\alpha$-276^{tyr}) MoFe Proteins

Table 12 lists the kinetic parameters determined for the catalyzed reduction of C_2H_2. The K_m values for all three MoFe proteins are the same. When the K_i for CO inhibition of C_2H_2 reduction was measured, we found that C_2H_2 reduction catalyzed by both of the altered MoFe proteins was less sensitive to CO than that of the wild-type. The observations suggest that the substitutions flanking the α-275-Cys residues introduced in the DJ609 and DJ610 mutant strains do not appreciably affect the binding of the C_2H_2. These mutations, however, certainly affect the sensitivity to CO although the non-competitive inhibition pattern is unchanged from the wild type. The effect on CO sensitivity, but not on C_2H_2 binding, suggests that these subtle changes of the FeMoco environment are affecting a site of CO binding in this portion of FeMoco. In the ATP hydrolysis studies, it was found that none of the altered MoFe protein (α-276^{his} and α-$274^{gln}/\alpha$-276^{his}) had changed ATP-hydrolysis rates compared to the wild type, indicating that the individual substitutions at these positions did not affect the

Table 10. Purification steps and specific activities at each purification stage for MoFe proteins from DJ609, DJ610 and wild-type cells

MoFe protein	MoFe protein specific activity (nmol H_2/min•mg)		
	Crude extract[a]	DE-52 partial pure[b]	S-200 pure[c]
DJ609 (α-274^{his}/α-276^{his})	130	462	1190
DJ610 (α-274^{gln}/α-276^{his})	94	305	830
Wild-type (α-274^{his}/α-276^{tyr})	305	1110	1980

[a] Crude extracts from the three listed strains were obtained following the procedures described in Experimental Procedure section. A heat step at 56°C for 5 min was included in crude extract preparations from all three strains.

[b] DE-52 partially pure MoFe protein is the major peak collected from the DE-52 anion exchange column.

[c] Sephacryl S-200 gel filtration column chromatography was used as a last purification step.

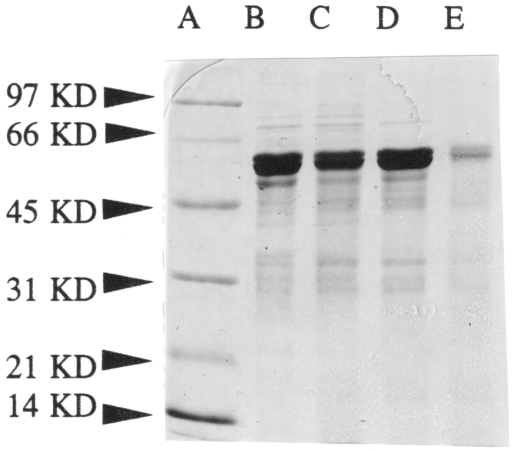

Figure 23. SDS-PAGE of MoFe proteins purified from DJ609, DJ610 and wild-type cells. Lane A: Molecular weight marker; Lane B: α-276^{his} MoFe protein from DJ609; Lane C: α-274^{gln}/α-277^{his} MoFe protein from DJ610; Lane D: wild-type MoFe protein; Lane E: purified wild-type MoFe protein standard.

Table 11. Kinetic parameters for the $\alpha 276^{his}$, $\alpha 274^{gln}/\alpha 276^{his}$ and wild-type ($\alpha 274^{his}/\alpha 276^{tyr}$) MoFe proteins.

Strain[a]	$K_m(C_2H_2)$ (atm)[b]	$K_i(CO)$ (atm)[c]
DJ609 (α-276^{his})	0.0060±0.0002	0.00078
DJ610 (α-$274^{gln}/\alpha$-276^{his})	0.0057±0.0008	0.0011
W-T (α-$274^{his}/\alpha$-276^{tyr})	0.0056±0.0003	0.00035

[a] Strain represents the source from which the MoFe protein was purified for the studies; the amino-acid substitutions made is in parentheses; W-T is wild type.

[b] K_m (C_2H_2) values are expressed as the concentration of C_2H_2 in atmosphere., determined in the acetylene-reduction reaction ($C_2H_2 \rightarrow C_2H_4$) catalyzed by the various MoFe proteins in the presence of wild-type Fe protein in a molar ratio of 1:20 under C_2H_2/Ar atmospheres.

[c] K_i (CO) values expressed as the concentration of CO in atmospheres, determined in the inhibition of catalyzed acetylene reduction by CO.

electron transfer route either intermolecularly or intramolecularly.

4.3.5 Rapid Quench Turn-over Experiments

Since two sets of EPR signals were observed in both mutants, a question arose, "Is it possible that only one set of the signals is actually functional, with the other one representing a nonproductive state of FeMoco?" First, the attempted correlation among the relative intensities of the two sets of EPR signals for each altered MoFe protein and specific activity produced some interesting possibilities. For the α-276^{his} MoFe protein, the two g values at 3.64 and 3.45 are in a 2:1 intensity ratio. If only the FeMoco species giving rise to g =3.64 signal were active, then an expected specific activity (compared to wild type) would be 1300 (1970 $\times$ 0.66) nmol H_2 per minute per mg protein. A specific activity of 1200 is actually found. However, for the nitrogenase from the double mutant, the α-274^{gln}/α-276^{his} MoFe protein, the EPR intensity ratio is 4:1, suggesting that either 80% or 20% of wild-type activity might be expected. In fact, the α-274^{gln}/α-276^{his} MoFe protein has -42% of wild-type specific activity. In order to pursue this question further, pre-steady state EPR studies were carried out using rapid-quench techniques, which ares described as follows.

An experiment was performed on each of the three altered MoFe proteins, α-276^{his}, α-274^{gln}/α-276^{his} and α-277^{his} along with wild type, in which a 3:1 Fe protein to MoFe protein molar ratio was used. A simple device that consisted of a pair of 1.0 ml "Hamilton" gas-tight syringes (Becton Dickinson and Company, Franklin Lakes, NJ), which contained MoFe protein and Fe protein in one of the syringes and ATP-regenerating system in the other, was used. Simultaneous depression of the two syringe plungers delivers the mixture into an EPR tube through the attached hypodermic needle (22 gauge), thus initiating the nitrogenase turnover in the complete system. The reaction was terminated by immediately

freezing the EPR tube in an iso-pentane bath which is itself cooled by liquid nitrogen. A time course of 0s, 5s, 10s, 15s, 20s was performed, with the zero time point performed in the absence of ATP-regenerating system, which was replaced with buffer. Both sets of EPR signals of all the altered MoFe proteins at $g = 4$ region disappeared within 5s in the turnover experiments indicating they turned-over in the nitrogenase reaction under the conditions used for the experiment (23°C, 3:1 Fe-protein to MoFe-protein molar ratio). This results demonstrated that both FeMoco "states" represented by the two set of EPR signals are catalytically active. Further experiments under different conditions, such as lower temperature, high ratio of MoFe protein to Fe protein, or rapid freezing using a special device, are necessary in order to clarify the correlation of the $S = 3/2$ EPR signals with the their catalytic capabilities during nitrogenase turnover.

4.4 Discussion

The three-dimensional crystal structure of the MoFe protein from both *A. vinelandii* and *C. pasteurianum* nitrogenases reveal that, although they are located in proximity to the FeMoco, the side chains of the α-275-Cys flanking residues do not interact directly with the FeMoco. Rather, both structures show that they are pointing away from the FeMoco (Kim & Rees, 1992a; Kim *et al.*, 1993). In *A. vinelandii* MoFe protein, site-directed mutagenesis studies at the α-274-His and α-276-Tyr positions are consistent with their seemingly noncritical roles as almost all constructed mutants retain full nitrogenase activities. For example, most of the mutant strains are able to reduce dinitrogen efficiently at rates comparable to the wild type. It is, however, noticeable that many of the substitutions at α-274 (Ala, Cys, Pro, or Ser) and α-276 (Ala, Cys, Gly, Ser, Thr or Glu) produce nitrogenase that direct a greater percentage of electron flux ($\sim 20\%$ *vs.* $\sim 10\%$) under a 10% C_2H_2 atmosphere to the production of H_2 rather than C_2H_4. These mainly smaller,

non-polar or uncharged residues are, therefore, detrimental to the enzyme's activity to reduce acetylene and suggest the possibility that a site for acetylene binding and reduction may be located on the non-Mo sub-fragment of FeMoco. Major disruptions of acetylene reduction occur in the mutant strains with α-274-His replaced by Arg which has a Nif$^-$ phenotype and no C_2H_2- or H^+-reduction activity with α-274-His replaced by Pro, which gave a Nif^{slow} phenotype; and the strain with α-276-Tyr substituted by Lys, which also yielded a Nif^{slow} phenotype. These two Nif^{slow} phenotypes appear to be due to different dislocations of the active site as shown by some substrate and inhibition studies. The α-274^{pro} nitrogenase, as mentioned above, distributes a larger portion of its electron flux to H_2 evolution (22%) rather than to C_2H_2 reduction compared to wild type (8%) but shows similar sensitivity of C_2H_2 reduction to CO, *i.e.*, less than 1% of its electron flux is used to produce C_2H_4 in the presence of $\sim$0.05 atm CO. In contrast, α-276^{lys} produces similar amounts of H_2 (11%) to wild type under 10% C_2H_2, but its C_2H_2 reduction is much less sensitive to inhibition by CO. In this strain, 29% of electron flux continues to be used to produce C_2H_4 in the presence of 0.05 atm CO. However, the α-274^{tyr} nitrogenases also shows a somewhat lowered sensitivity to CO (3% of flux to C_2H_4) and the α-274^{cys} nitrogenase has an apparently intermediate activity profile with 19% of flux producing H_2 under 10% C_2H_2/Ar and 3% of its flux going to C_2H_4 under 10% C_2H_2/5% CO/Ar. These differential effects of CO, together with the work described in Chapter 3 on the α-277^{his} MoFe protein, indicate that a CO-binding site may be located in this vicinity.

Proline is known to disrupt secondary structure so it is not surprising to see a Nif^{slow} strain upon its substituting for the α-274-His. Dramatic as the Pro residue may be to the local structure generally, when placed at the α-274 position, it does not completely abolish the diazotrophic growth capacity of the mutant

strain. This result indicates the flexible polypeptide backbone at the α-274 residue, which is consistent with its placement at the transition from a β sheet to a random coil structure (Kim & Rees, 1992b). Thus, because of its location, the α-274-His position may have no strict requirement for the type of residue occupying this position. This explanation is also in line with the variation observed at this position among the Mo-nitrogenase sequences known from different species (refer to Figure 2 for details). However, when substituted with an Arg at this position, a strict Nif^- strain was obtained, indicating increased disruption to the polypeptide structure around this position. Similarly, only the positively-charged, longer side-chain of Lys affects diazotrophic growth when substituting at the α-276-Tyr position. The structural basis for these disruptions is unclear. However, when the three-dimensional structure model of *A. vinelandii* nitrogenase is examined, the strictly conserved residues, α-277-Arg, α-389-Arg and α-385-Asp, plus α-284-Arg, which is conserved in most nitrogenase species except *C. pasteurianum* (Glu in *Cp* sequence), are located in the vicinity of the hydroxyl group on the α-276-Tyr side chain. Thus, the addition of yet another positively charged residue in the form of Lys substituting for Tyr may well disrupt this environment. Although α-274-His is located close to a number of strictly conserved residues, such as α-298-Asn and α-299-Phe, plus some mostly conserved residues, α-362-His (Thr in *Cp* sequence) and α-451-His (Ala in *Cp* sequence), the effect of adding a more positively-charged residue to this region is less obvious. Further, as for position α-274, there appears to be no clear requirement for specific types of residues at this position in order for nitrogenase to function properly.

The residues flanking α-275-Cys are not strictly conserved among all nitrogenases. The *Clostridium pasteurianum* α-subunit sequence is distinct among the common nitrogen-fixing species (for sequence comparison among some common nitrogen fixing organisms, refer to Figure 2 from Chapter 1).

Apparently, the *C. pasteurianum* nitrogenase has a unique primary sequence which gets complemented wherever necessary to ensure functionality because *C. pasteurianum* nitrogenase is as effective a dinitrogen fixer as is the *A. vinelandii* nitrogenase. This characteristic may be reflected in the region of the α-276-Tyr and α-274-His residues, where a high tolerance to substitutions in preserving normal nitrogenase functions is observed.

One possible manifestation of this situation is the reported (Morgan *et al.*, 1988) different relaxation properties of the $S = 3/2$ EPR spectrum from the wild - type *A. vinelandii* and *C. pasteurianum* MoFe proteins. The *C. pasteurianum* signal remains visible above 50 K, while the *A. vinelandii* spectrum is broadened beyond observability above 25 K. Comparisons of the primary sequence reveal significant differences, of interest here is the difference in residues immediately flanking α-275-Cys. *A. vinelandii* sequence of -His-Cys-Tyr- is replaced by -Gln-Cys-His- in the *C. pasteurianum* MoFe-protein α-subunit primary sequence. The location of His on opposite sides of the FeMoco-ligating α-275-Cys has been suggested previously (Dean *et al.*, 1990) to impose different constraints on the properties of the two MoFe proteins and this hypothesis was tested by constructing a mutant strain of *A. vinelandii* in which this three-residue sequence was replaced by that in *C. pasteurianum*. As expected, this substitution had only a minimal effect on diazotrophic growth of the mutant strain consistent with the fact that both *A. vinelandii* and *C. pasteurianum* MoFe proteins are functionally equivalent. However, the FeMoco within the altered protein has already been changed because of the two sets of $S = 3/2$ EPR signals that it exhibits. This observation has been followed by the study of the single individual substitutions to produce the strains with the sequences -His-Cys-His- and -Gln-Cys-His-. Whole-cell EPR spectroscopy was performed on these mutant strains. Those involving the His substitution at α-276, namely DJ609 (α-276^{his}) and DJ610 (α-274^{gln} / α-276^{his}) have

EPR spectra composed of two sets of lines around $g = 4$. The EPR spectrum from the mutant strain bearing the -H-C-H- sequence contains one set of lines identical to those of wild type plus a second more rhombic set. A tempting interpretation would be that each His could produce a particular orientation of FeMoco. However, when we replaced α-274-His with Gln (DJ672), resulting in a -QCY- sequence, a wild-type EPR spectrum was recorded indicating that the His residue is not strictly required for the observance of a wild-type EPR spectrum. Interestingly, cells of the double mutant also showed two set of EPR lines around $g = 4$ even though this sequence in *C. pasteurianum* MoFe protein produces only a single wild-type set of two lines. Neither set of signals corresponds to the wild-type signal and neither corresponds to the more rhombic set of lines exhibited by strain DJ609 (-H-C-H-).

Considering all the evidence collected with the wild-type and the mutant strains with substitutions at α-274-His and α-276-Tyr, the replacement of α-276-Tyr with His residue appears as the major contributor to the emergence of a second set of EPR signals. As we mentioned in Chapter 3, two sets of EPR signals were also observed when α-277-Arg was substituted by His (for details, refer to Chapter 3). Because of the close proximity of these two residues, the similar effect caused by their substitution by His likely has a common cause. The α-276-Tyr and α-277-Arg residues are probably involved in providing and preserving a proper environment for the FeMoco with the latter holding a more critical role than the former.

The reason why we see two sets of EPR signals may be the result of the FeMoco oscillating among two almost equivalent environments, the second of which has been introduced by the site-specific His substitution at the α-276-Tyr or α-277-Arg residues. Using purified MoFe protein, we sought to determine whether both FeMoco "orientation" are effective in enzyme turnover. To do so, a

manually driven mixing system was used to produce, and then freeze within 5 seconds, a turning-over solution involving each of these altered MoFe proteins in turn. It was found that both sets of EPR signals were completely gone for all three MoFe proteins in that time. This result indicates that both sets of signals, and, therefore, both FeMoco "orientations" were reduced during turnover and were, thus, likely involved in substrate reduction.

The kinetic studies using purified MoFe proteins from DJ609, DJ610 and the wild type revealed that no change in C_2H_2 binding in the altered MoFe proteins has been introduced compared to that of the wild type. Thus, the alterations at the flanking positions of α-275-Cys to either one His at the opposite position or two His residues did not affect the reactivity of the altered MoFe proteins toward C_2H_2 reduction. However, when we examined the K_i for CO as an inhibitor of the C_2H_2-reduction reaction catalyzed by the MoFe proteins, the α-276^{his} and α-274^{gln}/α-277^{his} MoFe proteins showed somewhat less CO sensitivity compared to that of the wild-type. In Chapter 3, we also examined the K_m values for C_2H_2 reduction and K_i values of CO on C_2H_2 reduction using purified α-277^{his} and wild-type (α-277^{arg}) MoFe proteins. The results indicated changed binding characteristics for substrate (C_2H_2), for the altered protein (α-277^{his} MoFe protein). However, the CO binding pattern in the altered α-277^{his} MoFe protein remains the same as the wild type. Therefore, the observation of a second set of EPR signals, resulting from the substitutions introduced at either α-276-Tyr or α-277-Arg, does not obviously correlate with their affinities for C_2H_2 as a substrate, nor with their sensitivity to CO as an inhibitor.

Chapter 5 Stopped-flow Spectrophotometric Studies on α-276^{his}, α-274^{gln}/α-276^{his} and α-277^{his} MoFe Proteins in Comparison with that of the Wild-type

I thank Dr. Karl Fisher for performing the stopped-flow spectrophotometric experiments.

5.1 Introduction

This investigation is principally concerned with the optical density changes (monitored at 430 nm) that take place as the MoFe-protein is reduced by electron transfer from the Fe protein to the various E_n states of the Lowe-Thorneley MoFe-protein cycle. Previous pre-steady-state stopped-flow spectrophotometric studies have been concerned with the primary electron transfer from the Fe-protein-$(MgATP)_2^{red}$ to the MoFe protein that is complete within 20 ms at 23°C, pH 7.5. Thorneley (1975) and Lowe & Thorneley (1984b) investigated the reduction of the dithionite-reduced resting state of the MoFe protein (E_0) that occurs as the first step in the MoFe-protein cycle. The oxidation of the Fe-protein-$(MgATP)_2^{red}$ was monitored at 430 nm and fitted to a single exponential function. Monitoring of the absorbance change of the Fe-protein by stopped-flow spectrophotometry at 430 nm permits the accurate measurement of the rate constant for electron transfer between the component proteins. Fisher *et al.* (1991) studied the corresponding electron transfer reaction with MoFe protein present initially as 50% E_0 and 50% E_1H (the one-electron reduced state). They concluded that electron transfer from Fe protein to MoFe protein occurred at the same rate with MoFe protein in either state. Recently, there has been an analysis of the absorbance changes at 430 nm that occur after the initial electron transfer reaction (Lowe *et al.*, 1992).

As described in Chapter 3 and Chapter 4, the altered MoFe proteins, from mutant strains DJ609 (α-276^{his}), DJ610 (α-274^{gln}/α-276^{his}) and DJ788 (α-277^{his}), all

have shown characteristics of altered substrate binding affinity and CO inhibition of C_2H_2-reduction activities, especially in the case of altered α-277^{his} MoFe protein, which showed CO-induced cooperativity in C_2H_2 binding. Based on the characteristics of its substrate reduction and CO inhibition, a model was proposed which involved the possibility of a non-existent E_4 state compared to the wild type. This hypothesis could be nicely tested with some pre-steady state kinetic studies. In order to probe for possible changes at the pre-steady state level with the altered MoFe protein, stopped-flow spectrophotometry studies were performed on all three altered MoFe proteins complemented with purified wild-type Fe protein, using wild-type MoFe protein and Fe protein as control. This chapter describes the reinvestigation of these absorbance changes, which occur over the first 500 ms as wild-type and altered α-276^{his}, α-277^{his} and α-274^{gln}/α-276^{his} MoFe proteins, from *A. vinelandii*, become reduced from E_0 through as far as E_4, and compares these changes with those observed previously with wild-type MoFe protein from *K. pneumoniae*.

5.2 Experimental Procedures

5.2.1 Solution Preparations

All solutions were prepared under argon except when N_2 was to be used as substrate. Argon was passed through a heated catalyst column to remove contaminating O_2. A manifold was used to evacuate and argon flush the sealed vials (8 ml volume) to be used in making up the protein solutions. Appropriate aliquots of acetylene, after gentle shaking in a 500-ml dropping funnel containing aqueous 5 mM $Na_2S_2O_4$ to remove any O_2, were added to the vials with gas tight syringes as needed. Protein and ATP solutions contained in sealed vials were taken into a high integrity glove box through which N_2, with an O_2 concentration below 1 ppm, was circulated. All solutions were taken into the glove box

dispensed in 2-ml aliquots immediately prior to performing each experiment to minimize the possible leakage of N_2 into samples through pierced butyl rubber septa. Samples were removed from sealed vials using gas-tight syringes with a wide bore needle attached. Precautions were taken to exclude N_2 from all the solutions unless the experiment was to be performed under an atmosphere of N_2, when the glove box atmosphere was allowed to equilibrate with the samples already prepared under N_2. All experiments to be conducted under an argon atmosphere were performed first and those under N_2 last. The stopped-flow apparatus was left filled with argon saturated buffer (25 mM Hepes-KOH, 10 mM $MgCl_2$, pH 7.4) containing 1 mM $Na_2S_2O_4$ overnight and flushed with similar argon-sparged buffer before filling with the first MgATP and protein solutions prepared under 1 atmosphere argon. The final concentrations after mixing in the stopped-flow spectrophotometer were MoFe protein (10 μM), Fe protein (80 μM) and MgATP (9 mM). All solutions contained $Na_2S_2O_4$ (10 mM), $MgCl_2$ (10 mM) and Hepes-KOH buffer (25 mM) at pH 7.4.

5.2.2 Protein Preparations

The altered MoFe proteins from mutant strains DJ788 (see Chapter 3), DJ609 and DJ610 (see Chapter 4), were purified as described earlier. Wild type MoFe protein and Fe protein were also prepared as before (see Chapter 2 for details). The purified proteins were concentrated using a Minicon concentrator and dialyzed into 200 mM NaCl, 10 mM $MgCl_2$ in 25 mM Hepes-KOH (pH 7.4) in the anaerobic glove box.

5.3 Results and Discussion

5.3.1 Determination of Primary Electron Transfer Rate

Table 12 summarizes the primary electron transfer rate of wild-type MoFe

Table 12. Summary of primary electron transfer rates for purified wild-type, α-276^{his}, α-274^{gln}/α-276^{his} and α-277^{his} MoFe proteins.

Gas Phase	Protein Name			
	wild-type	α-276^{his}	α-277^{his}	α-274^{gln} /α-276^{his}
100% Ar	189	N.D.	160	N.D.
100% N_2	208	226	177	234
100% C_2H_2	215	N.D.	188	N.D.

N.D. represents no data; units are s^{-1}.

protein as well as the three altered α-276^{his}, α-274^{gln}/α-276^{his} and α-277^{his} MoFe proteins under different gas phases at a Fe protein to MoFe protein molar ratio of 8:1. There are no significant differences in the rate constants determined for the three altered MoFe proteins when compared to the wild-type protein. According to the Lowe/Thorneley theory (Thorneley & Lowe, 1985) and the recent improvements (Lowe *et al.*, 1992) of the model, in the *K. pneumoniae* (*Kp*) nitrogenase system, the initial absorbance change up to 25 ms is due to the oxidation of the *Kp* Fe protein by *Kp* MoFe protein because the conversion of *Kp* MoFe protein from state E_0 to E_1 does not involve a significant absorbance change ($<0.5\%$ over the range 400 - 750 nm), and no other redox levels of *Kp* MoFe protein (beyond E_1) are significantly populated at the time (Lowe *et al.*, 1993). We conclude from these observations that the substitutions at the α-274-His, α-276-Tyr and α-277-Arg residues do not change the primary electron transfer from *A. vinelandii* (*Av*) Fe protein to *Av* MoFe protein and internally within *Av* MoFe protein to generate redox state of E_1. This result was not unexpected because, if the current hypothesis of electron flow through nitrogenase is correct, substitutions placed in the FeMoco environment, *i.e.*, at the substrate-binding and -reduction site, should have little or no effect on the early stages of intra-molecular electron transfer and acceptance and this is what has been observed. These results also are apparent indications of the overall MoFe protein structure remaining intact as well as of an unchanged, internal, electron-transfer pathway in the altered MoFe proteins.

5.3.2 Comparison of Absorbance Changes under N_2 for the α-276^{his}, α-274^{gln}/α-276^{his}, α-277^{his} and Wild-type Proteins

In Figure 24, the stopped-flow spectrophotometry absorbance trace for the first one second for all four MoFe proteins under a N_2 atmosphere are shown.

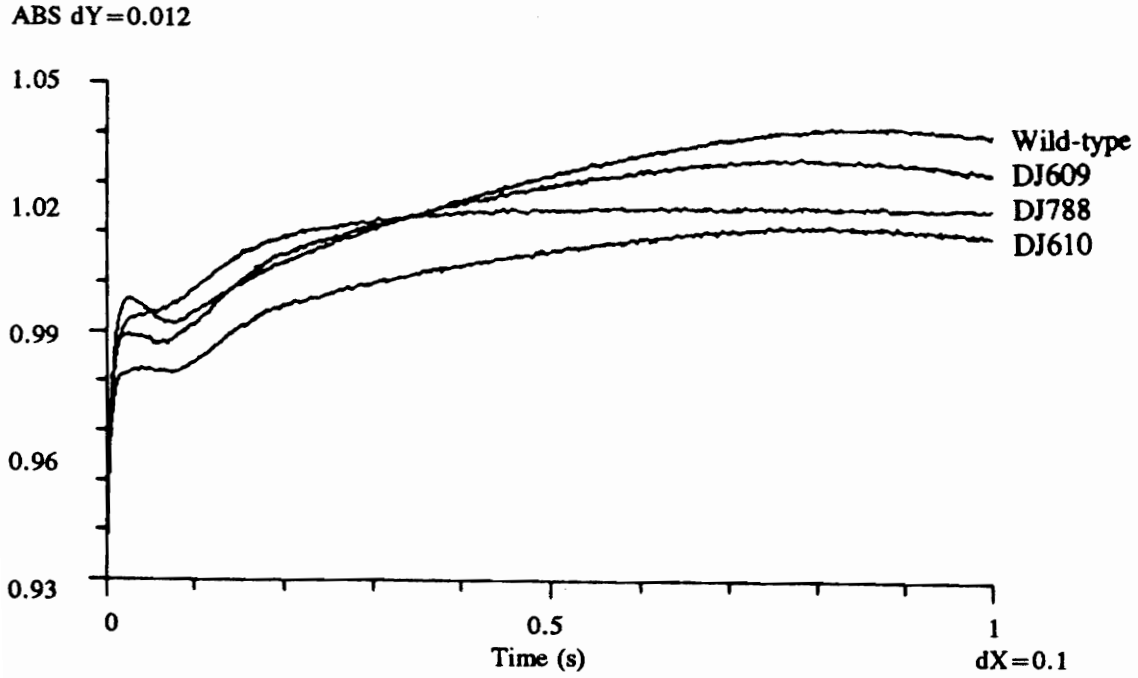

Figure 24. Absorbance change during the first 1 s reaction of MoFe proteins from the α-276^{his}, α-274^{gln}/α-276^{his}, α-277^{his} and wild-type strains under N_2 with Fe protein to MoFe protein molar ratio of 8:1.

According to the studies in the *K. pneumoniae* (*Kp*) nitrogenase system, ~16% of the *Kp* MoFe protein is in E_2 state at 50 ms, whereas at 150 ms, ~33% of the *Kp* MoFe protein is in E_2 state and <1% of the *Kp*1 is at levels other than E_0, E_1 and E_2. When E_3 is reduced to the E_4 state, there is a dramatic increase in absorbance compared to that associated with the prior redox changes ($E_n \rightarrow E_{n+1}$) (Lowe *et al.*, 1993). The stopped-flow data has not been simulated in the *A. vinelandii* nitrogenase system although it has similar trace compared to the *K. pneumoniae* system. In Figure 24, it is obvious that the traces for the α-276^{his}, α-274^{gln}/α-276^{his} and the wild-type proteins are similar, but that the α-277^{his} protein has a different trace in which no increase in absorbance is visible after ~200 ms. We interpret this result as the inability of α-277^{his} to reach the E_4 state. This agrees well with its Nif$^-$ phenotype, and its inability to bind N_2 (for details, see Chapter 3).

5.3.3 Comparison of the Absorbance Changes of the α-277^{his} and Wild-type Proteins under Ar, N_2 and C_2H_2 Atmosphere

As was mentioned above, the α-277^{his} MoFe protein cannot reach its E_4 redox state under a N_2 atmosphere, whereas the other proteins can. Therefore, we used 100% of both Ar and C_2H_2 atmospheres in the stopped-flow spectrophotometric studies in order for the further investigations. The results, shown in Figure 25, confirmed the nonexistent E_4 state under Ar, as was observed under N_2. Under a 100% C_2H_2 atmosphere, the same absorbance trace for both wild-type and the altered α-277^{his} MoFe protein are recorded which indicated similar behavior for both proteins before the E_4 state is reached (*i.e.*, for E_1, E_2 and E_3). Unfortunately, there is no absorbance change detectable for the change from the E_2 to the E_3 redox state (Lowe *et al.*, 1993), therefore, species distribution between the two redox states cannot be estimated.

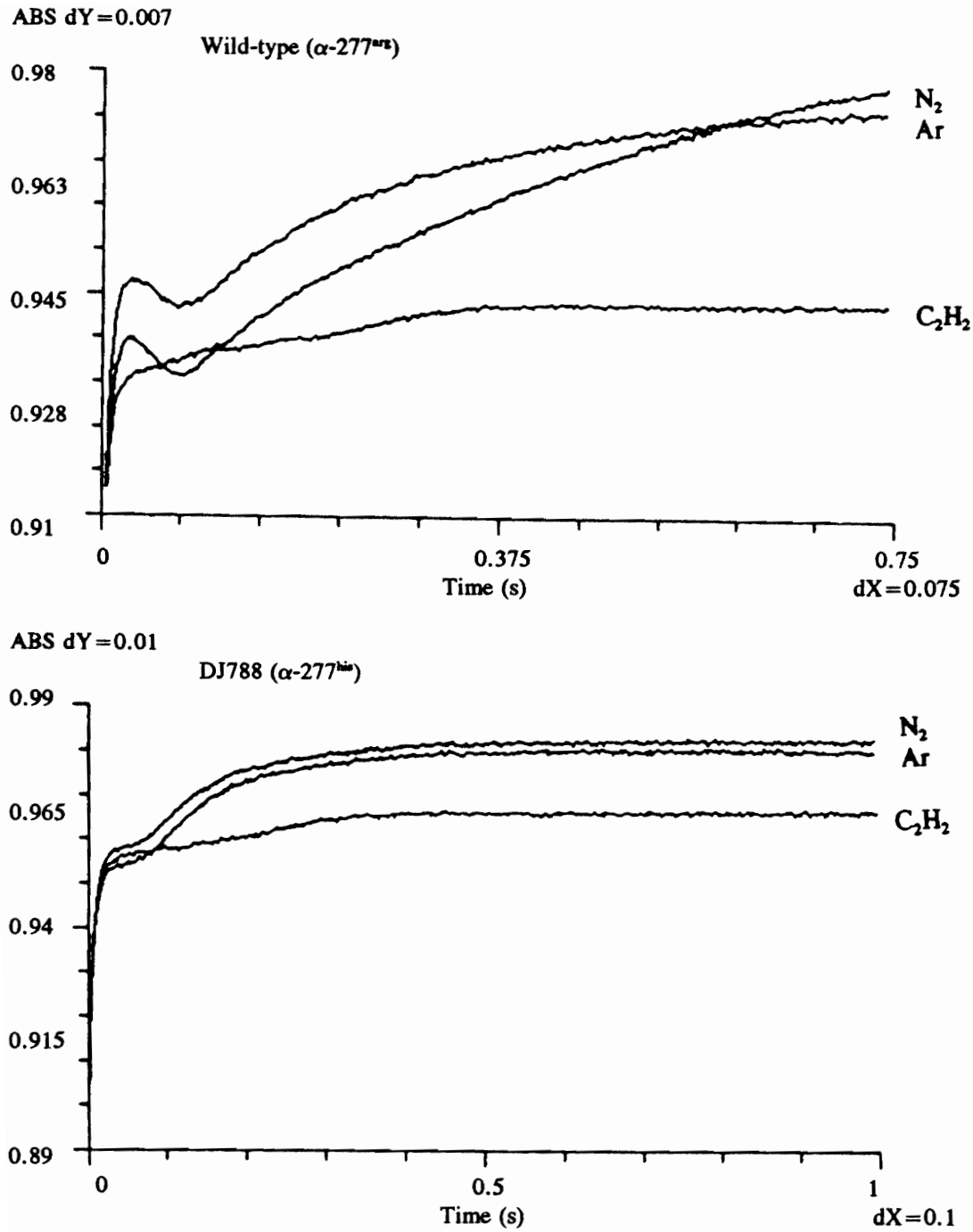

Figure 25. Comparison of the absorbance trace from the wild-type and the altered α-277^{his} MoFe protein under N_2, Ar and C_2H_2 atmosphere.

According to the Lowe/Thorneley theory, in the MoFe protein cycle, E_2 is the first state to evolve H_2, and upon doing so reverts to the E_0 state, which is probably the reason why H_2 always co-evolves with N_2 at a ratio of approximately 1 to 1. The fact that we always observe a higher ratio of H_2 evolution to C_2H_4 production in C_2H_2 reduction reaction could be explained on the basis of the nonexistence of the E_4 state in the altered α-277^{his} MoFe protein. Thus, the E_2 redox state becomes more abundant than in the wild-type MoFe protein cycle, resulting in the loss of electrons by evolving H_2 more readily than in the wild-type counterpart. This holds true for all the assay conditions we used, such as, high electron flux, low electron flux, high C_2H_2 concentration in the assays, different pHs or temperatures (see Chapter 3 for details). Therefore, by combining these data with the previous data, we propose a modified MoFe protein cycle for the altered α-277^{his} MoFe protein as shown in Figure 26.

5.4 Summary

By using the stopped-flow spectrophotometric method, we are able to record the time course of absorbance changes under different gas phases. The conclusions we can draw from these experiments are as follows.

1. Site-directed substitutions introduced in the mutant strains DJ609 (α-276^{his}), DJ610 (α-274^{gln}/α-276^{his}) and DJ788 (α-277^{his}) do not change the electron transfer pathway either intermolecularly (from *A. vinelandii* Fe protein to its MoFe protein) or intramolecularly (within *A. vinelandii* MoFe protein). Thus, the overall structure of the MoFe protein in the mutants constructed remains intact.
2. Because both α-276^{his} and α-274^{gln}/α-276^{his} MoFe proteins showed the same absorbance changes with time as the wild-type protein under a N_2 atmosphere, the mutations therein do not affect the normal functioning of nitrogenase (*i.e.*, they did not alter the oxidation-reduction cycle of the MoFe protein at least up to E_4 state).

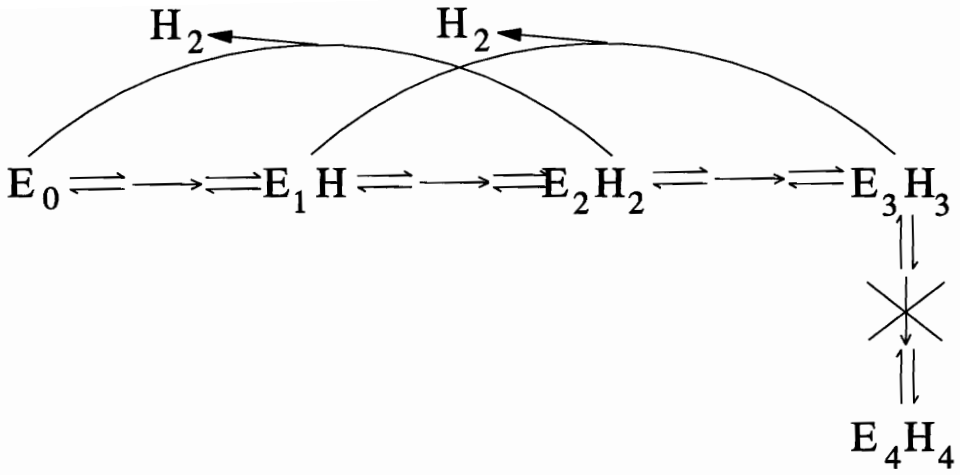

Figure 26. Modified MoFe protein cycle in the altered α-277^{his} MoFe protein.

3. In the case of DJ788 (α-277^{his}), the substitution of Arg by His disturbed the environment of the FeMoco, causing it to be unable to be reduced to the E_4 redox state, resulting in its Nif$^-$ phenotype. However, the absence of an E_4 state did not affect the C_2H_2- and H^+-reduction activities of the altered protein.

Chapter 6 Summary and Outlook

There has been a great deal of effort spent on locating the binding sites of the substrates, including physiological and nonphysiological ones, on the MoFe protein, and more recently, on FeMo-cofactor (FeMoco). With the help of the crystal structure, it is now understood that the substrate binding sites may involve the Fe atoms on the FeMoco (Deng & Hoffman, 1993; Dance, 1994). My research has been mainly aimed on the determination of the potential roles of the residues that are located close to the α-275-Cys, one of the two residues that are directly ligated to the FeMoco. Specifically, the question was what and how the α-274-His, α-276-Tyr and α-277-Arg residues contribute to the nitrogenase catalysis. By using a site-directed mutagenesis approach, individual substitutions at the corresponding positions enabled us to arrive at the conclusions summarized as follows.

First, none of the three residues is absolutely required for nitrogenase activities, although the α-277-Arg residue was found to be more sensitive to substitutions than the other two residues.

Second, some of the substitutions at either position α-276-Tyr or α-277-Arg resulted in the more dramatic change of EPR signals, more specifically, the emergence of a second set of EPR signal at $g = 4$ region. The fact that both signals disappeared during enzyme turnover suggests that they are both catalytically active; however, it is not clear at this point whether or not the two states of FeMoco represented by the two sets of EPR signals are equally active.

Third, it was found in some of the mutants at all three positions that the altered MoFe proteins were able to allocate a higher percentage of electron flux to H_2 evolution than to C_2H_2 reduction under a 10% C_2H_2 /90% Ar atmosphere. In addition, when the inhibition patterns by CO of C_2H_2-reduction reactions were

examined, patterns of CO sensitivity compared to the wild-type MoFe protein were observed ranging from no difference to less sensitive. These variations indicated the possible existence of a CO-binding site in the vicinity, specifically, in the vicinity of α-274-His and/or α-276-Tyr. Among all the mutants examined, none of them exhibited CO-sensitive H_2 evolution activity.

Fourth, none of the purified altered nitrogenases showed any changed ATP hydrolysis rates compared to the wild type, indicating that the electron transfer route has not been disturbed due to the individual substitutions at any of the three residues.

Fifth, and most important of all, through the detailed characterization using purified α-277^{his} MoFe protein and comparing it against the wild type (α-277^{arg}) MoFe protein, we were able to gain some mechanistic insight. Although the altered α-277^{his} MoFe protein lost its dinitrogen-reduction ability, it can still effectively reduce alternative substrates, such as C_2H_2 and H^+, at approximately 60% of the rate of wild type. When CO was present in minute amounts to only partially inhibit the C_2H_2 reduction activity, a CO-induced cooperativity of acetylene-reduction was obtained with the α-277^{his} MoFe protein, which involves two acetylene binding sites and CO acting as a noncompetitive inhibitor to C_2H_2 reduction. This CO-induced cooperativity is present under all electron flux conditions. Therefore, in the altered α-277^{his} MoFe protein, the binding of CO is affecting the enzymatic affinity for C_2H_2. The ten times higher K_m value for C_2H_2-reduction by the α-277^{his} MoFe protein compared to wild-type MoFe protein also supports the proposal that the substitution at this α-277-Arg position is directly affecting the C_2H_2 binding site(s). We have, for the first time, visualized the two C_2H_2 binding sites via altered α-277^{his} MoFe protein, and this phenomenon was induced by the binding of CO.

Furthermore, the altered α-277^{his} MoFe does not bind N_2 because the

presence of N_2 does not affect the catalyzed reduction of the other substrates, such as C_2H_2 and H^+. The substrate-reduction studies, using the altered α-277^{his} MoFe protein, have definitely demonstrated the validity of a previous proposal of C_2H_2 binding to the earlier redox states (E_1 and E_2) of the enzyme than those responsible for binding N_2 (E_3 and E_4) as shown by stopped-flow spectrophotometric experiments. The absence of a more-reduced enzyme state (beyond E_3) in the altered α-277^{his} MoFe protein created a useful model system to study the binding and reduction of other substrates. The results, using different substrates (acetylene, proton, azide and cyanide), have provided confirmation of some of the earlier studies of substrate binding and reduction at different enzymatic states.

Finally, although the three altered MoFe proteins from DJ788 (α-277^{his}), DJ609 (α-276^{his}) and DJ610 (α-274^{gln}/α-276^{his}) all showed additional sets of EPR signals compared to the wild-type protein, there has been no direct correlation between their different spectroscopic behavior and the catalytic characteristics.

In conclusion, although these nonphysiological substrates and inhibitor, such as acetylene or CO, are unlikely to be reduced via exactly the same mechanism as dinitrogen, they share a great deal of structural similarity. Thus, these studies can still provide us with some mechanistic insights into the interaction of the substrate with the FeMoco and also the effect of the polypeptide environment on reactivity. Such studies as these are important if we are ever to understand the mechanism of biological nitrogen fixation and manipulation of biological nitrogen fixation and use it for Mankind's benefit. Biological nitrogen fixation involves the enzymatic reduction of N_2 to ammonia. The ammonia produced then can be incorporated by enzymatic means for the growth and maintenance of the cell. An understanding of biological N_2 fixation is essential to elucidate the dynamics of the global nitrogen cycle and because the biological input of fixed nitrogen to plant growth is by far the major one. By increasing the amount of N_2 fixed or by orienting it more

directly to our major crops, the possibility exists to alleviate some of the hunger and suffering in the World. Apparently, the efficiency of nitrogen fixation largely depends on the arrangement of active site, which is almost certainly on the FeMoco of nitrogenase. Thus, understanding how substrate binding and reduction happens provides crucial information which could lead to targets for the improvement of the nitrogenase system using genetic manipulations of the microorganism. This could lead to a microbial system that is an improved supplier of fixed nitrogen to crops.

In addition, the Habor-Bosch process, the industrial nitrogen fixation process, requires high temperature and high pressure, must operate year-round to be economical (although fertilizer application is seasonal), and be of large capacity (thus, involving transportation costs to the sites of application). On this basis, compared to the biologically efficient nitrogen fixation system in some bacteria, which operates at ambient temperature, on-site and as needed, it seems very energy consuming and inefficient. Therefore, a better understanding of the biological system, in terms of how FeMoco and its polypeptide environment is organized for the dinitrogen reduction, may eventually prove beneficial for industrial nitrogen fixation in the sense of designing some more effective catalyst to improve efficiency. Thus, research on nitrogenase, one of the most important enzyme systems developed by Nature, should pay off in the longer term and produce improved enzymes and microorganisms that are beneficial to Mankind.

Substitution of α-277-Arg residue by His generated an interesting phenotype which allow us to visualize the CO-induced differential binding of C_2H_2 at two sites. However, we are unable to predict the structural change caused by the single mutation. Therefore, it will be more helpful if we could model the local structural change around the FeMoco environment caused by this point mutation. Further work will be needed in an attempt to crystalize the altered α-277^{his} MoFe

protein in order to better understand the reaction mechanism and explain the structural contribution imposed by the changed FeMoco environment on its function. Among all the mutants constructed at the α-277-Arg, we observed these unusual catalytic properties only from the altered α-277^{his} MoFe protein. More insights concerning the substrate and inhibitor binding and interaction will be necessary if we are to understand the mechanism. Other mutants could be used in similar studies. Moreover, it would be interesting to see the effect of substituting the α-277-Arg with some negatively charged residues, such as glutamate and aspartate. Meanwhile, before the crystallographic studies using altered MoFe proteins advance far enough to provide us with structural insights, computer modeling could be performed to simulate the local structure changes introduced by the certain substitutions. Further work is needed to examine the catalytic consequences of the two sets of EPR signals displayed by some of the mutants, such as α-276^{his}, α-274^{gln}/α-276^{his} and α-277^{his}. Some work on the substitutions at α-276-Tyr and α-277-Arg concerning their potential functions as proton donors in nitrogenase catalysis would also provide information in line with the potential channel for the substrate and product entry/exit.

Literature Cited

Ashby, G.A., Dilworth, M.J. and Thorneley, R.N.F. (1987) *Klebsiella pneumoniae* nitrogenase: Inhibition of hydrogen evolution by ethylene and the reduction of ethylene to ethane. *Biochem. J.* **247**, 547-554.

Ashby, G.A. and Thorneley, R.N.F. (1987) Nitrogenase of *Klebsiella pneumoniae*: Kinetic studies on the Fe protein involving reduction by sodium dithionite, the binding of MgATP and a conformation change that alters the reactivity of the 4Fe-4S center. *Biochem. J.* **246**, 455-465.

Bolin, J.T., Ronco, A.E., Mortenson, L.E., Morgan, T.V., Williamson, M., and Xuong, N-h. (1990) Structure of the nitrogenase MoFe protein: Spatial distribution of the intrinsic metal atoms determined by X-ray anomalous scattering. *Nitrogen Fixation: Achievements and Objectives* (Gresshoff, P.M., Roth, L.E., Stacey, G., and Newton, W.E. eds.) Chapman and Hall, New York & London. pp.117-124.

Bolin, J.T., Ronco, A.E., Morgan, T.V., Mortenson, L.E., Xuong, N-h. (1993a) The unusual metal clusters of nitrogenase: Structural features revealed by x-ray anomalous diffraction studies of the MoFe protein from *Clostridium pasteurianum*. *Proc. Natl. Acad. Sci. USA* **90**, 1078-1082.

Bolin, J.T., Campobasso, N., Muchmore, S.W., Morgan, T.V., Mortenson, L.E. (1993b) The crystal structure of the nitrogenase MoFe protein from *Clostridium pasteurianum*. *New Horizons in Nitrogen Fixation* (Palacios, R., Mora, J., Newton, W.E. eds). Dordrecht: Kluwer Academic. pp.89-94,

Brigle, K.E., Weiss, M.C., Newton, W.E. and Dean, D.R. (1987a) Products of the iron-molybdenum cofactor-specific biosynthetic genes, *nifE* and *nifN*, are structurally homologous to the products of the products of the nitrogenase molybdenum-iron protein genes, *nifD* and *nifK*. *J. Bacteriol.* **169**, 1547-1553.

Brigle, K.E., Setterquist, R.A., Dean, D.R., Cantwell, J.S., Weiss, M.C., and Newton, W.E. (1987b) Site-directed mutagenesis of the nitrogenase MoFe protein of *Azotobacter vinelandii*. *Proc. Natl. Acad. Sci. USA* **84**, 7066-7069.

Brigle, K.E., Dean, D.R. (1988) Revised nucleotide sequence of the *Azotobacter vinelandii nifE* gene. *Nucleic Acids Res.* **16**, 5214.

Bulen, W.A. (1976) Nitrogenase from *Azotobacter vinelandii* and reactions affecting mechanistic interpretations. *Proc. 1st Symp. Nitrogen Fixation*, Vol 1, (Newton, W.E., and Nyman, C.J. eds.) Washington State University Press. pp.177-186.

Bulen, W.A. and LeComte, J.R. (1966) The nitrogenase system for *Azotobacter*: Two enzyme requirements for N_2 reduction, ATP dependent H_2 evolution and ATP hydrolysis. *Proc. Natl. Acad. Sci. USA* **56**, 979-986.

Bulen, W.A., Burns, R. and LeComte, J.R. (1965) Nitrogenase fixation:Hydrosulfite as electron donor with cell-free preparations of *Azotobacter vinelandii* and *Rhodospirillum rubrum*. *Proc. Natl. Acad. Sci., USA* **53**, 532-539.

Burgess, B.K., Stiefel, E.I. and Newton, W.E. (1980a) Oxidation-reduction properties and complexation reactions of the iron-molybdenum cofactor of nitrogenase. *J. Biol. Chem.* **255**, 353-356.

Burgess, B.K., Jacobs, D.B., and Stiefel, E.I. (1980b) Large-scale purification of high activity *Azotobacter vinelandii* nitrogenase. *Biochim. Biophys. Acta* **614**, 196-209.

Burgess, B.K., Wherland, S., Newton, W.E. and Stiefel, E.I. (1981) Nitrogenase reactivity: Insight into the nitrogen-fixation process through hydrogen-inhibition and HD-forming reactions. *Biochem.* **20**, 5140-5146.

Burns, A., Watt, G.D., and Wang, Z.C. (1985) Salt inhibition of nitrogenase catalysis and salt effects on the separate protein components. *Biochem.* **24**, 3932-3936.

Burris, R.H., Winter, H.C., Munson, T.O., and Garcia-Rivera, J. (1965) *Non-heme iron proteins, role in energy conversation* (San Pietro, A. ed.) Antioch Press, Yellow Springs, OH. pp.315.

Burris, R.H. (1979) *A Treatise on Dinitrogen Fixation*. (Hardy, R.W.F., Bottomly, F., and Burris, R.H., eds.) Wiley, New York, pp.515.

Chan, M.K., Kim, J., and Rees, D.C. (1993) The nitrogenase FeMo-cofactor and P-cluster pair: 2.2 Å resolution structures. *Science* **260**, 792-794.

Chen, K.C.-K., Chen, J.-S., and Johnson, J.L. (1986) Structural features of

multiple *nifH*-like sequences and very biased codon usage in nitrogenase genes of *Clostridium pasteurianum*. *J. Bacteriol.* **166**, 162-172.

Chisnell, J.R., Premakumar, R., and Bishop, P.E. (1988) Purification of a second alternative nitrogenase from a *nifHDK* deletion strain of *Azotobacter vinelandii*. *J. Bacteriol.* **170**, 27-33.

Cobin, J.L. (1978) A simple, automated apparatus for the rapid multiple flush of reaction (assay) vessels with gases. *Anal. Biochem.* **84**, 340-342.

Conradson, S.D. Burgess, B.K., and Holm, R.H. (1988) Fluorine-19 chemical shifts as probes of the structure and reactivity of the iron-molybdenum cofactor of nitrogenase. *J. Biol. Chem.* **263**, 13743-13749.

Cordewener, , J.H., Haaker, P., van Ewijk, P., and Veeger, C. (1985) Properties of the MgATP and MgADP binding sites on the Fe protein of nitrogenase from *Azotobacter vinelandii*. *Eur. J. Biochem.* **148**, 499-508.

Dance, I.G. (1994) The binding and reduction of dinitrogen at an Fe_4 face of the FeMo cluster of nitrogenase. *Aust. J. Chem.* **47**, 979-990.

Davis, L.C., Henzl, M.T., Burris, R.H., and Orme-Johnson, W.H. (1979) Iron-sulfur clusters in the molybdenum-iron protein component of nitrogenase. Electron paramagnetic resonance of the carbon monoxide inhibited state. *Biochem.* **18**, 4860-4869.

Davis, L.C. (1980) Hydrazine as a substrate and inhibitor of *Azotobacter vinelandii* nitrogenase. *Achiv. Biochem. Biophys.* **204**, 270-276.

Dean, D.R., Brigle, K.E., May, H.D. and Newton, W.E. (1988) Site-directed mutagenesis of the nitrogenases MoFe protein. *Nitrogen Fixation - Hundred Years After*. (Bothe, H., de Bruijn, F.J. and Newton, W.E., eds.) Gustav Fischer, New York, pp.107-113.

Dean, D.R., Scott, D.J. and Newton, W.E. (1990a) Identification of FeMoco domains within the nitrogenase MoFe protein. *Nitrogen Fixation: achievements and objectives* (Gresshoff, P.M., Roth, R.L., Stacey, G. and Newton, W.E., eds.) Chapman and Hall, New York, London. pp.95-102.

Dean, D.R., Setterquist, R.A., Brigle, K.E., Scott, D.J., Laird, N.F., and

Newton, W.E. (1990b) Evidence that conserved residues Cys-62 and Cys-154 within the *Azotobacter vinelandii* nitrogenase MoFe protein α-subunit are essential for nitrogenase activity but conserved residues His-83 and Cys-88 are not. *Mol. Microbiol.* **4(9)**, 1505-1512.

Dean, D.R. and Jacobson, M.R. (1992) Biochemical genetics of nitrogenase. *Biological Nitrogen Fixation*. (Stacey, G., Burris, R.H. and Evans, H.J., eds.) Chapman and Hall, New York. pp.763-834.

Dean, D.R., Bolin, J.T., and Zheng, L. (1993) Nitrogenase metalloclusters: Structures, organization, and synthesis. *J. Bacteriol.*, **175**, 6737-6744.

Deits, T.L., and Howard, J.B. (1990) Effects of salts on *Azotobacter vinelandii* nitrogenase activities. *J. Biol. Chem.* 265, 3859-3867.

Deng, H., and Hoffman, R. (1993) How N_2 might be activated by the FeMo-cofactor in nitrogenase. *Angew. Chem. Int. Ed. Engl.* **32**, 1062-1065.

Derose, V.J., Kim, C.-H., Newton, W.E., Dean, D.R., and Hoffman, B.M. (1994) Spin echo envelope modulation spectroscopic analysis of altered nitrogenase MoFe proteins from *Azotobacter vinelandii*. *Biochem.* submitted.

Dikanov, S.A., and Tsvetkov, Y.D. (1992) Electron spin echo envelope modulation (ESEEM) spectroscopy. CRC Press, Baco Raton, Ann Arbor, London, Tokyo.

Dilworth, M.J. (1966) Acetylene reduction by nitrogen-fixing preparations from *Clostridium pasteurianum*. *Biochim. Biophys. Acta*. **127**, 285-294.

Dilworth, M.J. and Thorneley, R.N.F. (1981) Nitrogenase of *Klebsiella pneumoniae*: Hydrazine is a product of azide reduction. *Biochem. J.* **193**, 971-983.

Dilworth, M.J., Eady, R.R., Robson, R.L. and Miller, R.W.(1987) Ethane formation from acetylene as a potential test for vanadium nitrogenase *in vivo*. *Nature* (London) **327**, 167-168.

Dilworth, M.J., Eady, R.R. and Eldridge, M.E. (1988) The vanadium nitrogenase of *Azotobacter chroococcum*: Reduction of acetylene and ethylene to ethane. *Biochem. J.* **249**, 745-751.

Dilworth, M.J., Eldridge, M.E. and Eady, R.R. (1992) Correction for creatine interference with the direct indophenol measurement of NH_3 in steady-state nitrogenase assays. *Anal. Biochem.* **206**, 6-10.

Eady, R.R., Lowe, D.J. and Thorneley, R.N.F. (1978) Nitrogenase of *Klebsiella pneumoniae*: A pre-steady-state burst of ATP hydrolysis is coupled to electron transfer between the component protein. *FEBS Lett.*, **95**, 211-213.

Eady, R.R. (1986) Enzymology in free-living diazotrophs. *Nitrogen Fixation, Molecular Biology*, Vol.4 (Broughton, W.J. and Pühler, A., eds.) pp.1-49.

Eady, R.R. (1992) The dinitrogen-fixing bacteria. *The procaryotes*, second edition, vol. 1. (Balows, A., Truper, H.G., Dworkin, M., Harder, W., Schleifer, K.H. eds.) Springer-Verlag. pp.534-553.

Emerich, D.W., and Burris, R.H. (1976) Interaction of heterologous nitrogenase components that generate catalytically inactive complexes. *Proc. Natl. Acad. Sci. USA* **73**, 4369-4373.

Emerich, D.W., Ljones, T., and Burris, R.H. (1978) Nitrogenase: Properties of the catalytically inactive complex between *Azotobacter vinelandii* MoFe protein and the *Clostridium pasteurianum* Fe protein. *Biochim. Biophys. Acta* **527**, 359-369.

Ennor, A.H. (1957) Determination and preparation of N-phosphates of biological origin. *Methods in Enzymol.* **3**, 850-856.

Farid, R.S., Moser, C.C., and Dutton, P.L., (1993) Electron transfer in proteins. *Curr. Opin. Struct. Biol.* **3**, 225-233.

Filler, W.A., Kemp, R.M., Ng, J.C., Hawkes, T.R., Dixon, R.A., and Smith, B.E. (1986) The *nifH* gene product is required for the synthesis or stability of the iron-molybdenum cofactor of nitrogenase from *Klebsiella pneumoniae*. *Eur. J. Biochem.* **160**, 371-377.

Fisher, K., Thorneley, R.N.F., and Lowe, D.J. (1990) Nitrogenase of *Klebsiella pneumoniae*: Mechanism of acetylene reduction. *Biochem. J.* **272**, 621-625.

Fisher, K., Lowe, D.J., and Thorneley, R.N.F. (1991) *Klebsiella pneumoniae* nitrogenase: The pro-steady-state kinetics of MoFe-protein reduction and hydrogen

evolution under conditions of limiting electron flux show that the rates of association with the Fe-protein and electron transfer are independent of the oxidation level of the MoFe-protein. *Biochem. J.* **279**, 81-85.

Fisher, K., Lowe, D.J., and Pau, R.N. (1993) *Klebsiella pneumoniae* nitrogenase MoFe protein: Chymotryptic proteolysis affects function by limited cleavage of the β-chain and provides high-specific-activity MoFe protein. *Biochem. J.* **291**, 309-314.

Georgiadis, M.M., Chakrabati, P. and Rees, D.C. (1990) Crystal structure of the nitrogenase iron protein from *Azotobacter vinelandii*. *Nitrogen Fixation: Achievements and Objectives*. (Gresshof, P.M., Roth, L.E., Stacey, G., and Newton, W.E. eds). Chapman and Hall, New York & London. pp.111-116.

Georgiadis, M.M., Komiya, H., Chakrabati, P., Woo, D., Kornuc, J.J. and Rees, D.C. (1992) Crystallographic structure of the nitrogenase iron protein from *Azotobacter vinelandii*. *Science* **257**, 1653-1659.

Gosink, M.M., Franklin, N.M., and Roberts, G.P. (1990) The product of the *Klebsiella pneumoniae nifX* gene is a negative regulator of the nitrogen fixation (*nif*) regulon. *J. Bacteriol.* **172**, 1441-1447.

Govezensky, D., and Zamir, A. (1989) Structure-function relationship in the α-subunit of *Klebsiella pneumoniae* nitrogenase MoFe protein from analysis of *nifD* mutants. *J. Bacteriol.* **171**, 5729-5735.

Guth, J.H., and Burris, R.H. (1983) Inhibition of nitrogenase-catalyzed NH_3 formation by H_2. *Biochem.* **22**, 5111-5122.

Gutteridge, S., Tanner, S.J., and Bray, R.C. (1978) The molybdenum center of native xanthine oxidase. *Biochem J.* **175**, 869-878.

Haaker, H. and Veeger, C. (1977) Involvement of the cytoplasmic membrane in nitrogen fixation by *Azotobacter vinelandii*. *Eur. J. Biochem.* **77**, 1-10.

Hageman, R.V., and Burris, R.H. (1978) Nitrogenase and nitrogenase reductase association and dissociation with each catalytic cycle. *Proc. Natl. Acad. Sci. USA* **75**, 2699-2706.

Hageman, R.V., Orme-Johnson, W.H. and Burris, R.H. (1980) Role of

magnesium adenosine 5'-triphosphate in the hydrogen evolution reaction catalyzed by nitrogenase from *Azotobacter vinelandii*. *Biochem.* **19**, 2333-2342.

Hageman, R.V., and Burris, R.H. (1980) Electron allocation to alternative substrates of *Azotobacter vinelandii* nitrogenase is controlled by the electron flux through dinitrogenase. *Biochim. Biophys. Acta* **591**, 63-75.

Hageman, R.V. and Burris, R.H. (1979) Changes in the EPR signal of dinitrogen from *Azotobacter vinelandii* during the lag period before hydrogen evolution begins. *J. Biol. Chem.* **254**, 11189-11192.

Hagen, W.R., Eady, R.R., Dunham, W.R. and Haaker, H. (1985) A novel $S=3/2$ EPR signal associated with native Fe-proteins of nitrogenase. *FEBS Lett.* **189**, 250-254.

Hales, B.J., Case, E.E., Mornigstar, J.E., Dzeda, M.F., and Mauterer, L.A. (1986) Isolation of a new vanadium-containing nitrogenase from *Azotobacter vinelandii*. *Biochem.* **25**, 7251-7255.

Hales, B.J., Langosch, D.J., and Case, E.E. (1986) Isolation and characterization of a second nitrogenase Fe-protein from *Azotobacter vinelandii*. *J. Biol. Chem.* **261**, 15301-15306.

Hardy, R.W.F., Holsten, R.D., Jackson, E.K., and Burns, R.C. (1968) The acetylene-ethylene assay for N_2 fixation: Laboratory and field evaluation. *Plant Physiol.* **43**, 1185-1207.

Hardy, R.W.F., Burns, R.C., and Holsten, R.D. (1973) Applications of the acetylene-ethylene assay for measurements of nitrogen fixation. *Soil Biol. Biochem.* **5**, 47-81.

Hardy, R.W.F. (1979). *A Treatise on Dinitrogen Fixation*, Section 2, (Hardy, R.W.F. and Burns, R.C. eds.) Wiley and Sons, New York, pp.515-568.

Hardy, R.W.F., and Knight, E. (1968) Biochemistry and postulated mechanisms of nitrogen fixation. *Progress in Phytochemistry*. Vol.1 (Reinhold, L., and Liwschitz, Y., eds.) Wiley, New York, pp.407-489.

Harris, G.S., White, T.C., Flory, J.E., and Orme-Johnson, W.H. (1990) Genes required for formation of the apoMoFe protein of *Klebsiella pneumoniae*

nitrogenase in *Escherichia coli*. *J. Biol. Chem.* **265**, 15909-15919.

Hausinger, R.P., and Howard, J.B. (1983) Thiol reactivity of the nitrogenase Fe-protein from *Azotobacter vinelandii*. *J. Biol. Chem.* **258**, 13486-13492.

Hawkes, T.R., and Smith, B.E. (1983) Purification and characterization of the inactive MoFe protein of the nitrogenase from *nifB* mutants of *Klebsiella pneumoniae*. *Biochem. J.* **209**, 43-50.

Hawkes, T.R., McLean, P.A. and Smith, B.E. (1984) Nitrogenase from *nifV* mutants of *Klebsiella pneumoniae* contains an altered form of the iron-molybdenum cofactor. *Biochem J.* **217**, 317-321.

Hill, S., and Kavanagh, E.P. (1980) Roles of *nifF* and *nifJ* gene products in electron transport to nitrogenase in *Klebsiella pneumoniae*. *J. Bacteriol.* **141**, 470-475.

Hoch, G.E., Schneider, K.C., and Burris, R.H. (1960) Hydrogen evolution and exchange, and conversion of N_2O to N_2 by soybean root nodules. *Biochim. Biophys. Acta.* **37**, 273-279.

Homer, M.J., Paustian, T.D., Shah, V.K., and Roberts, G.P. (1993) The *nifY* product of *Klebsiella pneumoniae* is associated with apodinitrogenase and dissociates upon activation with the iron-molybdenum cofactor. *J. Bacteriol.* **175**, 4907-4910.

Hoover, T.R., Robertson, A.D., Cerny, R.L., Hayes, E.N., Imperial, J., Shah, V.K., and Ludden, P.W. (1987) Identification of the V factor needed for synthesis of the iron-molybdenum cofactor of nitrogenase as homocitrate. *Nature*, **329**, 855-857.

Hoover, T.R., Imperial, J., Ludden, P.W., and Shah, V.K. (1988) Homocitrate cures the *NifV*$^-$ phenotype in *Klebsiella pneumoniae*. *J. Bacteriol.* **170**, 1978-1979.

Hoover, T.R., Imperial, J., Ludden, P.W., and Shah, V.K. (1989) Homocitrate is a component of the iron-molybdenum cofactor of nitrogenase. *Biochem.* **28**, 2768-2771.

Howard, K.S., McLean, P.A., Hansen, F.B., Lemley, P.V., Koblan, K.S., and

Orme-Johnson, W.H. (1986) *Klebsiella pneumoniae nifM* gene product is required for stabilization and activation of nitrogenase iron protein in *Escherichia coli*. *J. Biol. Chem.* **261**, 772-778.

Howard, J.B., Davis, R., Moldenhauer, B., Cash, V.L. and Dean, D. (1989) Fe:S cluster ligands are the only cysteine required for nitrogenase Fe protein activities. *J. Biol. Chem.* **264**, 11270-11274.

Howard, J.B., and Rees, D.C. (1994) A nucleotide-dependent molecular switch. *Annu. Rev. Biochem.* **63**, 235-264.

Hwang, J.C., and Burris, R.H. (1972) Nitrogenase-catalyzed reactions. *Biochim. Biophys. Acta* **283**, 339-350.

Hwang, J.C., Chen, C.H., and Burris, R.H. (1973) Inhibition of nitrogenase-catalyzed reductions. *Biochim. Biophys. Acta* **292**, 256-270.

Jackson, E.K., Parshall, G.W., and Hardy, R.W.F. (1968) Hydrogen reactions of nitrogenase: Formation of the molecule HD by nitrogenase and by an inorganic model. *J. Biol. Chem.* **243**, 4952-4958.

Jacobson, M.R., Cash, V.L., Weiss, M.C., Laird, N.F., Newton, W.E., and Dean, D.R. (1989b) Biochemical and genetic analysis of the *nifUSVWZM* cluster from *Azotobacter vinelandii*. *Mol. Gen. Genet.* **219**, 49-57.

Jacobson, M.R., Cantwell, J.S., and Dean, D.R. (1990) A hybrid *Azotobacter vinelandii-Clostridium pasteurianum* nitrogenase iron protein that has *in vivo* and *in vitro* catalytic activity. *J. Biol. Chem.* **265**, 19429-19433.

Kelly, M. (1969) Comparisons and cross reactions of nitrogenase from *Klebsiella pneumoniae*, *Azotobacter chroococcum* and *Bacillus polymyza*. *Biochim. Biophys. Acta* **191**, 527-540.

Kennedy, I.R., Morris, J.A., and Mortenson, L.E. (1968) N_2 fixation by purified components of the N_2-fixing system of *Clostridium pasteurianum*. *Biochim. Biophys. Acta.* **153**, 777-786.

Kent, H.M., Ioannidis, I., Gormal, C., Smith, B.E., and Buck, M. (1989) Site-directed mutagenesis of the *Klebsiella pneumoniae* nitrogenase. *Biochem. J.* **264**, 257-264.

Kent, H.M., Baines, M., Gormal, C., Smith, B.E., and Buck, M. (1990) Analysis of site-directed mutations in the α- and β-subunits of *Klebsiella pneumoniae* nitrogenase. *Mol. Microbiol.* **4(9)**, 1497-1504.

Kim, J., Woo, D., and Rees, D.C. (1993) X-ray crystal structure of the nitrogenase molybdenum-iron protein from *Clostridium pasteurianum* at 3.0-Å resolution. *Biochem.* **32**, 7104-7115.

Kim, C.-H., Newton, W.E., and Dean, D.R. (1994) Studies on the role of the MoFe protein α-subunit histidine-195 residue in FeMo-cofactor binding and nitrogenase catalysis. *Biochem.* in press.

Kim, J. and Rees D.C. (1992a) Structural models for the metal centers in the nitrogenase molybdenum-iron protein. *Science* **257**, 1677-1659.

Kim, J., and Rees, D.C. (1992b) Crystallographic structure and functional implications of the nitrogenase molybdenum-iron protein from *Azotobacter vinelandii*. *Nature* **360**, 553-560.

Kim, J., Rees, D.C. (1994) Nitrogenase and biological nitrogen fixation. *Biochem*, **33**, 389-397.

Knowles, P.F., Marsh, D., and Rattle, H.W.E. (1976) *Magnetic resonance of biomolecules*. Wiley, New York.

Kraulis, P. (1991) MOLSCRIPT:A program to produce both detailed and schematic plots of protein structures. *J. Appl. Cryst.* **24**, 946-950.

Kurtz, D.M., Jr., McMillan, R.S., Burgess, B.K., Mortenson, L.E., and Holm, R.M. (1979) Identification of iron-sulfur centers in the iron-molybdenum centers in the iron-molybdenum proteins of nitrogenase. *Proc. Natl. Acad. Sci. USA* **80**, 4723-4727.

Laemmli, U.K. (1970) Cleavage of structural proteins during the assembly of the head of bacteriophage T_4. *Nature* (London) **227**, 680-685.

Leigh, G.J. (1981) The signifance of current research on chemical nitrogen fixation. *Chemistry and Industry*. 664-667.

Li, J.-G., Burgess, B.K. and Corbin, J.L. (1982) Nitrogenase reactivity: Cyanide

as a substrate and inhibitor. *Biochem.* **21**, 4393-4402.

Liang, J., Madden, M., Shah, V.K., and Burris, R.H. (1990) Citrate substitutes for homocitrate in nitrogenase of a *nifV* mutant of *Klebsiella pneumoniae*. *Biochem.* **29**, 8577-8581.

Lindahl, P.A., Papaefthymiou, V., Orme-Johnson, W.H., and Münck, E. (1988) Mössbauer studies of solid thionine-oxidized MoFe protein of nitrogenase. *J. Biol. Chem.* **263**, 19412-19418.

Lowe, D.J. and Thorneley, R.N.F. (1984a) The mechanism of *Klebsiella pneumoniae* nitrogenase action: Pre-steady-state kinetics of H_2 formation. *Biochem. J.* **224**, 877-886.

Lowe, D.J. and Thorneley, R.N.F. (1984b) The mechanism of *Klebsiella pneumoniae* nitrogenase action: The determination of rate constants required for the simulation of the kinetics of N_2 reduction and H_2 evolution. *Biochem. J.* **224**, 887-911.

Lowe, D.J., Thorneley, R.N.F., and Smith, B.E. (1985) Metal proteins with redox roles. *Metalloprotein 1* (Harrison, P.M. ed.) pp.207-249.

Lowe, D.J., Fisher, K., and Thorneley, R.N.F. (1990) *Klebsiella pneumoniae* nitrogenase mechanism of acetylene reduction and its inhibition by carbon monoxide. *Biochem. J.* **272**, 621-625.

Lowe, D.J. (1992) Multiple-electron transfer processes in nitrogen fixation and other natural systems. *Electron and proton transfer in chemistry and biology*. (Muller, A., Ratajczak, H., Jungle, W., and Diemann, E., eds.) Elsevier, Amsterdam. pp.149-165.

Lowe, D.J., Fisher, K. and Thorneley, R.N.F. (1993) *Klebsiella pneumoniae* nitrogenase: pre-steady-state absorbance changes show that redox changes occur in the MoFe protein that depend on substrate and component protein ratio; a role for P-centers in reducing dinitrogen? *Biochem. J.* **292**, 93-98.

Lowe, D.J., Fisher, K., Thorneley, R.N.F., Vaughn, S.A., and Burgess, B.K. (1989) Kinetics and mechanism of the reaction of cyanide with molybdenum nitrogenase from *Azotobacter vinelandii*. *Biochem.* **28**, 8460-8466.

Lowery, R., Chang, C., Davis, L., McKenna, M.C., Stephens, P.J., and Ludden, P. (1989) Substitution of histidine for arginine-101 of dinitrogenase reductase disrupts electron transfer to dinitrogenase. *Biochem.* **28**, 1206-1212.

Madden, M.S.,Kindon, N.D., Ludden, P.W., and Shah, V.K. (1990) Diastereomer-dependent substrate reduction properties of a dinitrogenase containing 1-fluorohomocitrate in the iron-molybdenum cofactor. *Proc. Natl. Acad. Sci. USA* **87**, 6517-6521.

Martin, A.E., Burgess, B.K., Iismaa, S.E., Smartt, C.T., Jacobson, M.R., and Dean, D.R. (1989) Construction and characterization of an *Azotobacter vinelandii* strain with mutations in the genes encoding flavodoxin and ferredoxin I. *J. Bacteriol.* **171**, 3162-3167.

Mascharak, P.K., Smith, M.C., Armstrong, W.H., Burgess, B.K., and Holm, R.H. (1982) Fluorine-19 chemical shifts as structural probes of metal-sulfur clusters and the cofactor of nitrogenase. *Proc. Natl. Acad. Sci. USA* **79**, 7056-7060.

May, H.D., Dean, D.R., and Newton, W.E. (1991) Altered nitrogenase MoFe proteins from *Azotobacter vinelandii*. *Biochem. J.* **277**, 457-464.

Menon, A.L., Stults, L.W., Robson, R.L., and Mortenson, L.E. (1990) Cloning, sequencing and characterization of the [NiFe] hydrogenase-encoding structural genes (*hoxK* and *hoxG*) from *Azotobacter vinelandii*. *Gene* **96**, 67-74.

Mensink, R.E., Wassink, H., and Haaker, H. (1992) A reinvestigation of the pre-steady-state ATPase activity of the nitrogenase from *Azotobacter vinelandii*. *Eur. J. Biochem.* **208**, 289-294.

McLean, P.A., Smith, B.E. and Dixon, R.A. (1983) Nitrogenase of *Klebsiella pneumoniae nifV* mutants. *Biochem. J.* **211**, 589-597.

McLean, P.A., Papaefthymiou, V., Orme-Johnson, W.H., and Münck, E. (1987) Isotopic hybrids of nitrogenase: Mössbauer study of MoFe protein with selective ^{57}Fe enrichment of the P clusters. *J. Biol. Chem.* **262**, 12900-12903.

Miller, A.F., and Orme-Johnson, W.H. (1992) The dependence on iron availability of allocation of iron to nitrogenase components in *Klebsiella pneumoniae* and *Escherichia coli*. *J. Biol. Chem.* **267**, 9398-9408.

Morgan, T.V., Mortenson, L.E., McDonald, J.W., and Watt, G.D. (1988) Comparison of redox and EPR properties of the molybdenum iron proteins of *Clostridium pasteurianum* and *Azotobacter vinelandii* nitrogenases. *J. Inorg. Biochem.* **33**, 111-120.

Morgan, T.V., McCracken, J., Orme-Johnson, W.H., Mims, W.B., Mortenson, L., and Peisach, J. (1990) Pulsed EPR studies of the interaction of magnesium-ATP and deuterated water with the iron protein of nitrogenase. *Biochem.* **29**, 3077-3082.

Mortenson, L.E. (1964) Ferredoxin and ATP, requirements for nitrogen fixation in cell-free extracts of *Clostridium pasteurianum. Proc. Natl. Acad. Sci. USA* **52**, 272-279.

Mortenson, L.E. and Thorneley, R.N.F. (1979) Structure and function of nitrogenase. *Ann. Rev. Biochem.* **48**, 387-418.

Moustafa, E., and Mortenson, L.E. (1967) Acetylene reduction by nitrogen fixation extracts of *Clostridium pasteurianum*: ATP requirement and inhibition by ADP. *Nature* **216**, 1241-1242.

Murrell, S.A., Lowery, R.G., and Ludden, P.W. (1988) ADP-ribosylation of dinitrogenase reductase from *Clostridium pasteurianum* prevents its inhibition of nitrogenase from *Azotobacter vinelandii*. *Biochem. J.* **251**, 609-612.

Newton, W.E, Bulen, W.A., Hadfield, K.L., Stiefel, E.O., and Watt, G.D. (1977) HD formation as a probe for intermediates in N_2 reduction. *Recent developments in nitrogen fixation.* (Newton, W.E., Postgate, J.R., and Rodriguez-Barrueco, C., eds.) Academic Press, London, New York, San Francisco. pp. 119-130.

Newton, W.E., Gheller, S.F., Hedman, B., Hodgson, K.O., Lough, S.M., and McDonald, J.W. (1985) Redox and compositional insights into the iron-molybdenum cofactor of *Azotobacter vinelandii* nitrogenase as a guide to synthesis of new Mo-Fe-S clusters. *Nitrogen Fixation Research Progress*. (Evans, H.J., Bottomley, P.J., and Newton, W.E., eds.) Dordrecht: Martinus Nijhoff. pp. 605-610.

Newton, W.E. (1992) Isolated Iron-Molybdenum Cofactor of Nitrogenase. *Biological Nitrogen Fixation*. (Stacey, G., Burris, R.H., and Evans, H.J., eds.)

Chapman & Hall, New York, London. pp. 877-929.

Newton, W.E., and Dean, D.R. (1993) Role of the iron-molybdenum cofactor polypeptide environment in *Azotobacter vinelandii* molybdenum-nitrogenase catalysis. *Molybdenum enzymes, cofactors, and model systems* (Stiefel, E.I., Coucouvanis, D., and Newton, W.E., eds.) American Chemical Society, Washington D.C. pp.216-230.

Orme-Johnson, W.H., Hamilton, W.D., Ljones, T., Tso, M.-Y., Burris, R.H., Shah, V.K. and Brill, W.J. (1972) Electron paramagnetic resonance of nitrogenase and nitrogenase components from *Clostridium pasteurianum W5* and *Azotobacter vinelandii OP*. *Proc. Natl. Acad. Sci. USA* **69**, 3142-3145.

Palmer, G. (1985) The electron paramagnetic resonance of metalloproteins. *Biochem. Soc. Trans.* **13**, 548-560.

Pau, R.N., Mitchenall, L.A., and Robson, R.L. (1989) Genetic evidence for an *Azotobacter vinelandii* nitrogenase lacking molybdenum and vanadium. *J. Bacteriol.* **171**, 124-129.

Paul, W., and Merrick, M. (1989) The roles of the *nifW, nifZ* and *nifM* genes of *Klebsiella pneumoniae* in nitrogenase biosynthesis. *Eur. J. Biochem.* **178**, 675-682.

Paustian, T. D., Shah, V.K. and Roberts, G.P. (1989) Purification and characterization of the *nifE* and *nifN* gene products from *Azotobacter vinelandii* mutant UW45. *Proc. Natl. Acad. Sci. USA* **86**, 6082-6086.

Paustian, T. D., Shah, V.K., and Roberts, G.P. (1990) Apo-dinitrogenase purification, association with a 20-kilodalton protein, and activation by the iron-molybdenum cofactor in the absence of nitrogenase. *Biochem.* **29**, 3515-3522.

Peters, P.W., Fisher, K., and Dean, D.R. (1994) Identification of a nitrogenase protein-protein interaction site defined by residues 59 through 67 within the *Azotobacter vinelandii* Fe protein. *J. Biol. Chem.* **269**, 28076-28083.

Pope, M.R., Murrell, S.A., and Ludden, P.W. (1985) Covalent modification of the iron protein of nitrogenase from *Rhodospirillum rubrum* by adenosine diphosphoribosylation of a specific arginine residue. *Proc. Natl. Acad. Sci. USA* **82**, 3173-3177.

Rawlings, J., Shah, V.K., Chisnell, J.R., Brill, W.J., Zimmermann, R., Münck, E. and Orme-Johnson, W.H. (1978) Noval metal cluster in the iron-molybdenum cofactor of nitrogenase. *J. Biol. Chem.* **253**, 1001-1004.

Rivera-Ortiz, J.M., and Burris, R.H. (1975) Interactions among substrates and inhibitors of nitrogenase. *J. Bacteriol.* **123**, 537-545.

Roberts, G.P., MacNeil, T., McNeil, D., and Brill, W.J. (1978) Regulation and characterization of protein products coded by the *nif* (nitrogen fixation) genes of *Klebsiella pneumoniae*. *J. Bacteriol.* **136**, 267-279.

Robinson, A.C., Dean, D.R., and Burgess, B.K. (1987) Iron-molybdenum cofactor biosynthesis in *Azotobacter vinelandii* mutant strains containing defined deletions within the nitrogenase structural gene cluster. *J. Bacteriol.* **166**, 180-186.

Robson, R.L., Eady, R.R., Richardson, T.H., Miller, R.W., Hawkins, M., and Postgate, J.R. (1986) The alternative nitrogenase of *Azotobacter chroococcum* is a vanadium enzyme. *Nature (London)* **322**, 388-390.

Rubinson, J.F., Burgess, B.K., Corbin, J.L. and Dilworth M.J. (1985) Nitrogenase reactivity: Azide reduction. *Biochem.* **24**, 273-283.

Schill, R. (1977) Instrumentation. *Modern Practice of Gas Chromatography*. (Grob, R.L., ed.) Wiley, New York, London, Sydney, Toronto, pp.289-364.

Schöllhorn, R., and Burris, R.H. (1967) Acetylene as a competitive inhibitor of N_2 fixation. *Proc. Natl. Acad. Sci. USA* **58**, 213-216.

Scott, D.J., May, H.D., Newton, W.E., Brigle, K.E. and Dean, D.R. (1990) Role for the nitrogenase MoFe protein α-subunit in FeMo-cofactor binding and catalysis. *Nature* **343**, 188-190.

Scott, D.J., Dean, D.R., and Newton, W.E. (1992) Nitrogenase-catalyzed ethane production and CO-sensitive hydrogen evolution from MoFe proteins having amino acid substitutions in an α-subunit FeMo cofactor-binding domain. *J. Biol. Chem.* **267**, 20002-20010.

Segal, I.H. (1975) *Enzyme Kinetics: Behavior and analysis of rapid equilibrium and steady-state enzyme systems*. Wiley. New York, Chichester, Brisbane,

Toronto, Singapore.

Sellman, D. (1993) X-ray structure analysis of FeMo nitrogenase - Is the problem of N_2 fixation solved? *Angew. Chem. Int. Ed. Engl.* **32**, 64-67.

Shah, V.K., and Brill. W.J. (1977) Isolation of an iron-molybdenum cofactor from nitrogenase. *Proc. Natl. Acad. Sci. USA* **78**, 3249-3253.

Shah, V.K., Stacey, G. and Brill, W.J. (1983) Electron transport to nitrogenase: Purification and characterization of pyruvate:flavodoxin oxidoreductase, the *nifJ* gene product. *J. Biol. Chem.* **258**, 12064-12068.

Shah, V.K., Ugalde, R.A., Imperial, J., and Brill, W.J. (1984) Molybdenum in nitrogenase. *Ann. Rev. Biochem.* **53**, 231-257.

Shah, V.K., Imperial, J., Ugalde, R.A., Ludden, P.W., and Brill, W.J. (1986) *In vitro* synthesis of the iron-molybdenum cofactor of nitrogenase. *Proc. Natl. Acad. Sci. USA* **83**, 1636-1640.

Shah, V.K., Hoover, T.R., Imperial, J. Paustian, T.D., Roberts, G.P., and Ludden, P.W. (1988) Role of *nif* gene products and homocitrate in the biosynthesis of iron-molybdenum cofactor. *Nitrogen Fixation: Hundred Years After.* (Bothe, H., de Bruijn, F.J., and Newton, W.E., eds.) Stuttgart: Gustav Fischer. pp.115-120.

Simpson, F.B., and Burris, R.H. (1984) A nitrogen pressure of 50 atmospheres does not prevent evolution of hydrogen by nitrogenase. *Science* **224**, 1095-1097.

Smith, B.E., Lowe, D.J., Chen, G.-X., O'Donnell, M.J., and Hawkes, T.R. (1983) Evidence on intramolecular electron transfer in the MoFe protein of nitrogenase from *Klebsiella pneumoniae*. *Biochem. J.* **207**, 207-213.

Smith, B.E. and Lang, G. (1974) Mössbauer spectroscopy of the nitrogenase proteins from *Klebsiella pneumoniae*. *Biochem. J.* **137**, 169-180.

Smith, B.E., Bishop, P.E., Dixon, R.A., Eady, R.R., Filler, W.A., Lowe, D.J., Richards, A.J.M., Thompson, A.J., Thorneley, R.N.F. and Postgate, J.R. (1985) The iron-molybdenum cofactor of nitrogenase. *Nitrogen Fixation Progress.* (Evans, H.J., Bottomley,P.J. and Newton, W.E., eds.) pp. 597-603.

Smith, B.E., and Eady, R.R. (1992) Metalloclusters of the nitrogenase. *FEBS.* **205**, 1-15.
Smith, P.K., Krohn, R.I., Hermanson, G.T., Mallia, A.K., Gartner, F.H., Provenzano, M.D., Fujimoto, E.K., Goeke, N.M., Olson, B.J., and Klenk, D.C. (1985) Measurement of protein using bicinchoninic acid. *Anal. Biochem.* **150**, 76-85.

Stephens, P.J., McKenna, C.E., Smith, B.E., Nguyen, H.T., McKenna, M.-C., Thomas, A.J., Devlin, F., and Jones, J.B. (1979) Circular dichroism and magnetic circular dichroism of nitrogenase proteins. *Proc. Natl. Acad. Sci. USA* **76**, 2585-2590.

Stiefel, E.I. (1973) Proposed molecular mechanism for the action of molybdenum in enzymes: Coupled proton and electron transfer. *Proc. Natl. Acad. Sci. USA* **70**, 988.

Strandberg, G.W., and Wilson, P.W. (1968) Formation of the nitrogen-fixing enzyme systems in *Azotobacter vinelandii*. *Can. J. Microb.* **14**, 25-31.

Sullivan, J.J., and O'Brien, M.J. (1977) Detectors. *Modern Practice of gas chromatography*. (Grob, R.L., ed.) John Wiley & Sons, New York, Sydney, Toronto, pp. 213-288.

Sundaresan, V., and Ausubel, F.M. (1981) Nucleotide sequence of the gene coding for the nitrogenase Fe protein from *Klebsiella pneumoniae*. *J. Biol. Chem.* **256**, 2808-2812.

Thomann, H., Morgan, T.V., Jin, H., Burgmayer, S.N.J., Bare, R.E. and Stiefel, E.I. (1987) Protein nitrogen coordination to the FeMo center of nitrogenase from *Clostridium pasteurianum*. *J. Am. Chem. Soc.* **109**, 7913-7914.

Thomann, H., Bernardo, M., Newton, W.E., and Dean, D.R. (1991) N coordination of FeMo-cofactor requires His-195 of the MoFe proteins α subunit and is essential for biological nitrogen fixation. *Proc. Natl. Acad. Sci. USA* **88**, 6620-6623.

Thorneley, R.N.F. (1975) Nitrogenase of *Klebsiella pneumoniae*: A stopped-flow study of magnesium-adenosine triphosphate-induced electron transfer between the component proteins. *Biochem. J.* **145**, 391-396.

Thorneley, R.N.F., Yates, M.G. and Lowe, D.J. (1976) Nitrogenase of *Azotobacter chroococcum*: Kinetics of the reduction of oxidized iron-protein by sodium dithionite. *Biochem. J.* **155**, 137-144.

Thorneley, R.N.F., Eady, R.R. and Lowe, D.J. (1978) Biological nitrogen fixation by way of an enzyme-bound dinitrogen-hydride intermediate. *Nature* **272**, 557-558.

Thorneley, R.N.F. and Lowe, D.J. (1983) Nitrogenase of *Klebsiella pneumoniae*: Kinetics of the dissociation of oxidized iron protein from molybdenum-iron protein: Identification of the rate-limiting step for substrate reduction. *Biochem. J.* **215**, 393-403.

Thorneley, R.N.F. and Lowe, D.J. (1984a) The mechanism of *Klebsiella pneumoniae* nitrogenase action: Pre-steady-state kinetics of an enzyme-bound intermediate in N_2 reduction and of NH_3 formation. *Biochem. J.* **224**, 886-894.

Thorneley, R.N.F. and Lowe, D.J. (1984b) The mechanism of *Klebsiella pneumoniae* nitrogenase action: Simulation of the dependence of the H_2 evolution rate on component-protein concentration and ratio and sodium dithionite concentration. *Biochem. J.* **224**, 903-909.

Thorneley, R.N.F. and Lowe, D.J. (1985) Kinetic and mechanism of the nitrogenase enzyme system. *Molybdenum Enzymes*. (Spiro, T.G., eds) Wiley & Sons, pp.221-284.

Thorneley, R.N.F, and Deistung, J. (1988) Electron-transfer studies involving flavodoxin and a natural redox partner, the iron protein of nitrogenase: Conformational constraints on protein-protein interactions and the kinetics of electron transfer within the protein complex. *Biochem. J.* **253**, 587-595.

Thorneley, R.N.F., and Ashby, G.A. (1989) Oxidation of nitrogenase iron protein by dioxygen without inactivation could contribute to high respiration rates of *Azotobacter vinelandii* and facilitate nitrogen fixation in other aerobic environments. *Biochem. J.* **261**, 181-187.

Thorneley, R.N.F., Ashby, G.A., Howarth, J.V., Millar, N.C., and Gutfreund, H. (1989) A transient kinetic study of the nitrogenase of *Klebsiella pneumoniae* by stopped-flow calorimetry. *Biochem. J.* **264**, 657-661.

True, A.E., Nelson, M.J., Ventors, R.A., Orme-Johnson, W.H., and Hoffman, B.M. (1988) ^{57}Fe hyperfine coupling tensors of the FeMo cluster in *Azotobacter vinelandii* MoFe protein: Determination by polycrystalline ENDOR spectroscopy. *J. Am. Chem. Soc.* **110**, 1935-1943.

Ulgalde, R.A., Imperial, J., Shah, V.K., and Brill, W.J. (1984) Biosynthesis of iron-molybdenum cofactor in the absence of nitrogenase. *J. Bacteriol.* **159**, 888-893.

Wherland, S., Burgess, B.K., Stiefel, E.I. and Newton, W.E. (1981) Nitrogenase Reactivity: Effects of component ratio on electron flow and distribution during nitrogen fixation. *Biochem.* **20**, 5132-5140.

White, T.C., Harris, G.S., and Orme-Johnson, W.H. (1992) Electrophoretic studies on the assembly of the nitrogenase molybdenum-iron protein from the *Klebsiella pneumoniae nifD* and *nifK* gene products. *J. Biol. Chem.* **267**, 24007-24016.

Willing, A.H., Georgiadis, M.M., Rees, D.C., and Howard, J.B. (1989) Crosslinking of nitrogenase components: Structure and activity of the covalent complex. *J. Biol. Chem.* **264**, 8499-8503.

Willing, A.H., and Howard, J.B. (1990) Cross-linking site in *Azotobacter vinelandii* complex. *J. Biol. Chem.* **265**, 6596-6599.

Winter, H.C., and Burris, R.H. (1968) Stoichiometry of the adenosine triphosphate requirement for N_2 fixation and H_2 evolution by a partially purified preparation of *Clostridium pasteurianum*. *J. Biol. Chem.* **243**, 940-944.

Wolle, D., Kim, C.-H., Dean, D.R., and Howard, J.B. (1992) Ionic interactions in the nitrogenase complex. *J. Biol. Chem.* **267**, 3667-3673.

Wuttke, D.S., Bjerrum, M.J., Winkler, J.R., and Gray, H.B. (1992) Electron-tunneling pathways in cytochrome c. *Science* **256**, 1007-1009.

Yang, S.-S., Pan, W.-H., Friesen, G.D., Burgess, B.K., Corbin, J.L., Stiefel, E.I., and Newton, W.E. (1982) Iron-molybdenum cofactor from nitrogenase. *J. Biol. Chem.* **257**, 8042-8048.

Yates, M.G. (1992) The enzymology of molybdenum-dependent nitrogen fixation.

Biological Nitrogen Fixation. (Stacey, G., Burris, G.P., and Evans, H.J., eds.) Chapman and Hall. pp. 685-735.

Zheng, L., White, R.H., Cash, V.L., Jack, R.F., and Dean, D.R. (1993) Cysteine desulfurase activity indicates a role for *NIFS* in metallocluster biosynthesis. *Proc. Natl. Acad. Sci. USA* **90**, 2754-2758.

Zovoisky, E.J. (1945) Paramagnetic relaxation of liquid solutions for perpendicular fields. *J. Phys. U.S.S.R.* **9**, 211-216.

Zumft, W.G., Mortenson, L.E., and Palmer, G. (1974) Electron-paramagnetic-resonance studies on nitrogenase. *Eur. J. Biochem.* **46**, 525-535.

ROLES OF MoFe PROTEIN α-274-HISTIDINE, α-276-TYROSINE AND α-277-ARGININE RESIDUES IN *Azotobacter vinelandii* NITROGENASE CATALYSIS

by

JOAN SHEN

Dissertation submitted to the faculty of the
Virginia Polytechnic Institute and State University
in partial fulfillment of the requirements for the degree of

DOCTOR OF PHILOSOPHY

in

Biochemistry and Anaerobic Microbiology

APPROVED:

William E. Newton, Chairman

Jiann-Shin Chen

Dennis R. Dean

Eugene M. Gregory

Thomas O. Sitz

November, 1994
Blacksburg, Virginia

Vita

Joan Shen was born on June 5, 1967, in Shanghai, P. R. China. She graduated from FuDan University in Shanghai with a Bachelor of Science in Biochemistry in 1989. She came to Virginia Polytechnic Institute and State University after graduation, and started her graduate program in the Department of Biochemistry and Nutrition in August, 1989. The department was later merged together with the Anaerobic Microbiology into Department of Biochemistry and Anaerobic Microbiology where she completed her Ph.D. requirements in November, 1994.